University of Southampton

Faculty of Natural and Environmental Sciences

School of Ocean and Earth Science

SINK OR SWIM: THE FATE OF PARTICULATE ORGANIC CARBON IN THE INTERIOR OCEAN

by

Emma Cavan

A thesis presented for the degree of

Doctor of Philosophy

2016

University of Southampton

Abstract

Faculty of Natural and Environmental Sciences
Ocean and Earth Sciences

Doctor of Philosophy

Sink or swim: The fate of particulate organic carbon in the interior ocean

by Emma Louise Cavan

Without small oceanic organisms atmospheric CO_2 levels would be about 200 ppm higher than they are today; phytoplankton convert dissolved inorganic carbon (DIC) to particulate organic carbon (POC) during photosynthesis, influencing the air-sea exchange of CO_2. Eventually some of this POC is exported out of the upper ocean, often as either phytodetrital aggregates or zooplankton faecal pellets. Because of the complexity of this biological carbon pump (BCP), the fate of the exported POC in the mesopelagic zone is difficult to predict. To make things more complex all of these processes vary temporally and spatially.

Marine snow catchers (MSCs) were used to analyse fast and slow sinking particles separately, which is a unique approach as slow sinking POC fluxes are not often quantified. To investigate what controls the fate of particles in the upper mesopelagic zone (50 - 500 m) particles were collected from three contrasting oceanic regions: the Southern Ocean (SO), Equatorial Tropical North Pacific (ETNP) oxygen minimum zone (OMZ) and the temperate North Atlantic. In all sampling areas the slow sinking POC flux was as large if not larger than the fast sinking POC flux. This emphasises the importance of slow sinking particles in the upper mesopelagic zone.

The main outcome from this thesis is the importance of the role of zooplankton in BCP processes. For instance the efficiency which particles were exported from the mixed layer varied inversely with primary production in the SO, and was likely due to the zooplankton grazing down the phytoplankton. When extending the data to include the ETNP and the North Atlantic this relationship still held, conflicting the long-standing theory that as primary production increases export efficiency increases.

In the ETNP oxygen minimum zone a high proportion of exported POC sank through the mesopelagic zone. Microbial oxygen uptake incubations showed for the first time that fast sinking particles are turned over significantly slower than slow sinking particles (0.13 d^{-1} and 5 d^{-1} respectively). Microbial degradation of POC could explain most of the fast sinking POC attenuation with depth, with the remainder lost due to abiotic fragmentation. Therefore it is likely that zooplankton degradation of particles is reduced in OMZs as their abundance and metabolism are lowered. This reduces the overall remineralistion of POC, hence a higher fraction of POC is transferred to depth in OMZs. Phytoplankton lipid biomarkers dominated lipid particle composition throughout the upper mesopelagic zone in the ETNP, further emphasising the minor role of zooplankton in OMZs.

Comparing the observations with an ecosystem model output at all three oceanic sites further emphasised the importance of zooplankton in the BCP. The model poorly parameterises zooplankton processing of particles and thus the observations and model matched best in the ETNP, where zooplankton processing of particles is naturally low.

Changes in climate will effect the abundance and distribution of these small organisms. Further understanding of how zooplankton community structure and metabolism may change in the future will be important to predict how atmospheric CO_2 levels may change.

Contents

List of Figures

List of Tables

Author's declaration

I, Emma Cavan, declare that the thesis entitled "Sink or swim: The fate of particulate organic carbon in the interior ocean" and the work presented in the thesis are both my own, and have been generated by me as the result of my own original research. I confirm that:

- this work was done wholly or mainly while in candidature for a research degree at this University;
- where any part of this thesis has previously been submitted for a degree or any other qualification at this University or any other institution, this has been clearly stated;
- where I have consulted the published work of others, this is always clearly attributed;
- where I have quoted from the work of others, the source is always given. With the exception of such quotations, this thesis is entirely my own work;
- I have acknowledged all main sources of help;
- where the thesis is based on work done by myself jointly with others, I have made clear exactly what was done by others and what I have contributed myself;
- parts of this work have been published separately;

In which my contribution was the development and handling of the reported analytical work, sample analysis, writing the papers with advice from the co-authors, producing the figures and leading the responses to the peer reviews.

Signed .....

Date .....

Acknowledgements

Thank you to Richard Sanders for spending the last 4 years turning me into a real scientist. I've thoroughly enjoyed our Monday morning chats, where often the topic of conversation would not be science! I appreciate the freedom I've been given and Richard's ability to deal with my opinionated personality. Thanks to Adrian Martin for telling Richard about my interview, as without this conversation this thesis wouldn't exist. I'm extremely grateful to Alex Poulton as he wasn't an official supervisor but somehow got roped into the role. Alex made sure I was always on course and guided me through many unnecessarily tough panel sessions. I'm also grateful for all the advice he has given me. It's been amazing to work with Richard Lampitt, who helped me improve my scientific writing and this whole thesis. I've also really appreciated help and advice from Steph Henson, who has always felt like a supervisor and is a great role model for female scientists. Thanks too to Debbie Yarrow, the 'mum' of OBE. As well I feel like I owe a lot to Google, I don't understand how people did a PhD pre-Google.

In addition I'd like to thank my fellow PhD'ers and NOC friends, particularly those who would have a breakfast bap with me, which would be the highlight of my week at NOC: Victoria Hemsley, Lou Jenkins and Chris Daniels. I had a lot of fun times with Jason Hopkins who undoubtedly was the best office mate in the world. We put the 'science' world to right many times. I was very relieved when Anna Belcher chose to also do a marine snow catcher PhD, it has been amazing to have someone else's brain to pick about even the simplest problems. Thank you so much to the people that have read this work: Lou, Mandy Sibbick and my parents. My parents and sister have always been very supportive of my career choice and I am so grateful for this. It makes all the difference. I'm also grateful to Mick Sibbick for his constant supply of wine!

The last 4 years would have been very different without the awesome Fran James, who would be willing to let off steam with me, even on a 'school' night when everyone else would be behaving. Which brings me to the Platform Tavern, where people have no idea what I do and that has been a blessing. Having friends who don't understand what you do is very important during a PhD so you can talk about something else other than science!

My biggest thank you is to Ned. For being so understanding and supportive of such a chaotic career choice. Your graciousness with my frequent and sometimes extended absences due to work has been so appreciated. Although as promised I won't go away for 10 weeks again! Your support means the world to me, as do you...thank you!

Abbreviations

1D	One Dimensional
ANCOVA	Analysis Of Co-Variance
ANOSIM	Analysis Of Similarities
ANOVA	Analysis Of Variance
b	Power function exponent
BCP	Biological Carbon Pump
BCPeff	Biological Carbon Pump Efficiency
BSi	Biogenic Silica
BSTFA	Bis-trimethylsilyl-trifluoroacetamide
C	Carbon
chl a	Chlorophyll a
CHN	Carbon Hydrogen Nitrogen
CO_2	Carbon dioxide
CTD	Conductivity Temperature Depth
DCM	Dichloromethane
DHA	Docosahexaenoic Acid
DIC	Dissolved Inorganic Carbon
DO	Dissolved Oxygen
DVM	Diel Vertical Migration
EPA	Eicosapentaenoic acid
ESD	Equivalent Spherical Diameter
ETNP	Equatorial Tropical North Pacific
ETSP	Equatorial Tropical South Pacific
eV	Activation energy
Fig.	Figure
FlowCAM	Flow Camera
FOV	Field Of View
FP	Faecal Pellet
GCMS	Gas Chromatograph Mass Spectrometer
GMT	Greenwich Mean Time
Gt	Gigatonne

HNLC	High Nutrient Low Chlorophyll
IRS	Indented Rotating Sphere
JGOFS	Joint Global Ocean Flux Study
k	Carbon-specific respiration rate
L	Litre
LOD	Limit Of Detection
m^{-2}	per metre squared
MDS	Multi-Dimensional Scaling
MEDUSA	Model of Ecosystem Dynamics and Utilisation, Sequestration an Acidification
MIZ	Marginal Ice Zone
MLD	Mixed Layer Depth
MSC	Marine Snow Catcher
MSC_{Ex}	Export sampling depth
N_2	Nitrogen
NA	Not Applicable
MSC_D	Deep sampling depth
MUFA	Mono-Unsaturated Fatty Acid
NOAA	National Oceanic and Atmospheric Administration
NOC	National Oceanography Centre
O_2	Oxygen
OCIMP	Ocean Carbon Model Intercomparison Project
OMZ	Oxygen Minimum Zone
PAP	Porcupine Abyssal Plain
PDA	Phytodetrital Aggregate
PEeff	Particle Export Efficiency
PELAGRA trap	Particle Export using a LAGRAngian trap
PF	Polar Front
Pg	Petagram
POC	Particulate Organic Carbon
PON	Particulate Organic Nitrogen
PP	Primary Production
ppm	parts per million

PTFE	Polytetrafluoroethylene
PUFA	Poly-Unsaturated Fatty Acid
Q_{10}	Temperature Coefficient
R	Global R result from ANOSIM
RLS	Reminerlisation Length Scale
SACCF	Southern Antarctic Circumpolar Front
SAF	Subantartic Front
SAP	Stand Alone Pump
SBDY	Southern Boundary of the SACCF
SETCOL	Settling Column
SFA	Saturated Fatty Acid
SIZ	Seasonal Ice Zone
SG	South Georgia
SSI	South Sandwich Islands
SO	Southern Ocean
sp	species
T*eff*	Transfer Efficiency
TEP	Transparent Exopolymer Particles
^{234}Th	Thorium-234
^{238}U	Uranium-238
USFA	Unsaturated Fatty Acid
w	Sinking rate
yr^{-1}	per year
z	Depth
z^*	Reminerlisation length scale

Chapter 1

Introduction

1.1 Global carbon cycle and climate

The ocean stores 39 000 Gt of carbon (Falkowski *et al.*, 2000), making it the second largest reservoir of carbon on Earth after the Lithosphere (Fig 1.1). Most carbon in the oceans is stored as dissolved inorganic carbon (DIC) with a small amount stored as organic carbon (Kilops & Kilops, 2005). The emission of at least 244 Gt of carbon to the atmosphere since 1800, as a result of burning fossil fuels and cement production, has altered the fluxes between global carbon reservoirs (Sabine *et al.*, 2004). In pre-industrial times the carbon cycle appeared to be in a steady state, where the flux of carbon into the ocean equalled that back into the atmosphere. However by the 1980s the fluxes were no longer in equilibrium. About 90 Gt of carbon is exchanged every year between the atmosphere and oceans, with slightly more entering the oceans than is removed (Kilops & Kilops, 2005), thus the ocean is a net sink of carbon. There is spatial and temporal heterogeneity throughout the oceans, with different areas acting as net sources or sinks of CO_2. For example high latitude areas are often large sinks of CO_2 (Bopp & Le Quéré, 2009) as CO_2 is more soluble in cold, saline waters so sinks to the colder deep ocean (Falkowski *et al.*, 2000).

Even though only a small amount of organic carbon is stored in the oceans, biological processes that produce it can have a significant effect on CO_2 storage. Photosynthesis by phytoplankton (microscopic algae) in the euphotic zone (sunlit surface waters) converts CO_2 into particulate organic carbon (POC). About 42 % of CO_2 entering the surface ocean is taken up by photosynthesis (Fig. 1.1 (Bopp & Le Quéré, 2009)) with the remainder lost to the atmosphere or physically mixed to the deep ocean (the solubility pump). Eventually the surface-produced POC

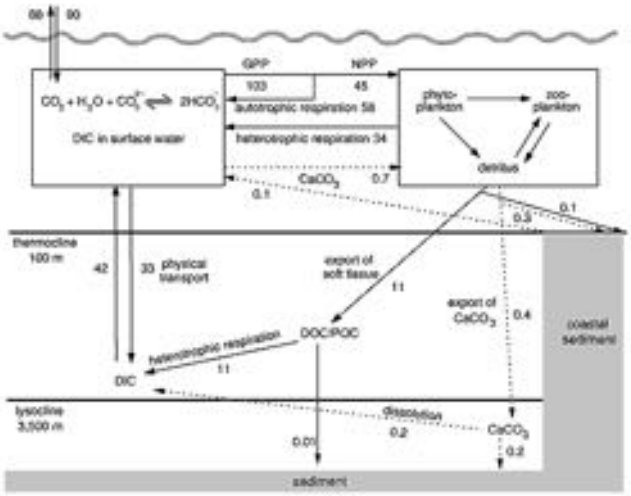

Figure 1.1: Post-industrial carbon cycle (Bopp & Le Quéré, 2009). Numbers are fluxes of carbon in Gt yr $^{-1}$.

sinks out of the upper ocean forming the biological carbon pump. The decrease in the CO_2 partial pressure gradient at the air-sea interface because of the carbon pumps provides the driving force for the invasion of CO_2 from the atmosphere into the ocean (Falkowski, 1998). In 2004 Sabine *et al.* estimated atmospheric CO_2 would be 55 ppm higher if the oceans did not take up any CO_2. Kwon *et al.* (2009) further emphasised this by showing that the depth at which POC is converted back to CO_2 (remineralised) directly influences how much CO_2 is in the atmosphere. However, a model study showed that the solubility pump would have a greater effect on reducing atmospheric CO_2 levels than the biological carbon pump (Volk & Hoffert, 1991).

Fig. 1.2 shows how high CO_2 emissions have increased the global temperature since 1870, and the projections of further CO_2 emissions and increasing temperature until 2100. Warming of the oceans is expected to increase heat storage in the surface ocean; leading to enhanced stratification and reductions in nutrient fluxes to the upper oceans, which will together increase the size of the oligotrophic (low nutrient) gyres and decrease the amount of photosynthesis (Falkowski, 1998). If this scenario holds, the effectiveness of the oceans as a sink of CO_2 may decrease and eventually they may become a net source of CO_2 to the atmosphere.

This thesis will contribute to our understanding of the organic carbon cycle in the ocean, as this directly links to climate by influencing the air-sea partial pres-

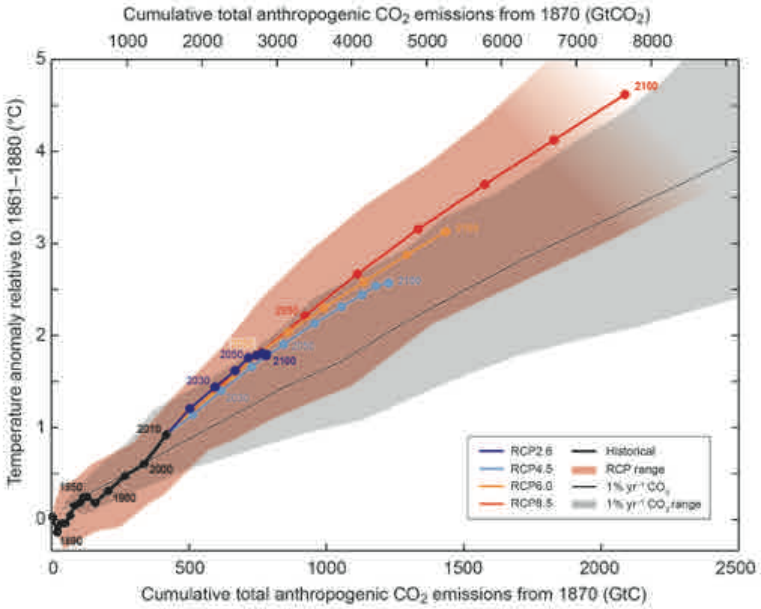

Figure 1.2: IPCC CO_2 projections. RCP = representative concentration pathways with RCP8.5 being considered 'business-as-usual'.

sure gradient of CO_2. Being able to construct a solid understanding of oceanic biological processes is important so we may then predict how further increases in CO_2 levels will change our oceans and atmosphere.

1.2 Biological carbon pump

Prior to the 1970s it was thought that the deep sea (below the permanent thermocline) was in steady state, with no seasonality, as food settled slowly and continuously from the surface ocean (Menzies *et al.*, 1973; Lampitt, 1985). However, seasonal reproductive behaviours were known to occur in deep sea organisms, conflicting this theory (Rokop, 1974). In 1979 photographs (Fig. 1.3) of the sea floor (< 4000 m) at temperate latitudes revealed the accumulation of detrital material during spring (Billett *et al.*, 1983). This showed that POC from the surface ocean is an energy source for organisms at the sea floor and revealed the existence of seasonality. This discovery opened a new field of oceanographic research; the biological carbon pump (BCP).

The BCP is the collective term for the processes by which DIC is fixed during phytoplankton photosynthesis in the euphotic zone and exported (transferred) out of the upper ocean to the deep ocean as particulate organic carbon (POC, see Fig. 1.4). Export processes include the passive sinking of organic particles (Alldredge & Gotschalk, 1988) and the active flux of particles through zooplankton

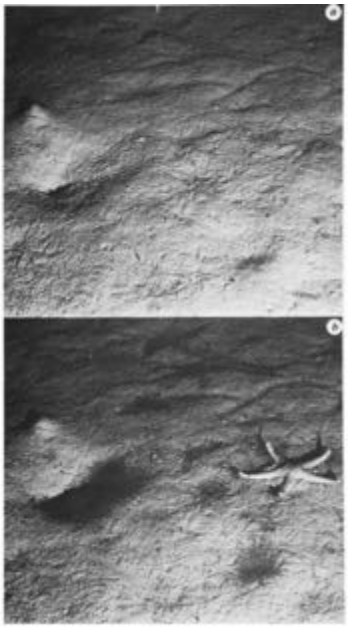

Figure 1.3: Arrival of phytodetritus on the sea floor (Billett *et al.*, 1983). Phytodetritus can be seen accumulating in the bottom image from the increase in the size of the dark areas compared to the top image.

(heterotrophic eukaryotic plankton) diel (daily) and ontogenetic (seasonal) vertical migration. (Steinberg *et al.*, 2000). Global oceanic net primary production (the rate at which organisms convert energy to organic compounds) is estimated to be between 45 and 60 Gt C yr^{-1}, yet only 11 - 16 Gt C yr^{-1} (18 - 45 %) is exported out of the upper ocean (Falkowski, 1998). Other estimates suggest only 1 - 40 % of surface primary production is exported (Herndl & Reinthaler, 2013) and of this exported material only a small fraction (ca. 1%) reaches the deep (> 1000 m) ocean (Henson *et al.*, 2011). This biological draw-down of POC sequesters (isolates) carbon on timescales of hundreds to thousands of years (Henson *et al.*, 2012).

Such a small proportion of surface produced POC reaches the deep ocean because most of the exported organic material is processed in the water column by heterotrophs (organisms whose energy source are organic compounds), which transform organic carbon back to DIC. This is known as remineralisation (Wakeham *et al.*, 1980). Processes included in the remineralisation of POC are respiration, zooplankton consumption and microbial gardening (Mayor *et al.*, 2014) by zooplankton. Particles are often mechanically broken either biologically by zooplankton (Lampitt *et al.*, 1990) or abiotically (Alldredge *et al.*, 1990) prior to remineralisation. If POC is remineralised in the upper water column then

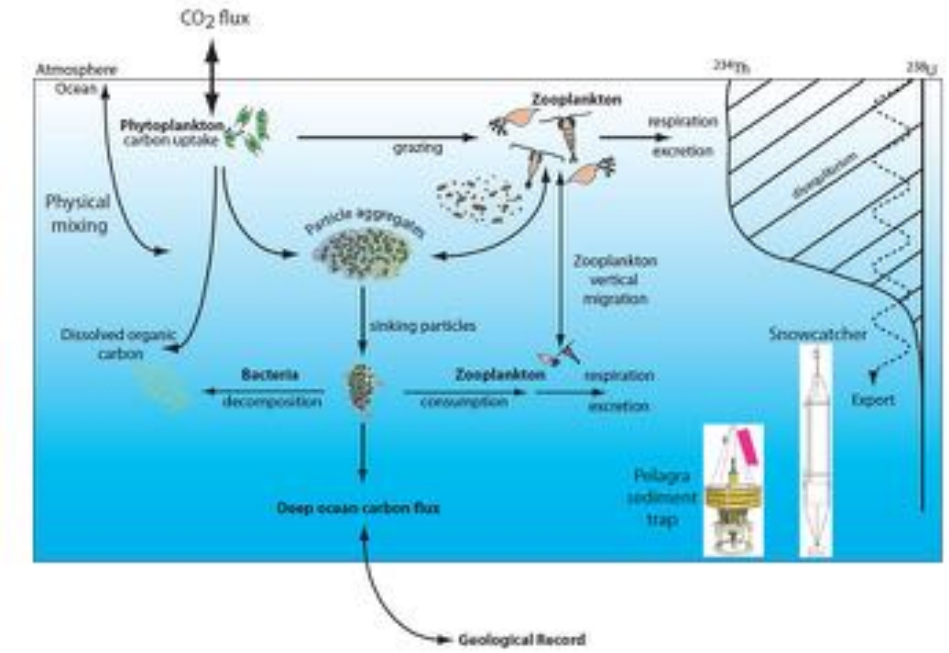

Figure 1.4: Biological Carbon Pump and methods of estimating particle flux (www.noc.ac.uk).

CO_2 may be physically mixed to the surface and lost to the atmosphere. If POC is remineralised deeper in the ocean, below the permanent thermocline, CO_2 is likely to remain in the deep ocean (Buesseler *et al.*, 2007*b*). There is huge temporal and spatial variability in the magnitude of POC export and subsequent remineralisation, making it difficult to ascertain a single controlling factor of the biological carbon pump.

The remineralisation of POC by heterotrophs results in a huge decrease in POC flux with depth. This was most notably described by Martin *et al.* (1987) from 123 POC flux estimates in the North Pacific, resulting in the depth profile shown in Fig. 1.5. Martin *et al.* fitted a power function to the data to show the logarithmic relationship between POC flux and depth, which quickly became the most popular algorithm to describe POC flux attenuation (equation 1.1):

$$F(z) = F_{100} * (z/z_{100})^{-b} \tag{1.1}$$

where F(z) is the POC flux (mg C m^{-2} d^{-1}) at depth z and b (dimensionless) is an exponent which represents the attenuation of POC with depth. The average b as depicted by Martin *et al.* was 0.86 and this value has been used widely in biogeochemical models, such as the ocean carbon model inter-comparison project (OCIMP) II runs (Doney *et al.*, 2004). However, it must be noted that earlier

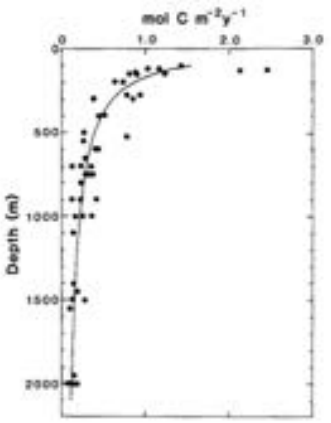

Figure 1.5: The 'Martin curve' (Martin *et al.*, 1987) showing the attenuation (decrease) of POC flux with depth. The fitted line is the power function (Equation 2.12) with an average b of 0.86.

algorithms exist such as that of Suess (1980) where POC flux is a function of primary production and depth.

More recent studies have shown b varies greatly globally (0.2 - 1.3) e.g. Van Mooy *et al.* (2002), Buesseler *et al.* (2007*b*) and Henson *et al.* (2012). Using one determined b value from the Pacific Ocean is not applicable globally and it is also likely to vary seasonally. Further concerns have been raised over the effect of sampling depth on determining b; at 0 m the curve approaches infinity emphasising that b is very sensitive to sampling depth, particularly at shallow depths (Buesseler & Boyd, 2009).

To exclude this bias Boyd & Trull (2007) suggested a different relationship between POC flux and depth using first order kinetics, i.e., rates are proportional to the amount of material present, where either degradation rates decrease (e.g. microbial respiration) with depth or particle sinking rates increase with depth. However, both degradation and sinking rates simultaneously effect the attenuation of POC. This resulted in the following exponential equation (equation 1.2):

$$F(z) = F(z_0) * e^{(z-z0/z*)} \tag{1.2}$$

Where $z*$ (m) is the 'decay length' or 'remineralisation length scale (RLS)'; the depth at which the flux has decreased by at least 63 % $(1/e)$ of the exported flux.

Boyd & Trull (2007) concluded in their review that there is a need for more particle studies in the upper ocean where POC attenuation is strongest and where particle fluxes can be measured as a function of their sinking speed. This

thesis does exactly that: improve our knowledge of upper ocean processes on fast and slow sinking particles separately. What controls or regulates biological carbon pump processes such as POC export and mesopelagic zone (100 - 1000 m) remineralisation is still unknown. Moreover, we have not yet determined if these controls are derived primarily from particle properties imprinted from the surface ocean or particle transformations deeper in the ocean (Boyd & Trull, 2007). Furthering our understanding of these factors will be an important aim of this thesis.

1.3 Particle type

The type of exported particles can affect the sinking rates and degradation rate of POC, hence the importance of determining the particle type. There are many different types of organic particles in the oceans, including marine snow, zooplankton faecal pellets and whole organisms or cells (Fowler & Knauer, 1986; Aksnes & Wassmann, 1993). In this thesis, I will focus mostly on marine snow and crustaceous zooplankton faecal pellets as these usually dominate particle flux.

1.3.1 Phytodetrital aggregates

Marine snow is defined as aggregates of detrital phytoplankton between 0.5 mm and 20 mm in diameter (Alldredge & Gotschalk, 1988). The term is thought to originate from Rachel Carson's award-winning book 'The Sea Around Us' (Carson, 1951), where she poetically describes 'The long snowfall...flake upon flake, layer upon layer' in the oceans. Marine snow occurs throughout the water column; at the surface the concentration of particles ($>$ 3 mm) is 1 - 10 L^{-1} and in deeper waters only 0.0001 - 2 L^{-1} (Lampitt *et al.*, 1993). As well as consisting of phytoplankton, detrital marine snow can also contain the gelatinous feeding structures of appendicularians, planktonic foraminifera and pteropods and can be formed from the physical coagulation of smaller particles or *via* the addition of particles collected as they sink (McCave, 1975; De La Rocha & Passow, 2007).

If certain physical conditions occur then large (metres long) aggregates (mucilages) form (see Fig. 1.6). This is a recurrent phenomenon in the upper water column of the Adriatic Sea where mucilages occur principally from chrysophytes and brown algae (Giani *et al.*, 2005). Mucilages reach almost neutral buoyancy at the pycnocline (density gradient) where their residence time increases, thus

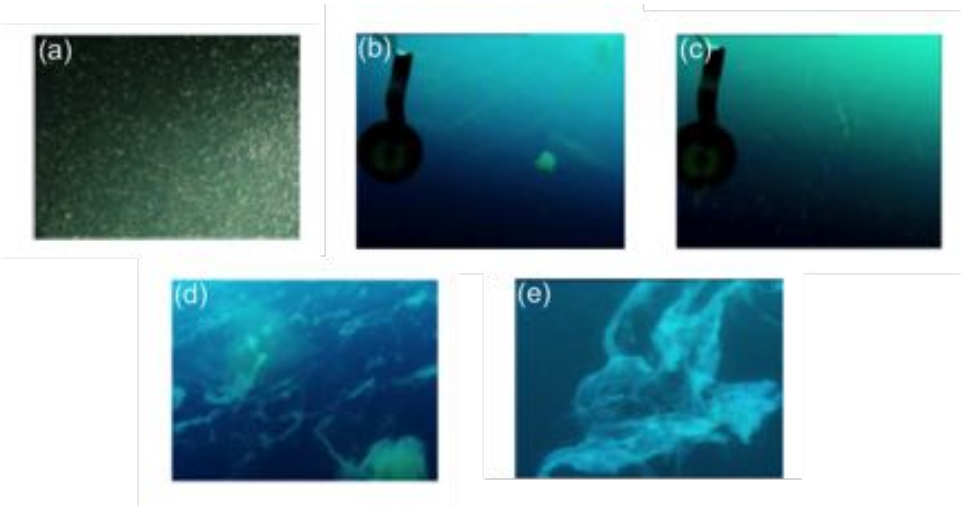

Figure 1.6: Macro-aggregates in the northern Adriatic Sea: a) 0.5 mm - 1 cm aggregates, b) 1 - 5 cm aggregates c) 2 - 25 cm elongated aggregates, d) 10 - 20 cm ribbon aggregates, e) web-like aggregates (Precali *et al.*, 2005).

they can grow into huge mucilages (Precali *et al.*, 2005). The composition of marine snow continuously changes as particles dis/aggregate and are remineralised (Abramson *et al.*, 2010).

Marine snow provide areas of enriched organic carbon and nutrients (Alldredge & Youngbluth, 1985) to microbial communities. This results in chemical microhabitats, where remineralisation can occur at highly elevated levels compared to the rates in surrounding waters (Alldredge, 1998). Therefore, high densities of metabolically active bacteria inhabit marine snow with more sparse free living populations in the surrounding water (Alldredge & Youngbluth, 1985). Carbon-specific respiration rates of particles by microbes range from 0.01-0.5 d^{-1} (Ploug & Grossart, 2000; Ploug *et al.*, 2008; Iversen & Ploug, 2013; Mcdonnell *et al.*, 2015; Belcher *et al.*, 2016). Zooplankton also inhabit marine snow for short periods of time whilst they graze. They can occur in abundance and some use chemical trails to detect particles (Lombard *et al.*, 2013).

The term marine snow defines detrital material that has aggregated together, mostly originating from photosynthesis. However, it is specifically for particles of a particular size (> 0.5 mm) and so in this thesis I will refer to phytodetrital aggregates (PDAs), which encompasses no size limits on particles.

1.3.2 Faecal pellets

Faecal pellets (FPs, here mostly assumed to be from crustaceous zooplankton) are discrete dense packages sometimes enclosed in a peritrophic membrane

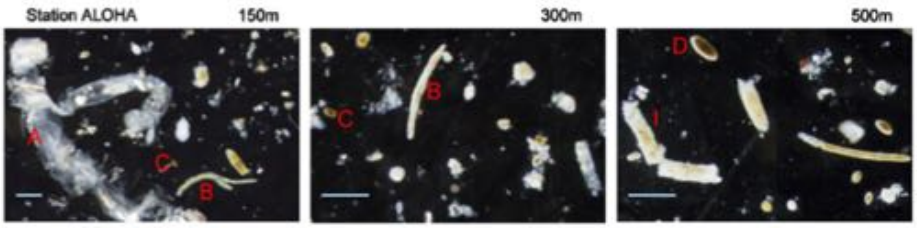

Figure 1.7: Zooplankton faecal pellets from sediment traps, scale bar = 0.5 mm: A) Heteropod, B) large copepod or euphausiid, C) small copepod, D) larvacean, I) broken pellet (Wilson *et al.*, 2008).

(Lampitt *et al.*, 1990). They are likely to contain a higher proportion of refractory material than phytodetrital aggregates, as some of the labile portion of POC will have been removed by the animal in the gut (Wilson *et al.*, 2008), particularly if coprophagy occurs; the ingestion of zooplankton faecal pellets by zooplankton (Frankenberg & Smith, 1967).

Faecal pellets do not disaggregate as easily as PDAs (Ploug *et al.*, 2008) and hence can form a large part (up to 90 %) of the vertical POC flux (Huskin *et al.*, 2004; Steinberg *et al.*, 2008; Abramson *et al.*, 2010; Wilson *et al.*, 2013; Hansen & Visser, 2016). Intact FPs have been found in the deep (200 - 900 m) ocean across the globe (Iseki, 1981; Abramson *et al.*, 2010). As well as their robustness they have low porosity (few holes) compared with marine snow (> 0.43 and > 0.96 respectively) and can have high (750 m d^{-1}) sinking rates (Ploug *et al.*, 2008). Zooplankton can release FPs into deep waters through diel vertical migration (DVM). This is where zooplankton migrate to the surface to feed at night and at dawn migrate into the mesopelagic zone, avoiding visual predators (Worthington, 1931). If they defecate at their daytime depth then these faecal pellets will have a greater chance of reaching the sea floor, as they will escape remineralisation where it is most intense in the upper mesopelagic zone (Martin *et al.*, 1987).

Different types of invertebrates produce different types of faecal pellets (Fig. 1.7): Euphausiids (e.g. krill) produce long (> 1 mm) cylindrical pellets; salps produce large (> 1 mm) tabular, fragile pellets; larvaceans ellipsoid pellets and copepod pellets vary greatly (Wilson *et al.*, 2008). The contribution of faecal pellets to POC flux varies greatly: in the Mediterranean faecal pellets comprised 18 - 87 % of POC flux (Abramson *et al.*, 2010); in the Northwest Pacific they only contributed to 3 - 48 % of the POC flux (Wilson *et al.*, 2013) and in the Panama basin they were only a minor component of flux (Asper, 1987). This high variability coupled with DVM makes quantifying the effect of zooplankton

on POC flux and parameterising it in models difficult. Throughout this thesis faecal pellets (FPs) will be defined as the pellets of crustaceous zooplankton unless stated otherwise.

1.4 Controls over sinking particle fluxes

One of the main aims of this thesis is to explore what controls the magnitude of particle export out of the upper ocean and its subsequent remineralisation at depth. These two processes indirectly influence atmospheric CO_2 levels (Kwon *et al.*, 2009). Parameters commonly calculated in analyses are particle export efficiency (PE*eff*) and transfer efficiency (T*eff*). PE*eff* is the ratio of the export flux at the base of the mixed layer to the primary production within the mixed layer, and T*eff* is the ratio of a deep flux to export flux (Henson *et al.*, 2012).

1.4.1 Controls on export fluxes

Export flux is the flux exported from the mixed layer (20-100 m deep). Highest export generally occurs after a peak in primary production (Laws *et al.*, 2000). It is important to measure and estimate how much POC is exported from the mixed layer as this determines the maximum amount that could reach the deep sea and sediments or be remineralised and mixed back to the surface ocean.

The export flux is formed of organic carbon that has been produced during primary production in the mixed layer. Therefore, factors that affect primary production, such as light, temperature and nutrients, are likely to affect the export flux. The dominant phytoplankton type could also be important, as shown by the ballast hypothesis (Armstrong *et al.*, 2002; Henson *et al.*, 2012) (see section 1.4.2). Additionally grazing by zooplankton influences the magnitude of export, but this is not just an upper-ocean process and can occur throughout the mesopelagic zone.

Temperature

The seminal paper by Laws *et al.* (2000) suggested that there is an inverse relationship between PE*eff* and temperature, such that warming the surface waters of the ocean will decrease PE*eff*. This is because warming would restrict vertical circulation and reduce allochthonous nutrient inputs in most areas of the oceans (Laws *et al.*, 2000). This relationship has also been shown using other models (Dunne *et al.*, 2005; Lima *et al.*, 2013). However, this has also been

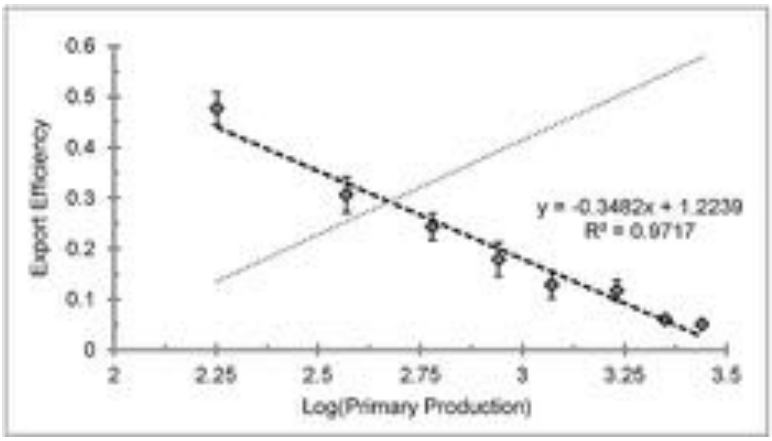

Figure 1.8: PE*eff* vs. primary production from Maiti *et al.* (2013) (dashed line) with the output of Laws *et al.* (2000) included (dotted line).

refuted as Maiti *et al.* (2013) found the relationship broke down at temperatures below 6 °C in the Southern Ocean.

Primary production and phytoplankton community structure

As with temperature, net primary production (NPP) and/or the dominant phytoplankton group are used to estimate export flux. NPP can be measured *in situ*, derived from satellite-measured surface chlorophyll-*a* concentrations or estimated using biogeochemical or food web models.

Micronutrients, such as iron, are known to limit primary production in the oceans (Martin, 1990; Sedwick & DiTullio, 1997). Iron fertilisation experiments have shown how increasing primary production can increase the export of particles. For example, Lam & Bishop (2007) showed (through *in situ* experiments in the Southern Ocean) that where there was already high export, export could be enhanced further by iron fertilisation. Whereas where export was low, iron fertilisation did not stimulate an increase in export. Thus a high phytoplankton biomass does not necessarily result in high export.

Laws *et al.* (2000) suggested a global positive relationship between primary production and PE*eff*, such that the higher the phytoplankton biomass, the more efficiently particles are exported from the mixed layer. Devol & Hartnett (2001) also hypothesised that a lower flux, measured by sedimentation rates off the Pacific coast of Mexico, was due to lower primary production rates. This relationship was challenged by Maiti *et al.* (2013) & Le Moigne *et al.* (2016) who used *in situ* data from the Southern Ocean to show that in this region there was actually an inverse relationship between primary production and PE*eff* (Fig. 1.8).

These studies highlight that there isn't a singular relationship between primary production and PE*eff* across the globe, even though global models often use a single simple relationship (Henson *et al.*, 2012). This thesis will determine if PE*eff* is positively or inversely related to primary production and what influences the relationship.

The dominant phytoplankton group is often used to estimate the magnitude of export flux; e.g. where there is a relatively high diatom abundance, PE*eff* is high (Lam *et al.*, 2011; Henson *et al.*, 2012; Laufkötter *et al.*, 2013; Lima *et al.*, 2013). This is associated with the mineral ballast hypothesis (see section 1.4.2); where biogenic minerals produced by certain phytoplankton groups, such as diatoms (siliceous) and coccolithophores (calciferous), are incorporated in sinking particles influencing flux through the mesoeplagic zone (François *et al.*, 2002).

High export at high latitudes is thought to be affected by the incomplete utilisation of mixed layer NO_3, resulting in a high diatom abundance and therefore high PE*eff* (Henson *et al.*, 2012), due to their large cell size. Analysis from a biogeochemical model agreed with this and showed the fraction of diatoms strongly correlated ($r^2 = 0.8$, $p = 0.1$) to PE*eff* in most global areas apart from the North Pacific and Antarctic Circumpolar Current (Laufkötter *et al.*, 2013). This further emphasises the findings of Maiti *et al.* (2013) that the Southern Ocean does not conform to the same single relationship when comparing primary production and export like the rest of the globe. Additionally, care must be taken when using mineral ballasting to infer the mixed layer ecosystem structure, as it does not necessarily reflect this (Lima *et al.*, 2013). For example if a particle flux in the mesopelagic zone has a high calcite content this does not necessarily mean that calcite-producing phytoplankton dominated the epipelagic phytoplankton community structure.

1.4.2 Controls on mesopelagic remineralisation

Sinking rates and degradation (turnover) rates of particles affect remineralisation. The remineralisation length scale (z^*) in metres can be calculated by dividing sinking rate (m d^{-1}) by degradation rate (d^{-1}). Hence understanding what regulates these two processes is important.

Sinking rates

The rate at which an exported organic particle sinks influences its residence time in the upper ocean and subsequently how long it may be subjected to

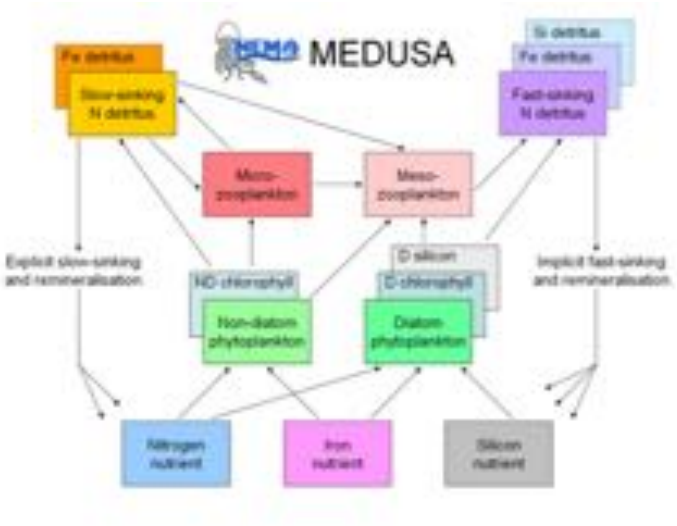

Figure 1.9: Schematic of MEDUSA model (Yool *et al.*, 2011). Note the separation of detrital fluxes into slow and fast sinking detritus.

degradation by heterotrophs (Goutx *et al.*, 2007; Kindler *et al.*, 2010). If a particle sinks slowly it has a long residence time in the upper ocean, thus a large proportion may be remineralised, allowing more DIC to be mixed back to the surface and re-exchanged with the atmosphere (Kwon *et al.*, 2009; Riley *et al.*, 2012). Being able to measure particle sinking rates *in situ* is key so these rates can be accurately modelled.

As a particle sinks through the water its sinking rate decreases due to decreases in temperature and increases in density with depth. Using sediment trap material Bach *et al.* (2012) showed that an increase of 9 °C in water temperature increased the sinking rate of particles by 40 %. Remineralisation of particles by zooplankton and bacteria will also effect their sinking rate as it reduces the amount of labile organic carbon and changes the shape, density, porosity and size of a particle. This will be discussed further in the following two sections.

Often in marine ecosystem models, sinking particles are separated into two pools: fast sinking and slow sinking (Slagstad *et al.*, 1999; Lampitt *et al.*, 2001; Yool *et al.*, 2011), as shown from the MEDUSA model in Fig. 1.9. The parametrized sinking rate of fast sinking particles ranges from 50 m d^{-1} (Fasham & Evans, 1995) to being too fast to be resolved by one time step of the model (Yool *et al.*, 2011) and for slow sinking particles from 2 - 6 m d^{-1} (Fasham & Evans, 1995; Yool *et al.*, 2013). However, estimating the magnitude and composition of the two pools separately *in situ* is a challenge and accurately measuring sinking rates, especially of slow sinking particles, an even greater one.

Early methods to determine particle sinking rates include collection of particles using SCUBA *in situ* and sinking in a lab and using time-lapsed cameras on the sea floor to calculate the time between production in the surface and arrival on the seafloor (Billett *et al.*, 1983; Asper, 1987). The latter method produced sinking rate estimates of 1 - 150 m d^{-1}. Another method was to measure the time it took for an aggregate to sink to a spot of neutrally buoyant fluorescent dye placed 3 cm below it, which generated a mean sinking rate of 117 m d^{-1} (Alldredge, 1998). Calculating the sinking rate of slow sinking particles is somewhat harder as they are often much smaller than fast sinking particles and therefore not visible to the naked eye.

This problem can be overcome by using the SETCOL method developed by Bienfang (1981); originally to measure the sinking rate of phytoplankton cells it can be applied to any measured substance (POC, chlorophyll-*a* e.t.c). It uses a settling column and compares the change in mass of a substance between the start and end of the settling time;

$$w\ (m\ d^{-1}) = \frac{(V_s * b_s - V_s * b_0)}{(V_t * b_0)} * \frac{l}{t} \tag{1.3}$$

where V_s is the volume of the base of the settling column (b_0), V_t is the total volume of sample in the column, b_0 is the total biomass initially within the column (taken at t = 0), b_s is the total POC concentration of the base settled at the end of the settling time (t) and l is the length of the column (m). Initial experiments yielded a mean sinking rate of 1.75 m d^{-1} using phytoplankton cells, much slower than fast sinking particles.

What determines particle sinking rate is still unknown. Some laboratory experiments show a positive linear relationship between the size and sinking rate of particles (Iversen & Ploug, 2013); however this relationship has rarely been observed in the field. One study used gel traps off the Western Antarctic Peninsular and observed sinking rates of 10 - 150 m d^{-1}, with small (< 100 μm diameter) and large (> 1000 μm diameter) particles sinking fastest (> 50 m d^{-1}) (McDonnell & Buesseler, 2010). Riley *et al.* (2012) assumed sinking rates of 9 m d^{-1} for slow sinking particles using marine snow catchers (see section 1.13). Both Riley *et al.* (2012) and Alonso-Gonzalez *et al.* (2010) observed that the slow sinking POC flux dominated the total flux by 63 % and up to 75 % respectively. This highlights the importance of slow sinking particles in POC

export and transfer through the upper mesopelagic zone (< 500 m).

Two standard methods for measuring POC flux *in situ* are sediment traps (Honjo, 1982; Buesseler *et al.*, 2008; Marsay *et al.*, 2015) or the Thorium-234 method (Buesseler *et al.*, 1992; Thomalla *et al.*, 2008; Le Moigne *et al.*, 2013*b*). Most sediment traps collect bulk particles which are not separated by sinking rate or size, making it impossible to quantify the proportion of fast or slow sinking particles to the total flux. Additionally, sediment traps are often deployed in the deep ocean, at depths of a few kilometres deep, meaning slow sinking particles are unlikely to reach these depths (Riley *et al.*, 2012). The Thorium-234 method involves collection of particles *via* stand alone *in situ* pumps (SAPs) which have two different size filters, 1 - 53 μm and > 53 μm (Le Moigne *et al.*, 2013*c*). Here the particles are separated into large and small fractions, but this does not necessarily reflect their sinking rate. See section 1.6 for more in-depth details on particle collection techniques.

It is widely believed that sinking rate, and so the percentage composition of the different sinking pools, affects how much particulate matter is remineralised and at what depth this occurs. However what has been observed in the ocean is not always translated into models, and the variability (spatially and temporally) is large. This thesis will focus on two sinking pools, the fast and slow, and develop methods to try to accurately measure the sinking rate of particles.

Ballast hypothesis

The ballast hypothesis suggests that minerals, such as calcite and opal, produced by plankton are incorporated into sinking particles, increasing the flux of POC through the mesopelagic. Either the minerals form a protective matrix and make remineralisation of POC more difficult or they increase the density, thus sinking rate, of the particle (Armstrong *et al.*, 2002; François *et al.*, 2002; Klaas & Archer, 2002). Up to 20 % of the organic carbon produced in euphotic zone can be by mineralizing phytoplankton (Poulton *et al.*, 2006), so it is highly likely some of this is exported. However, mineral ballasting is thought to have a greater affect on T*eff* than on PE*eff* (Lam *et al.*, 2011; Yool *et al.*, 2011; Lima *et al.*, 2013).

Armstrong *et al.* (2002) showed that POC flux must include both POC that is quantitatively associated with ballast minerals and that which is free (or excess),

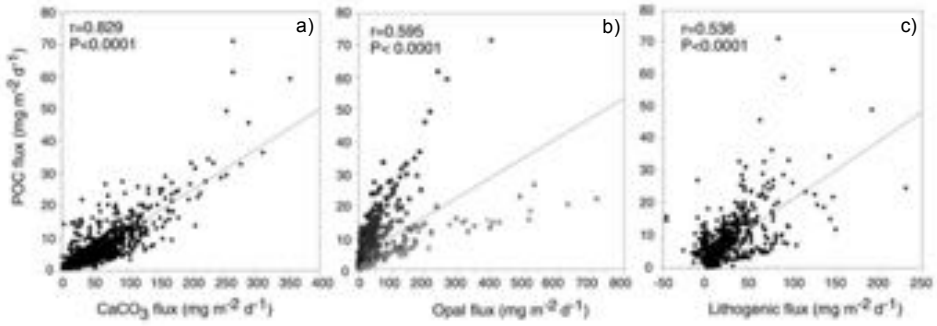

Figure 1.10: Scatter plots of $CaCO_3$, opal and lithogenic fluxes against POC flux from sediment traps at 1000 m (Klaas & Archer, 2002).

thus subject to remineralisation. POC export occurs even with negligible ballast fluxes (Le Moigne *et al.*, 2012) therefore ballast minerals are considered less important in the upper ocean than the deep (> 1800 m) (Armstrong *et al.*, 2002; Thomalla *et al.*, 2008; Le Moigne *et al.*, 2014).

Calcite is thought to be the dominant ballast mineral (Lam *et al.*, 2011; Henson *et al.*, 2012), with 83 % of global POC fluxes being associated with it, as it is denser than opal and more abundant in the oceans than lithogenic sources (Klaas & Archer, 2002) (Fig. 1.10). This conflicts with the long standing hypothesis that diatoms are the most important phytoplankton group controlling the magnitude of POC flux at > 2000 m (Boyd & Newton, 1999). François *et al.* (2002) showed a positive linear regression ($r^2 = 0.65$) between carbonate flux and the transfer efficiency of POC measured from traps and satellite estimates at 68 stations across the globe. They also calculated the carrying coefficients and used them to estimate transfer efficiency (T_{eff}) from ballast minerals and non-associated POC alone. There was a strong positive linear regression between measured and estimated T_{eff} with a r^2 of 0.85. After removing opal and lithogenics from the linear regression, the r^2 value only decreased to 0.84 (François *et al.*, 2002). This further emphasises the importance of calcite as a ballasting mineral compared to opal and lithogenics.

Another effect of minerals on particles other than ballasting is they can affect how zooplankton interact with POC. For example, when calcite was added to aggregates in a laboratory the rates of excretion of ammonia and phosphate by zooplankton (marine Rotifers) decreased, suggesting minerals may inhibit the destruction of POC by zooplankton (Le Moigne *et al.*, 2013*a*). However, microbial carbon-specific respiration rates of copepod FPs and aggregates were

similar with and without ballast minerals, hence the presence of minerals did not effect bacterial remineralisation of particles (Ploug *et al.*, 2008).

Finally the ballast hypothesis has led to the following geographical premise; in high latitude, cold, opal-dominated areas, export is high but the transfer of this export flux to depth is low; whereas in low latitude, warm, calcite-dominated areas, export is low but there is a high transfer to depth of the exported material (François *et al.*, 2002; Henson *et al.*, 2012). If the predicted shift from diatoms to small species occurs with climate change, then the ratio of ballast-associated and free POC may change, altering PE*eff* and T*eff* and potentially ocean atmospheric partitioning of CO_2 (Le Moigne *et al.*, 2012).

Remineralisation by heterotrophs

Cai *et al.* (2015) showed that the concentration of euphotic zone POC is not enough to control export alone; other factors such as aggregation, zooplankton repackaging and grazing and bacterial degradation must be important. Zooplankton and bacteria utilise sinking POC to support their metabolic demand (Steinberg *et al.*, 2008; Giering *et al.*, 2014).

Bacteria inhabit sinking detrital particles in much higher densities than free-living populations (Alldredge & Youngbluth, 1985). Lampitt *et al.* (1993) found that aggregates contained 1.4 - 4.3 x 10^5 bacteria per mm^3 in the upper 300 m of the Northeast Atlantic, at least one order of magnitude lower than free-living bacteria abundance (Li, 1998). Bacteria are able to hydrolyse the organic carbon by producing exoenzymes, with evidence that this is coordinated through quorum sensing (Gram *et al.*, 2002). Quorum sensing is the regulation of gene expression (such as for biofilm and antibody production) in response to cell-population density (Miller & Bassler, 2001). A modelling study showed this mechanism is useful as there is an abundance threshold of bacteria on aggregates at which producing exoenzymes is energetically beneficial for the whole group (Mislan *et al.*, 2014). It is estimated that 30 % of exported POC is remineralised by bacteria, which is a continuous processes (Buesseler & Boyd, 2009). However bacteria alone cannot explain the observed decrease in POC flux with depth.

Zooplankton have a slightly more complicated relationship with POC flux. They remineralise sinking POC through respiration, however they can also increase flux at depth through vertical migration and the egestion of FPs at depth.

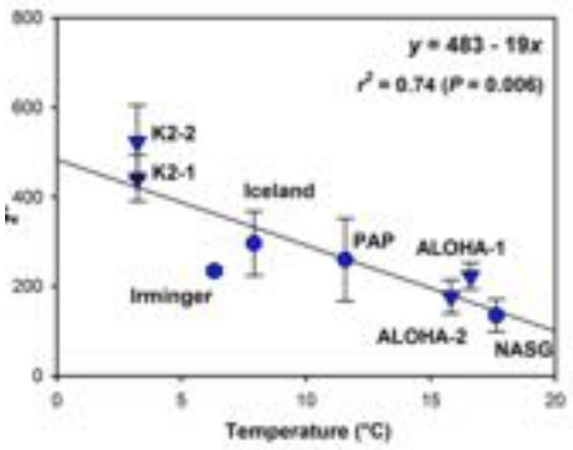

Figure 1.11: Median temperature (0 - 500 m) versus z^*. The inverted triangles are North Atlantic values and circles are North Pacific values. Error bars represent the standard error of z^* (Marsay *et al.*, 2015).

Zooplankton that actively migrate support up to 80 % of their metabolic carbon demand from surface production (Steinberg *et al.*, 2008) by transferring organic carbon from the surface to the mesopelagic zone. 40 % of organic carbon from an ingested particle is egested as a faecal pellet and the remainder lost through respiration and sloppy feeding (Buesseler & Boyd, 2009). However, zooplankton also consume sinking detritus and copepods have been shown to ingest faecal pellets even with other food sources available (Iversen & Poulsen, 2007). This is an important food source as no photoautotrophic production occurs in the mesopelagic zone (Steinberg, 1995).

Finally, physical variables such as sea temperature and oxygen concentrations affect the distribution and metabolism of both bacteria and zooplankton. For instance a recent study by Marsay *et al.* (2015) showed from *in situ* measurements that $z*$ (the remineralisation length scale, section 1.2) is negatively correlated with temperature. So where temperature is low, remineralisation occurs deeper and a higher proportion of particle flux reaches the deep ocean. This is hypothesised because remineralisation is slowed in colder waters (Marsay *et al.*, 2015).

In the MEDUSA model (see section 1.4.2) slow sinking particles are remineralised as a function of temperature, such that as temperature increases so does the remineralisation rate (Yool *et al.*, 2011). However fast sinking particles are remineralised as a function of ballasting. Lima *et al.* (2013) showed using a coupled physical-biogeochemical model that $z*$ is dependant on temperature, however at very low O_2 concentrations denitrification and lithogenic inputs be-

come important. This increases $z*$ in oxygen minimum zones (OMZs) (Lima *et al.*, 2013). This concurs with the study by Devol & Hartnett (2001), which compared an oxic and a sub-oxic site in the eastern Pacific and found decreased attenuation of POC flux in low O_2 regions, emphasising that low dissolved O_2 concentrations decrease remineralisation rates, thus more organic carbon reaches the seafloor.

1.5 Zooplankton dynamics

As discussed zooplankton are an important component in the biological carbon pump. They interact with particles throughout the water column; from grazing down phytoplankton at the surface to consuming particles and respiring dissolved inorganic carbon in the mesopelagic zone.

Zooplankton vary greatly in size and lifestyle. Some zooplankton are holoplanktonic meaning they spend their entire life cycle in the plankton whereas some are meroplanktonic eventually becoming sessile. Zooplankton are heterotrophic organisms with many feeding on phytoplankton in the upper sunlit water column. They can feed in many different ways; for instance some crustaceous zooplankton such as copepods are ambush feeders that actively find their prey whereas others such as appendicularians filter feed *via* a gelatinous web (Kiørboe, 2011).

Productivity cycles differ globally; micrograzers (2 - 200 μm length) and bacterioplankton constitute a greater portion of the mesozooplankton (0.2 - 20 mm length) food in the tropics than in polar and temperature regions (Fernández-Álamo & Färber-Lorda, 2006). This is because in tropical regions such as the Eastern Pacific the phytoplankton community are dominated by picophytoplankton (Olson & Daly, 2013) and temperate/polar regions by larger phytoplankton such as diatoms. As micrograzers feed on small particles, which are not efficiently utilized by mesozooplankton they make the production of nanno- and picoplankton accessible to higher order consumers (Landry & Hassett, 1982). In the Southern Ocean larger ($>$ 0.5 mm) zooplankton such as Calanoid copepods, krill and salps dominate the zooplankton community (Pakhomov & McQuaid, 1996).

A fraction of the carbon ingested by zooplankton will be egested as a faecal pellet (see section 1.3.2). These contribute to the export flux of particles out of the upper ocean and into the mesopelagic zone. In areas where zooplankton graz-

ing is high, increased fragmentation shallows the remineralisation depth and leads to faecal pellet-dominated, low POC fluxes (Ebersbach *et al.*, 2011). Often there is a temporal lag between peak primary production and export due to plankton speciation and zooplankton grazing, particularly in areas where seasonality exists such as the subtropical Pacific (Benitez-Nelson *et al.*, 2001).

Some zooplankton live deeper in the mesopleagic zone (> 200 m) either always residing here or migrating to surface waters on daily or seasonal timescales. The benefit of diel (daily) vertical migration (DVM) is to avoid visual predators whilst feeding (Gliwicz, 1986). As zooplankton consume phytoplankton and particles in the upper ocean at night they will egest faecal pellets, contributing to the flux. If they also egest FPs as they migrate back to deeper waters at dawn then these particles will escape the most intense areas of remineralisation in the upper few 100 m. Further zooplankton will continue to respire and excrete during the day releasing dissolved inorganic and organic carbon (obtained from the surface) into the mid-mesopelagic waters (Steinberg *et al.*, 2000). This is known as active flux. A nutrient-phytoplankton-zooplankton model estimated 27 % of export flux is a result of active transfer by zooplankton (Hansen & Visser, 2016). Seasonal migration also occurs because it is beneficial to some species of copepods to migrate below the permanent thermocline during winter months when food availability in the surface waters is low. To survive this the copepods produce large lipid stores during the spring and summer months and during winter slowly respire these, also releasing DIC into the deep ocean (Jónasdóttir *et al.*, 2015). This 'lipid pump' can release a similar amount of carbon (1-4 mg C m^{-2} d^{-1}) to the sinking flux (2 - 8 mg C m^{-2} d^{-1}) to depths of 600 - 1400 m in the North Atlantic (Jónasdóttir *et al.*, 2015).

1.6 Methods to estimate POC flux

1.6.1 Sediment traps

Sediment traps are likely the most commonly used equipment globally to collect and measure particle flux. Their use has been documented in aquatic science since the 1960s (Davis, 1968). Sediment traps are often either conical or cylindrical in shape and deployed on moorings at depths > 1000 m, surface-tethered or free-drifting. During the last few decades sediment traps have undergone various modifications to eliminate some of the biases associated with them, such as the

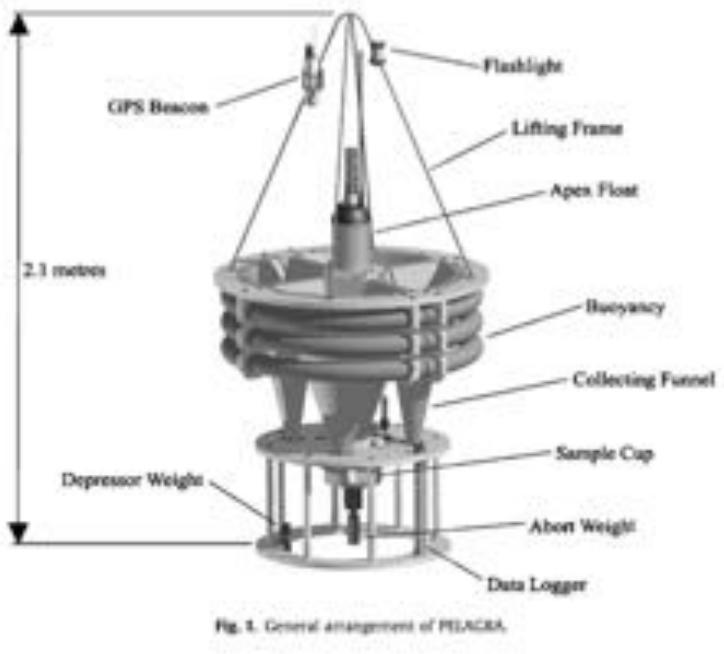

Figure 1.12: PELAGRA sediment trap (Lampitt *et al.*, 2008).

presence of swimmers, hydrodynamic biases and the solubilisation of particles (Buesseler *et al.*, 2007*a*).

The term 'swimmers' refers to zooplankton that can actively enter sediment traps and feed on the particles collected and/or produce faecal pellets (Buesseler *et al.*, 2007*a*). Therefore zooplankton can increase or decrease flux, although this is often more of a problem in shallower traps (< 1000 m) where zooplankton populations are larger. Zooplankton can be attracted to traps from the shear of the water or from oscillating mooring ropes that act as a feeding cue (Lampitt *et al.*, 2008).

One trap that is designed to eliminate the problem of swimmers is the indented rotating sphere trap (IRS). The particles are removed from contact with zooplankton by a rotating sphere, which can be programmed to collect particles based on sinking velocities (Peterson *et al.*, 2005). Once the sphere has rotated the sample carousel beneath rotates through 11 sample chambers over 24 hours at appropriate time intervals. This results in minimal settling rates for each sample tube between 0.68 and 980 m d^{-1} (Peterson *et al.*, 2005).

Another modification of a trap to avoid swimmers is the invention of neutrally buoyant sediment traps (NBSTs), such as PELAGRA (Particle Export measurement using a LAGRAngian trap (Lampitt *et al.*, 2008), Fig. 1.12). PELAGRA traps are neutrally buoyant with a compressibility close to seawater, so the trap

follows the motion of water. This reduces the number of zooplankton entering the trap as it has reduced shear and also reduces the hydrodynamic bias of particles entering. This allows PELAGRA to be deployed in shallower (< 1000 m) waters than traditional moored traps. PELAGRA deployments at the Porcupine Abyssal Plain site produced similar estimates of POC flux to those estimated by measuring new production (Lampitt *et al.*, 2008) and using marine snow catchers (section 1.6.3, (Riley *et al.*, 2012)).

1.6.2 Radionuclide

An alternative method to measure particle flux is using the radioactive disequilibrium between a naturally recurring particle-reactive daughter and its parent, such as ^{234}Th and ^{238}U (Thomalla *et al.*, 2006). Using radionuclides reduces the complex biological system to simple terms providing a measure of seasonal or daily average rates of carbon export (Buesseler *et al.*, 1992). One drawback is that you cannot use this method on the same time scale as sediment traps, e.g. for a year, as the particles are mostly collected *via in situ* Stand Alone Pumps (SAPs) on ship time. The pumps are deployed along a wire, often at multiple depths, and left in the water to pump water (1500 - 2000 L) over a few hours through > 53 μm and < 53 μm polycarbonate filters (Le Moigne *et al.*, 2012). An advantage of using ^{234}Th is its short half life (24.1 days) so particle fluxes can be estimated on timescales of days to weeks (Buesseler *et al.*, 1992).

To calculate POC flux vertical profiles of ^{234}Th activity are converted to estimates of downward ^{234}Th flux using a 1D steady state model and then converted to POC flux using measured POC/Th ratio (Le Moigne *et al.*, 2012). The POC/Th ratio is a crucial part of the method in calculating POC flux but is highly variable depending on the site, season, year or sampling method (Thomalla *et al.*, 2006). The ^{234}Th method is used frequently to look at the effect of ballasting minerals on POC flux (Thomalla *et al.*, 2008; Sanders *et al.*, 2010; Le Moigne *et al.*, 2013*c*, 2014), however if using SAPS it does not separate particles by sinking rate.

1.6.3 Marine Snow Catcher

This thesis presents only flux measurements made by Marine Snow Catchers (MSCs). These are large water bottles (95 or 300 L) with two detachable sections used to collect sinking particles from the water column (Lampitt *et al.*, 1993). They are deployed to depth one at a time with water passing through the bottle

on its descent. A messenger is fired which closes the bottle and it is left on deck upright for two hours allowing particles time to sink. It was designed by Richard Lampitt at the National Oceanography Centre, Southampton (NOC) and first used as part of the UK JGOFS programme in the Northeast Atlantic to estimate how much POC flux was actively transported (Lampitt *et al.*, 1993).

The basic principle of the MSC is to use it as a settling column; after a certain amount of time stood still, particles will settle out along different heights of the MSC depending on their sinking rates. Fast sinking particles are collected from the bottom of the base of the MSC, slow sinking particles from the base of the MSC and suspended particles are assumed to be spread out homogeneously throughout the MSC (Fig. 1.13, (Riley *et al.*, 2012)). Being able to separate particles by sinking speed is unique as most methods of estimating flux (e.g. sediment traps, SAPs) do not allow this kind of separation. Additionally, onboard experiments can be done on the particles collected, such as for sinking rates or particle respiration incubations. The importance of slow sinking and suspended particles in the biological carbon pump is largely ignored due to the reliance on sediment traps, even though metabolic activity in the interior ocean is closely linked to the suspended pool (Herndl & Reinthaler, 2013).

The MSCs were not used for a while after Lampitt *et al.* (1993) until Becquevort & Smith (2001) used them in the Ross Sea in the Southern Ocean to look at bacterial processes in the cycling of organic material. Becquevort & Smith (2001) used the previously described SETCOL (Bienfang, 1981) method (equation 1.3) to calculate sinking rates of the slow sinking particles, resulting in rates of 0 - 1 m d^{-1}. More recently Riley *et al.* (2012) used MSCs in the Northeast Atlantic at the Porcupine Abyssal Plain (PAP) site. They estimated slow sinking particle sinking rates of 9 m d^{-1} based on the height of the MSC and a homogeneous distribution of particles prior to settling. Fast sinking particle sinking rates were calculated by dropping particles collected from the MSC into a measuring cylinder filled with seawater and recording the time to sink between two discrete points. This gave average sinking rates of 200 m d^{-1}. POC fluxes were estimated to be 146 mg C m^{-2} d^{-1}, which was close to estimates from a PELAGRA trap deployed in parallel of 84 mg C m^{-2} d^{-1} (Riley *et al.*, 2012), emphasising the MSC can be a useful tool in estimating POC flux in the oceans.

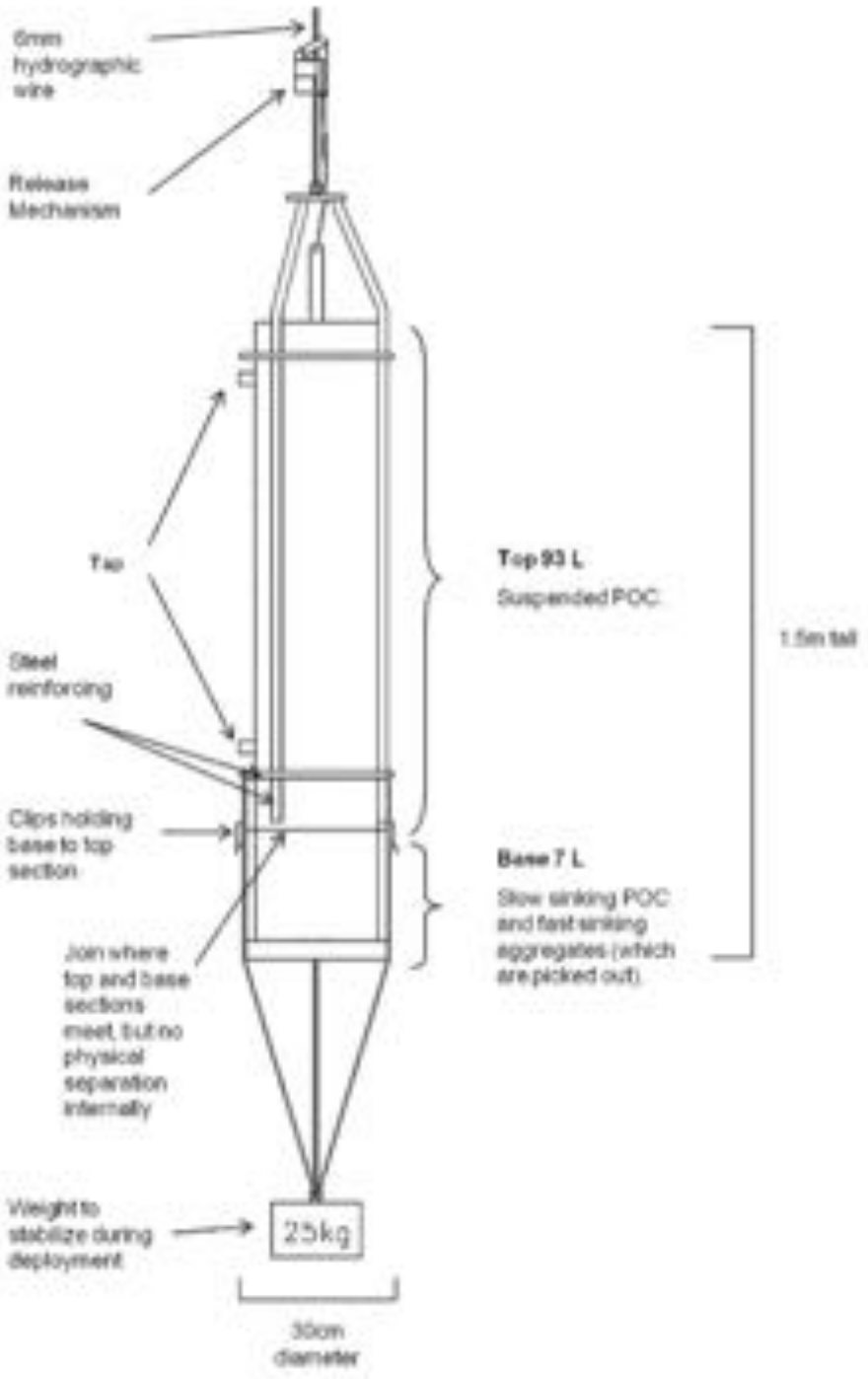

Figure 1.13: Schematic of a Marine Snow Catcher (Riley *et al.*, 2012).

Applicability of the Marine Snow Catcher

The main purpose of this thesis is to investigate processes within the biological carbon pump separately for slow and fast sinking particles. This distinction in sinking rate is often made in models but not with *in situ* measurements. Using marine snow catchers (MSCs) allows measurements of fast (> 20 m d^{-1}) and slow sinking (< 20 m d^{-1}) POC to be made separately, a unique tool.

As with all methods there are benefits and limitations. One of the main concerns is what happens inside the MSC during the 2 hour settling period. For instance zooplankton might consume and fragment particles as they come into contact with them, thus the particles are not in the same form as when collected. Some sediment traps fix particles as they settle into the base so they cannot be transformed, either using gels or chemicals which would be harmful to zooplankton. Adding gels or fixing agents would be difficult in the MSC due to its design and this has not yet been trialled. It is possible that zooplankton can avoid entering the MSC and they were only found to contribute to < 4 % of particle composition in the MSC. Therefore in this thesis it is assumed that during the settling time of the MSCs any change in particle composition abiotically or by zooplankton is not large enough to significantly alter particle sinking rates or flux.

Another issue is that deploying the MSC can be temperamental. It is closed by a manual messenger-release system which sometimes does not shut the MSC correctly and another deployment has to be made. Also the MSC can leak if the o-rings become dislodged during deployment, entailing an additional deployment. These problems are generally easily addressed onboard. What is more difficult to fix is if the MSC closes before the release is triggered, at a shallower depth than desired. This could be caused by too much movement or swinging on the wire when deploying or if the MSC is jolted vertically in the water by surface waves. Early closure can be noticed either on deck or after the MSC had been recovered and settled, by the very fast clogging of filters by biological particles. The best way to determine if the MSCs have collected water from the desired depth is by checking the temperature and salinity of the water with a TS probe.

A huge benefit of the MSCs is that individual particles can be collected and a whole suite of ship-board (or laboratory if frozen) experiments can be done such as: measuring sinking rates, microbial respiration, carbon, nitrogen and

phosphorous remineralisation, nitrification and lipid and isotopic composition. Further, it is possible to characterise the particles using microscopes, unlike with sediment traps where the particles have often aggregated together. Finally, flux measurements are instantaneous, rather than those integrated over a few days, weeks or months as with other methods. This makes high resolution temporal studies possible.

The MSC will feature heavily in this thesis as it gives instantaneous fluxes, allows the separation of particles by sinking rate and the opportunity for further experiments on collected particles.

1.7 Thesis aims and outline

The aim of this thesis is to further our understanding of processes in the upper ocean biological carbon pump as these influence atmospheric CO_2 levels; primarily particle export and remineralisation. It is important we understand how biological processes in the ocean operate now, so we may be able to model how they may be affected by global change. There are three main hypotheses for this thesis:

1. Particle export efficiency is positively related to primary production
2. Diel vertical migration by zooplankton strongly influences particle flux in the Southern Ocean
3. Zooplankton behaviour in oxygen minimum zones results in the high proportion of POC reaching the deep ocean.

Both particle export efficiency and the attenuation of POC have been computed in many flux studies. Some suggest using temperature is enough to estimate these parameters accurately, but does this apply ubiquitously in the ocean? Processes in the Southern Ocean often do not comply with simple algorithms used elsewhere. This project has the opportunity to study these processes in the Southern Ocean.

Both remineralisation and sinking rates affect the attenuation of POC flux, however obtaining sinking rates of particles can be challenging. Moreover only the sinking rates of fast sinking particles are typically measured; so in this thesis both the rates of fast and slow sinking particles will be measured and compared. This thesis will investigate what affects sinking rates of particles.

The dominant heterotroph responsible for remineralisation will be investigated: microbes or zooplankton. This research will be focussed in the Eastern Tropical North Pacific oxygen minimum zone where there are still uncertainties as to why the proportion of particle flux is so high at depth in low oxygen waters.

Additionally the type of particle will be determined and the proportion of each type quantified. For fast sinking particles this can be done *via* microscopy with simple classification into faecal pellets and phytodetrital aggregates. However, using organic geochemical techniques, this thesis will explore the composition of both fast and slow sinking particles in more detail.

Finally, *in situ* data from the Southern Ocean, equatorial Pacific and North Atlantic will be compared with an ecological model output. The aim is to test the role of zooplankton on the biological carbon pump efficiency and see if model parameters could be improved to achieve greater fidelity with observations.

This thesis has four result chapters:

Chapter 2: Particle export and flux attenuation in the Southern Ocean

Chapter 3: Remineralisation of organic carbon in a Pacific oxygen minimum zone

Chapter 4: Particle composition in the Eastern Tropical North Pacific

Chapter 5: The role of zooplankton in determining the efficiency of the biological carbon pump.

Chapter 2

Particle export and flux attenuation in the Southern Ocean

Note, this chapter was published by Cavan *et al.* (2015) in Geophysical Research Letters. Extra data on slow sinking and total sinking flux data have been added.

2.1 Overview

In this chapter Marine Snow Catchers were used to collect fast and slow sinking particles separately in the upper mesopelagic zone in the Southern Ocean. Particulate organic carbon (POC) fluxes were calculated for both sinking fractions and subsequently particle export efficiency and the attenuation coefficient Martin's *b*. These two parameters were used to determine what controls particle export and POC attenuation in the Atlantic sector of the Southern Ocean.

2.2 Introduction

The Southern Ocean (SO) accounts for ca. 20 % of the global ocean CO_2 uptake (Takahashi *et al.*, 2002; Park *et al.*, 2010). Although it can be a large source of CO_2 to the atmosphere as deep water, rich in CO_2, formed in the North Atlantic upwells in the SO (Barker *et al.*, 2003). The SO is a large high-nutrient-low-chlorophyll region (HNLC), likely due to limited iron availability (Martin, 1990). Nevertheless, iron from oceanic islands and melting sea ice can cause intense phytoplankton blooms, which may lead to high particulate organic carbon (POC) export (Pollard *et al.*, 2009). In the Scotia Sea (Atlantic Southern Ocean)

intense blooms form downstream from the island of South Georgia (Whitehouse *et al.*, 2012). This can lead to high export fluxes in this area (Schlitzer, 2002). Thus this HNLC area is more likely to affect atmospheric CO_2 levels compared to other HNLC regions globally (Falkowski, 1998).

Diatoms are thought to dominate the phytoplankton community composition in the SO (Arrigo *et al.*, 1999) and they are found in sediments from 20,000 years ago (Zielinski & Gersonde, 1997; Abelmann *et al.*, 2006), with *Phaeocystis sp.* being the next dominant group (DiTullio *et al.*, 2000). Zooplankton are abundant in the SO, particularly *Euphausia superba* (krill) who are prey for charismatic animals such as baleen whales, penguins and seals (Hill *et al.*, 2006). Copepods are important grazers in the SO ingesting up to 50 % of primary production daily (Gleiber *et al.*, 2015). Model results have suggested that zooplankton grazing may explain the low phytoplankton biomass in the SO during summer, rather than iron limitation (Le Quéré *et al.*, 2015). Due to their high abundances, both krill and copepod faecal pellets (FPs) are important in the SO biological carbon pump (Hopkins & Torres, 1989; Smith *et al.*, 2011; Sailley *et al.*, 2013; Gleiber *et al.*, 2015; Manno *et al.*, 2015; Rembauville *et al.*, 2015) as FPs can sink rapidly (300 m d^{-1}) through the mesopelagic zone (Atkinson *et al.*, 2012). Salps are also found in the SO and produce large, fast sinking FPs that contribute to export (Ducklow *et al.*, 2001).

Simple algorithms are sometimes applied globally, such as those describing the relationship between particle export efficiency (PE*eff*) and temperature or primary production ((Laws *et al.*, 2000), Chapter 1). Yet, these do not always apply in the SO (Maiti *et al.*, 2013; Le Moigne *et al.*, 2016). This raises questions as to whether other relationships hold in the SO, such as the latitudinal trend in T*eff* as described by Henson *et al.* (2012) and the ballasting hypothesis (Armstrong *et al.*, 2002). According to these theories, the SO with cold temperatures, high nutrients, diatom-dominated phytoplankton communities has a high PE*eff* but low T*eff*. This chapter will investigate if the upper mesopelagic zone in the SO conforms to these patterns and if it does experience high PE*eff* and low T*eff* (with T*eff* being expressed as the attenuation of POC).

The objectives of this chapter are to calculate PE*eff* and flux attenuation in the Southern Ocean, for both fast and slow sinking particles. For fast sinking particles the hypothesis is that PE*eff* will be high and flux attenuation will be low

in line with estimates by Armstrong *et al.* (2002) & Henson *et al.* (2012). Slow sinking particles are hypothesised to be rapidly remineralised in the mesopelagic, so are also expected to yield a low transfer efficiency (Riley *et al.*, 2012). The controls over both PE*eff* and flux attenuation will be identified using measurements of primary production, sea surface temperature and zooplankton abundance. Finally, the use of the SETCOL method (Bienfang, 1981) to estimate slow sinking rates of particles in the Marine Snow Catchers (MSCs) shall be described.

2.3 Methods

2.3.1 Cruise Location

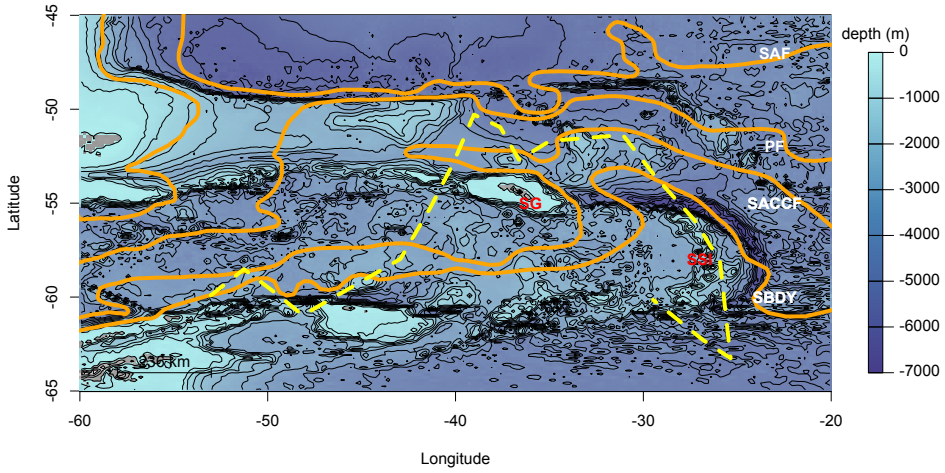

Figure 2.1: Cruise track (yellow dashed line) of JR274 in the Scotia Sea. Orange lines are fronts labelled in white, data from Orsi *et al.* (1995), SAF = Subantarctic Front, PF = Polar Front, SACCF = Southern Antarctic Circumpolar Front and SBDY = Southern Boundary of the SACCF. In red SG = South Georgia and SSI = South Sandwich Islands. Contours are bathymetry from NOAA database, Longitude is in ° E and Latitude ° N.

Observations were made in the Scotia Sea (Fig. 2.1) during the *RRS James Clark Ross* cruise JR274 (11 January to 5 February 2013) as part of the UK Ocean Acidification program. Many ecosystem studies have occurred in the Scotia Sea (Korb *et al.*, 2012; Tarling *et al.*, 2012; Venables *et al.*, 2012) however few estimates of export exist here (Le Moigne *et al.*, 2013*b*). The cruise track was south of the Polar Front but crossed the mean position and southern boundary of the Antarctic Circumpolar Current (Fig. 2.1). Stations south of 60 °S were in the seasonal ice zone (SIZ), and one station (# 12, > 15 % ice cover) was in the marginal ice zone (MIZ) (Tarling, 2013). 18 different stations were sampled close to 06:00 local time (Appendix Table A.1).

2.3.2 Phytoplankton Composition and Production

Samples for mixed layer chlorophyll *a* (chl *a*), biogenic silica, and primary production were taken using Niskin bottles mounted on a conductivity-temperature-depth (CTD) rosette sampler by other members of the scientific party, also from the National Oceanography Centre, Southampton (NOCS).

Chl *a* was measured by passing 0.2 L of seawater through a 0.7 μm glass fibre filter or 2, 5, 10, or 20 μm membrane filters (Whatman). Chl *a* was extracted in 90 % acetone overnight in a refrigerator and fluorescence quantified the following morning using a fluorometer (Turner Trilogy) calibrated with a solid standard and chl *a* extract. The chl *a* concentrations were averaged over the mixed layer. The mixed layer depth was determined subjectively from prior CTD (conductivity, temperature, depth) casts by the depth with the strongest gradients in temperature and salinity.

Biogenic silica concentration was measured by filtering 1 L of seawater through a 10 μm membrane filter, digesting it with sodium hydroxide, neutralizing with hydrochloric acid, and measuring the silicate concentration using an autoanalyzer (Brown *et al.*, 2003). Concentrations were averaged over the mixed layer.

Daily rates of primary production were measured following Poulton *et al.* (2014). Water samples (70 mL, 3 light, 1 formalin killed) from the middle of the mixed layer were inoculated with 28–30 μCi of ^{14}C-labelled sodium bicarbonate and either incubated for 24 h in chilled surface seawater with the light depth replicated using Misty-blue optical filters (LEETM) or in a refrigeration container (Richier *et al.*, 2014). The average relative standard deviation of triplicate (light) measurements was 20 % (2–51 %). Rates of primary production were integrated over the mixed layer.

2.3.3 Zooplankton

Zooplankton abundance was also measured by other members of the scientific party from the British Antarctic Survey, Cambridge. A motion-compensated bongo net system was deployed between 0 and 200 m at approximately 05:00 and 17:30 local time. The nets had a mesh size of 200 μm mesh and diameter mouth openings of 0.61 m (Ward *et al.*, 2012*a*).

Whole samples were examined, and moderately abundant, large, and /or rare taxa were enumerated. The sample was then split using a Folsom plankton splitter to provide total counts of 100 – 200 of the larger organisms (1/2 –

1/64) and 1 – 2 further splits for the smaller organisms (1/32 – 1/512), resulting in around 500 – 750 individual organisms per sample. Data from splits were standardized to per catch and then to individual m^2 using a calculation of mouth area multiplied by the vertical sampling interval (200 m). No flowmeters were used on the net as the slow hauling speed employed is at the bottom end of the calibration range for most flowmeters. 100 % sampling efficiency was assumed as no obvious clogging of the nets occurred.

2.3.4 Particle flux

Marine Snow Catcher sampling

The Marine Snow Catchers (MSCs) were deployed following the protocol laid out in Riley *et al.* (2012). MSCs were deployed to 10 m and 110 m below the mixed layer depth (MLD) (henceforth referred to as the export depth MSC (MSC_{Ex}) and the deeper MSC (MSC_D), respectively) at each station sampled. The MLD ranged from 20 to 70 m, and all deployments occurred around 06:00 local time. Once the MSC reached the required depth a messenger was used to close the device and it was immediately returned to deck. Only one MSC can be deployed at a time so MSC_D was deployed approximately 30 minutes after MSC_{Ex}. After recovery, 1 L of water was sampled from the bottom tap to represent a homogeneous distribution of particles (t_0). Then the MSCs were left to stand for 2 h, allowing the particles inside to settle.

After 2 h, 1 L of water was sampled from the base tap representing the suspended particles (t_2) and the tap was opened to drain away the water inside the top section. Once emptied, the top was removed and 1 L of water siphoned from the base to collect slow sinking and suspended particles (b_2). Most of the remaining water was siphoned out leaving the visible, fast sinking particles.

Fast sinking particles

Fast sinking particles visible to the naked eye were picked out from the MSC base using a Pasteur pipette (4 mm opening) and placed in well plates. Using a microscope (Olympus SZX16) at 100 x magnification the particles were classified as either phytodetrital aggregates (PDAs) or faecal pellets (FPs, Fig 2.2). Photographs (Canon T2-EOS) were uploaded to SigmaScan Pro 4, where PDAs were drawn around manually and the software then determined the equivalent spherical diameter of each particle. This was then converted to volume. For FPs the diameter and length were measured from the photographs to calculate vol-

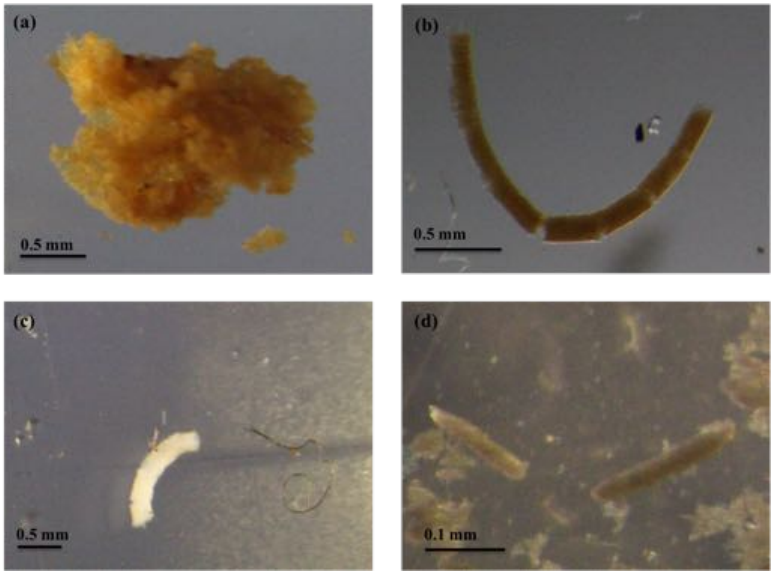

Figure 2.2: Images of fast sinking particles collected by the MSC a) Phytodetrital Aggregate (PDA), b) *Euphausiid sp.* brown faecal pellet (FP), *Euphausiid sp.* white FP and d) copepod FP. Black line is scale bar.

ume. Conversion factors from Alldredge (1998) were used to estimate the POC mass from particle volume:

$$\text{PDA POC } (\mu g) = 1.09 * v^{0.52} \tag{2.1}$$

$$\text{FP POC } (\mu g) = 1.05 * v^{0.51} \tag{2.2}$$

where v is the estimated volume of the particle in cubic millimetres.

Fast sinking particle sinking rates were measured using a glass measuring cylinder filled with seawater at *in situ* temperature (Riley *et al.*, 2012). Particles were individually placed a few inches above a marked point on the cylinder and the time for particles to pass between the two marked points was timed. Sinking rates were calculated by dividing the distance travelled by the time it took, and expressed as m d^{-1}.

Slow sinking particles

All 1 L water samples (t_0, t_2, b_2) collected from the MSC were filtered individually onto ashed (400 °C, overnight) 0.7 μm glass fibre filters (Whatman). The filters were dried and stored at room temperature until return to NOCS. The filters were acid fumed in hydrochloric acid overnight to remove inorganic carbon and ran on a CHN elemental analyser to determine the mass of POC. To determine the mass of slow sinking particles, the mass of POC sampled from the

top (t_2) was subtracted from the mass of POC in the base (b_2), as the base of the MSC contained both suspended and slow sinking particles.

Slow sinking rates

As briefly described in Chapter 1, sinking rates of particles too small to be seen by the naked eye can be estimated using the SETCOL (settling column) method (Bienfang, 1981). This uses the difference in biomass between the base of a settling column (here the MSC) and the biomass before settling with the time spent settling and height of the column to estimate an overall sinking rate for the column. One mean slow sinking rate is calculated per MSC deployment, not one for each particle. The equation is as follows:

$$w\ (m\ d^{-1}) = \frac{(V_s * b_s - V_s * b_0)}{(V_t * b_0)} * \frac{l}{t} \tag{2.3}$$

where V_s is the volume of the base of the settling column, V_t is the total volume, b_0 is the initial POC mass at the start of settling, b_s is the POC mass of the base settled after settling, l is the length of the column and t the settling duration. Applying this to the MSC and the samples collected from it forms this equation:

$$w\ (m\ d^{-1}) = \frac{(V_b * b_2 - V_b * t_0)}{(V_t * t_0)} * \frac{l}{t} \tag{2.4}$$

where V_s is the volume of the base of the MSC (8 L), V_t is the total volume (95 L), t_0 is the initial POC mass at the start of settling, b_2 is the POC mass of the base settled after settling, l is the length of the MSC (1.5 m) and t the settling duration (2 h). This equation initially yields sinking rates in m h^{-1}, which are converted to m d^{-1}. This method is used to calculate slow sinking rates throughout this thesis.

Particle flux calculations

POC sinking fluxes were calculated using a similar equation to Riley *et al.* (2012) but instead of using a sinking time of 2 h in the equation, the mean calculated sinking rate was converted to sinking time:

$$\text{Sinking time } (d) = \frac{l}{w} \tag{2.5}$$

where l is the height of the MSC (m) and w is the sinking rate m d^{-1}. For fast sinking particles this was 0.003 d, which was less time to sink than assumed by

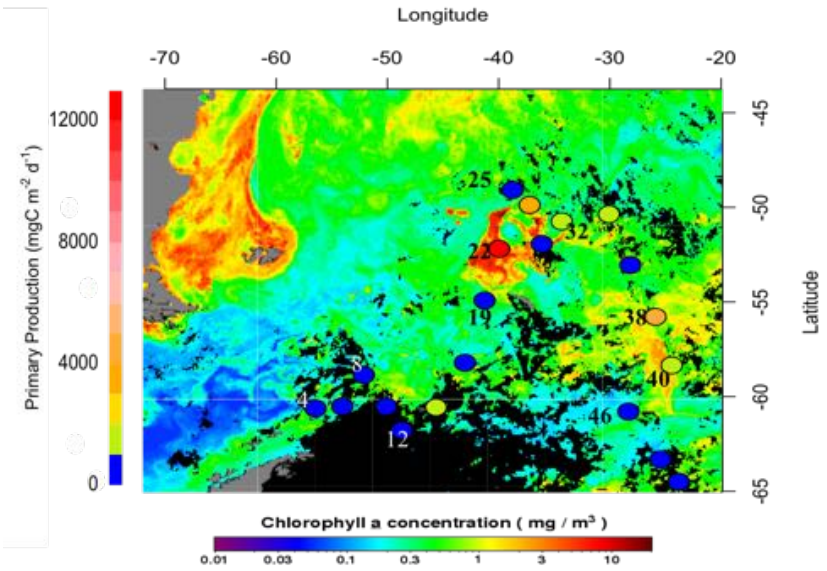

Figure 2.3: Satellite chlorophyll *a* image (Aqua Moderate Resolution Imaging Spectroradiometer from www.oceancolor.gsfc.nasa.gov, monthly composite for January 2013) with measured *in situ* primary production rates (circles). The numbers represent station numbers. Black represents cloud and sea ice cover. The continuous black coverage below station 12 is due to sea ice. Longitude is in ° E and Latitude ° N.

Riley *et al.* (2012) of 0.08 d. For slow sinking particles the mean sinking time was 1.7 d. The same equation was used to calculate fast and slow sinking POC fluxes:

$$\text{POC flux } (mgCm^{-2}d^{-1}) = m/a/t \tag{2.6}$$

where m is the mass of POC (mg, fast or slow sinking), a is the area of the base of the MSC (0.06 m^2) and t is the average time the particles took to sink (d, equation 2.5, fast or slow sinking). This equation is also used to calculate all POC fluxes in this thesis.

2.4 Results

2.4.1 Mixed Layer Plankton

Phytoplankton

Primary production showed a similar distribution to chl *a* (Pearson's product-moment correlation, r = 0.96, $p < 0.001$, n = 18), with peak values of > 12 g C m^{-2} d^{-1} north-west of South Georgia and > 4.5 g C m^{-2} d^{-1} north of the South Sandwich Islands (Fig. 2.3).

Peak total mixed layer chl *a* concentrations were also observed northwest of South Georgia (17 μg L^{-1}) and north of the South Sandwich Islands (11

Table 2.1: Averaged mixed layer Chl *a* concentrations, Primary Production (integrated over mixed layer) and Zooplankton abundance over 200 m.

Station ID	**Time** (local)	**Chl *a*** (μg L^{-1})	**PP** (mgC m^{-2} d^{-1})	**Zooplankton** (ind m^{-2})
6	08:45	1.05	935.99	35866
8	05:15	0.80	826.07	219026
10	07:00	0.87	431.10	37754
12	08:50	0.37	355.56	16195
16	06:30	0.98	584.71	300750
19	08:30	1.63	630.25	478393
22	06:45	16.90	12512.84	376310
25	06:50	1.00	997.48	282848
27	06:45	6.39	3621.28	467339
29	09:15	0.45	667.14	166726
32	06:45	2.78	1395.85	233370
34	06:45	4.11	1464.87	461288
36	06:40	0.83	269.23	222834
38	06:45	10.89	4563.46	103629
40	08:30	3.89	1616.60	69385
43	06:40	0.21	59.13	62864
44	06:45	0.94	409.86	45968
46	06:50	0.55	217.11	33796

μg L^{-1}, Table 2.1). These areas both had high (16 and 10 μg L^{-1}, respectively) concentrations of chl $a > 20$ μm and biogenic silica suggesting high concentrations of diatoms in these regions (Appendix Fig. A.1).

Zooplankton

Euphausiids were present in the study region, but net avoidance meant that no quantitative data on their abundance is available. Total zooplankton levels were low (< 15,000 ind m^2) in the SIZ and also at the South Sandwich Islands, even though chl *a* was relatively high (Table 2.1). Highest abundances (> 200,000 ind m^2) were generally found northwest of South Georgia.

2.4.2 Particulate organic carbon concentration

Total POC concentration ranged from 40 μg L^{-1} at station 19 near South Georgia to 358 μg L^{-1} at station 38 near the South Sandwich Islands (Appendix Tables A.2 and A.3). POC concentration from the MSCs at both depths was significantly correlated with mixed layer chlorophyll ($p < 0.05$, $r = 0.5$ and $p < 0.01$, $r = 0.6$). POC concentration was significantly higher at MSC_{Ex} than MSC_D ($t = -2.5$, $p < 0.01$) with total means ($\pm$ standard error of the mean) of 152 ($\pm$ 14) and 84 ($\pm$ 17) μg L^{-1} respectively (Fig. 2.4). This was due to significant decreases in the suspended fraction, with no significant change in

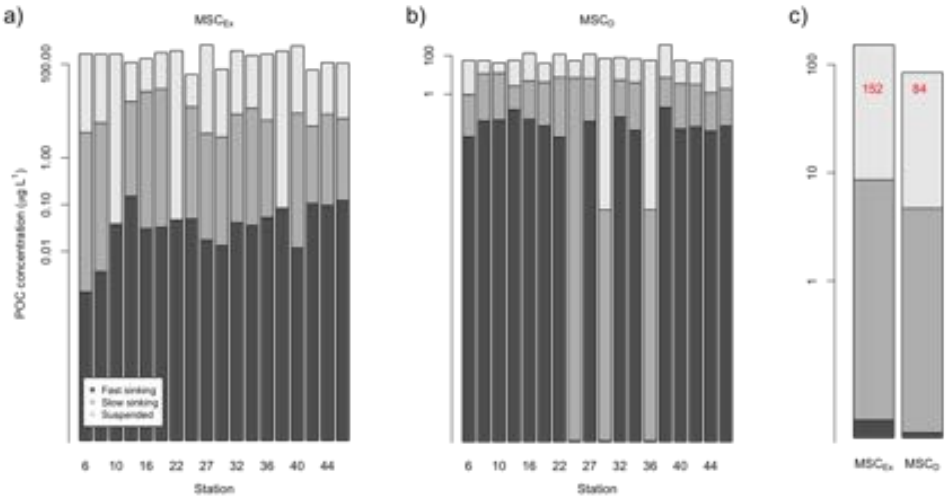

Figure 2.4: POC concentration of all stations from a) MSC_{Ex}, b) MSC_D and c) the mean at both MSC_{Ex} and MSC_D. Red numbers on c) are total concentration (μg L^{-1}). Note the log scale on the y-axes. Fast sinking particle concentrations are in dark grey, slow sinking mid-grey and suspended particles light grey.

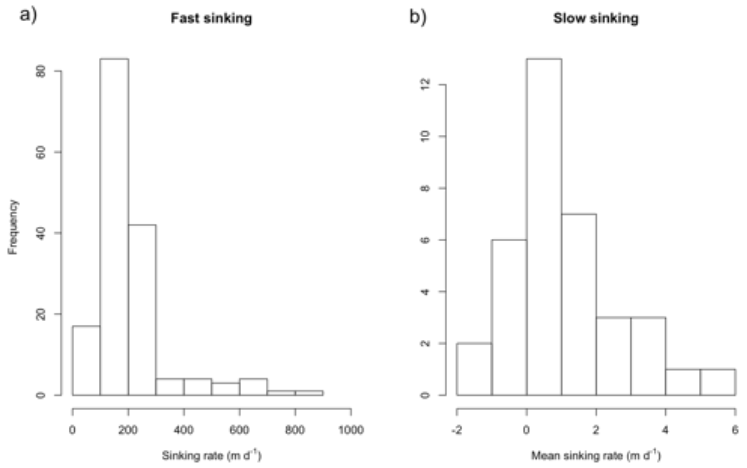

Figure 2.5: Particle sinking rate frequency distribution for a) fast sinking rates and b) mean estimate for slow sinking particles, at all stations.

either the slow or fast sinking POC concentrations. The absence of fast sinking POC concentrations at 3 stations in Fig. 2.4 b is a limitation of using the human eye to pick out particles.

The largest fraction of POC by concentration was the suspended, followed by the slow sinking and then the fast sinking with at least an order of magnitude between each fraction. At some stations there was no slow or fast sinking POC (Fig. 2.4). No observation of slow sinking POC occurs when there is a greater mass in the top of the MSC than in the base. This suggests particles are positively buoyant and therefore rising.

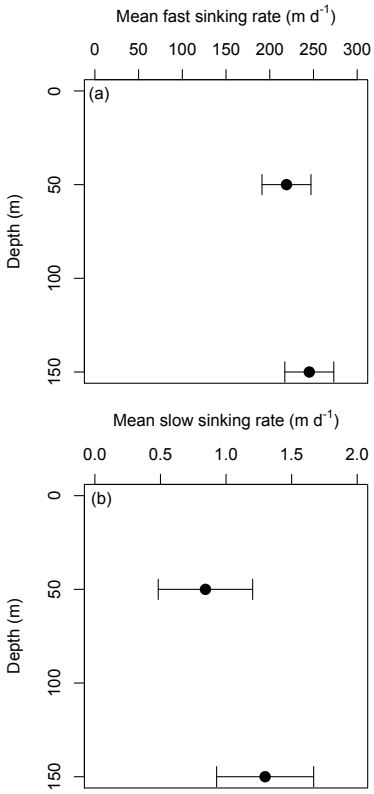

Figure 2.6: Particle sinking rates with depth for a) fast sinking and b) slow sinking particles. Error bars are standard errors of the mean.

2.4.3 Particle sinking rates

Fast sinking particles

The fast sinking rates of 161 particles were measured, 37 of these were phytodetrital aggregates (PDA) and 124 were faecal pellets (FPs). Fast sinking rates ranged from 50 to 828 m d^{-1} (Fig. 2.5), with one particle sinking at 6480 m d^{-1} . This sinking rate was removed from analysis as an anomaly, as it was greater than the mean ± two standard deviations. PDAs sank statistically faster than FPs (t-test, df = 41, $p < 0.05$) with mean (± standard errors of the mean) rates of 268 (± 33) and 188 (± 10) m d^{-1} respectively. Most (76 %) particles sank between 100 - 300 m d^{-1} (Fig. 2.5). There was no significant (t-test, $p > 0.05$) change in fast sinking rate with depth (Fig. 2.6), although the mean sinking rate increased from 219 to 245 m d^{-1}.

Slow sinking particles

As described in section 2.3.4 only one average sinking rate for each MSC deployment can be calculated when using the SETCOL method. Estimated mean slow sinking rates ranged from -1.5 to 5 m d^{-1} (Table 2.2). Negative sinking rates show there were more rising particles than sinking. 6 negative rates were observed at MSC_{Ex} compared to just 2 at MSC_D. Most particles sank

Table 2.2: Fast and slow particle sinking rates at export depth (MSC_{Ex}) and deep depth MSC_D.

	MSC_{Ex}			MSC_D		
Station	**Depth**	**Fast sink**	**Slow sink**	**Depth**	**Fast sink**	**Slow sink**
ID	(m)	(m d^{-1})	(m d^{-1})	(m)	(m d^{-1})	(m d^{-1})
6	50	NA	1.16	150	125.77	0.99
8	50	NA	0.49	150	200.98	4.86
10	25	147.00	-0.76	125	124.38	5.09
12	75	187.70	3.48	175	183.82	1.54
16	50	426.58	3.71	150	185.39	0.83
19	50	331.33	-0.95	150	457.14	0.08
22	75	132.01	0.25	175	109.41	0.76
25	75	199.39	1.49	175	NA	3.33
27	50	50.49	-0.74	150	447.79	1.29
29	75	NA	2.12	175	NA	1.34
32	50	105.48	0.94	150	349.39	0.35
34	50	NA	0.66	150	293.33	2.33
36	50	462.34	-1.03	150	NA	0.26
38	50	NA	2.50	150	NA	0.08
40	50	NA	-0.37	150	NA	0.22
43	50	222.91	1.78	150	327.31	-0.14
44	50	145.28	1.96	150	138.01	-0.66
46	25	NA	-1.52	125	NA	0.80

between -1 to 2 m d^{-1} (Fig. 2.5).

As with fast sinking particles there was no significant difference in slow sinking rates with depth, although the mean sinking rate did also increase from 0.8 m d^{-1} at MSC_{Ex} to 1.3 m d^{-1} at MSC_D (Fig. 2.6).

2.4.4 Particulate Organic Carbon Flux

Fast sinking POC fluxes ranged from 0 to 91 mg C m^{-2} d^{-1}, with the maximum flux observed at MSC_D at station 12 in the MIZ (Fig. 2.8 b); this was due to high FP fluxes, which increased at depth at this station, but not in the other stations south of 60 °S (Figs. 2.8 c & d). FP fluxes ranged between 0 and 78 mg C m^{-2} d^{-1}. The PDA flux was much smaller, only ranging from 0 to 36 mg C m^{-2} d^{-1} (Figs. 2.8 e & f), with most PDA fluxes decreasing with depth. The FP flux was strongly correlated (Pearson's product-moment correlation) with the total fast sinking mass at both depths (MSC_{Ex}, $r = 0.92$, $p < 0.001$, $n = 19$; MSC_D, r

Table 2.3: Fast and slow sinking POC fluxes at MSC_{Ex} and MSC_D.

	MSC_{Ex}			MSC_D		
Station	**Depth**	**Fast flux**	**Slow flux**	**Depth**	**Fast flux**	**Slow flux**
ID	(m)	(mg C m^{-2} d^{-1})	(mg C m^{-2} d^{-1})	(mg C m^{-2} d^{-1})	(mg C m^{-2} d^{-1})	
6	50	0.79	3.90	150	3.59	0.91
8	50	2.16	2.66	150	24.06	54.75
10	25	22.54	0.00	125	26.58	59.99
12	75	87.61	52.98	175	90.89	3.73
16	50	17.89	93.45	150	28.62	3.86
19	50	19.17	0.00	150	12.98	0.27
22	75	27.51	0.00	175	1.76	5.46
25	75	28.87	17.62	175	0.00	22.64
27	50	10.23	0.00	150	22.47	8.44
29	75	7.79	5.68	175	0.00	0.00
32	50	23.95	7.71	150	38.15	1.83
34	50	20.93	7.31	150	7.61	9.03
36	50	30.76	0.00	150	0.00	0.00
38	50	2.23	0.00	150	13.82	0.56
40	50	2.68	0.00	150	9.07	0.74
43	50	61.52	7.96	150	11.74	0.00
44	50	55.96	16.08	150	7.00	0.00
45	25	67.30	0.00	125	12.79	1.47

= 0.90, p < 0.001, n = 19). However, correlations between PDA flux and mass, although significant (p < 0.05), were not as strong (MSC_{Ex}, r = 0.48, n = 19; MSC_D, r = 0.49, n = 19) highlighting that FPs drove much of the variability in POC flux. The proportion of total POC flux due to FPs was 66 – 100 % in the SIZ and MIZ and 0 – 68 % at South Georgia and the South Sandwich Islands. At half the stations fast sinking POC flux increased with depth. High FP export was observed in the SIZ (stations 43–46) and the MIZ at MSC_{Ex} (Figs. 2.8 c & d) even though total zooplankton abundance was low in this region. Antarctic krill (*Euphausia superba*) were most likely responsible for this high FP export as throughout the sampling region, 82 % of the FPs were of Euphausiid origin, the remainder being recognisable copepod pellets (Figs. 2.2 b-d). There was an increase in FP flux at MSC_D relative to MSC_{Ex} in the MIZ, whereas in the SIZ, there was a large decrease in FP flux with depth. This pattern was not reflected in the PDA flux.

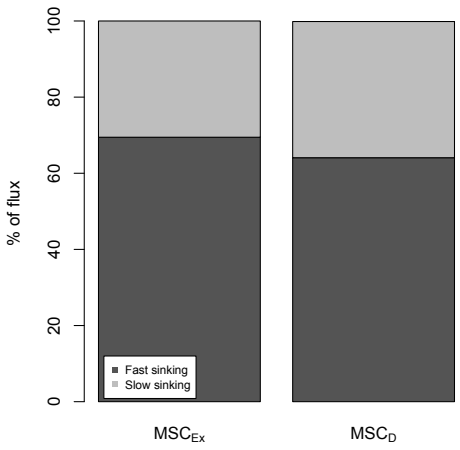

Figure 2.7: Percentage contribution of fast (dark grey) and slow (light grey) sinking particles the total sinking flux.

Slow sinking POC fluxes ranged from 0 to 93 mg C m^{-2} d^{-1} (Figs. 2.8 g & h), which is similar to the fast sinking POC flux range. However most (ca. 95%) of the slow sinking fluxes were less than 60 mg C m^{-2} d^{-1}. Even with this large range, on average the slow sinking flux was only 1/3 of the total sinking flux at both depths (Fig. 2.7). Also at over half the stations slow sinking POC flux increased with depth.

2.5 Discussion

2.5.1 Mixed layer ecosystem

The cruise track crossed low and high areas of primary production (PP) with highest PP (12 g C m^{-2} d^{-1}) near the oceanic islands of South Georgia and the South Sandwich Islands (Fig. 2.3). This suggests terrestrial iron inputs could be stimulating the phytoplankton blooms (Gilmartin *et al.*, 1974; Jones *et al.*, 2012). In the MIZ (station 12) and SIZ (stations 43 - 46) PP was low (< 1 g C m^{-2} d^{-1}).

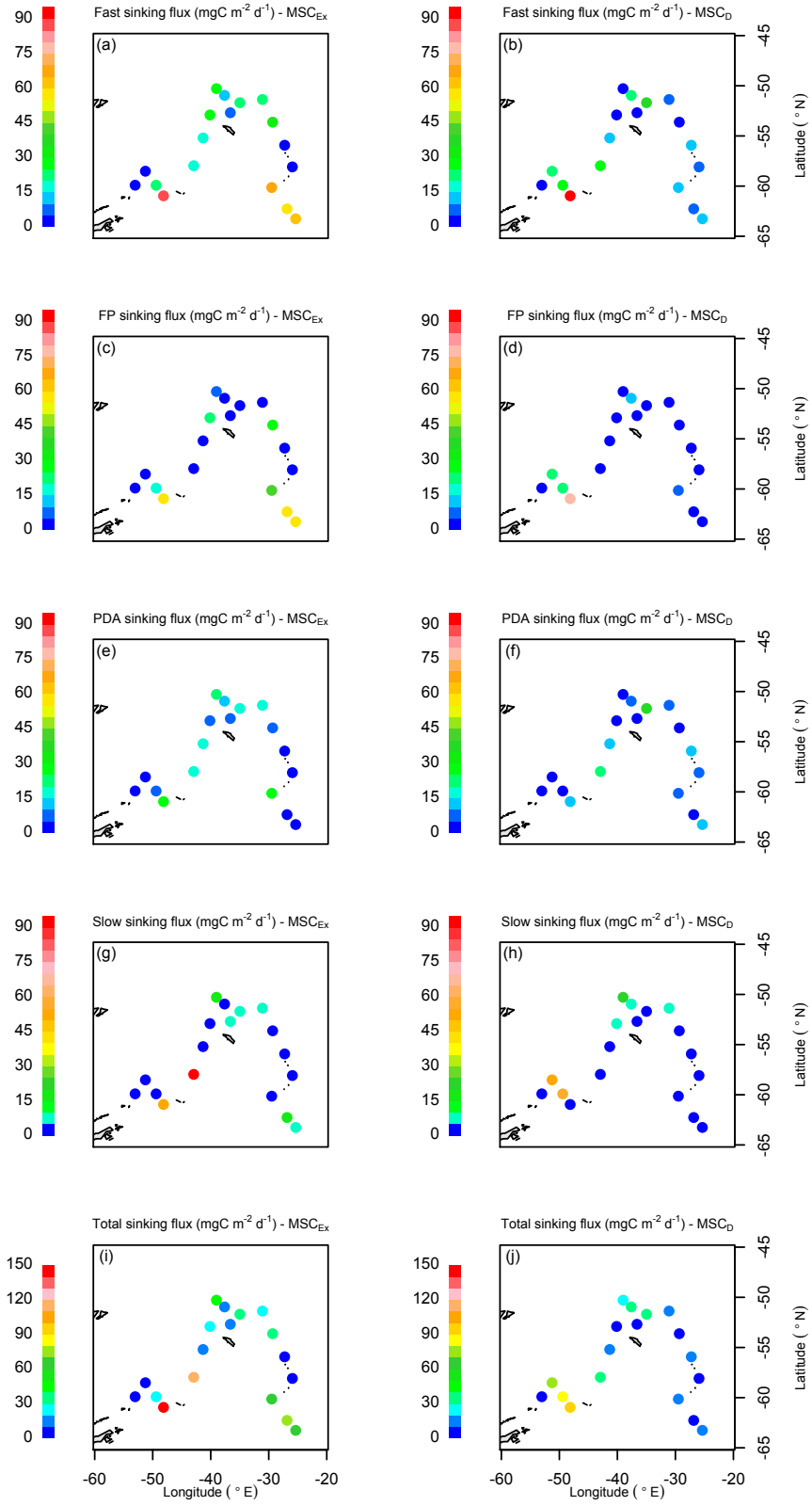

Figure 2.8: Geographical distribution of POC flux (mg C m^{-2} d^{-1}) at the export depth (left column) and 100 m below it (right column).

Zooplankton catches were numerically dominated by Cyclopoid copepods (Appendix Fig. A.1), which may have a role in the degradation and remineralisation of faecal pellets (Gonzalez & Smetacek, 1994; Iversen & Poulsen, 2007). Calanoid copepods were the next most abundant taxa including many species known to graze on phytoplankton and to perform DVM (Atkinson *et al.*, 1992). Highest zooplankton abundance (< 500,000 ind. m^{-2}, Table 2.1) was observed north-west of South Georgia at station 19, which had the second highest primary production rates. Around the South Sandwich Islands where PP was high, zooplankton abundances were much lower (100,000 ind. m^{-2}). These mismatches between phytoplankton and zooplankton abundance may be due to the dynamics of sea ice retreat in this region (Clarke & Peck, 1990) and/or the seasonal vertical migrations of late-stage copepodites ascending into surface waters after spending the preceding winter at depth (Tarling *et al.*, 2004). Low estimates of zooplankton abundance occurred in the MIZ and SIZ however this may be due to the lack of *Euphausiid sp.* represented in the samples.

2.5.2 Comparison of flux estimates

The POC concentrations measured at both depths were very similar to those measured by Riley *et al.* (2012) using MSCs at the Porcupine Abyssal Plain, in the North Atlantic; where there was an order of magnitude difference in the concentrations of the different particle fractions. In this study suspended particles contributed on average to 94 % of the total POC concentration, slow sinking particles 5.5 % and the fast sinking the small remainder. Fast sinking particles sank at 200 m d^{-1} with no influence of depth on sinking rate even though it is hypothesised that with increasing depth sinking rates decrease due to increasing density (Bach *et al.*, 2012). Other mean estimates of fast sinking particles range from 25 - 326 m d^{-1} (Asper, 1987; Alonso-Gonzalez *et al.*, 2010; McDonnell & Buesseler, 2010; Riley *et al.*, 2012). Sinking rate is a continuous measurement and thus there is no cut off of when a particle is slow or fast sinking. However, the minimum fast sinking rate measured in this study was 50 m d^{-1} and the maximum slow sinking rate was 5 m d^{-1}.

This study is the first to show net negative sinking rates of exported slow sinking particles. As the SO is often dominated by diatoms it is possible they could be responsible as they are known to exhibit positive buoyancy (Villareal, 1988). The MSCs have previously been used as settling columns following the SETCOL

method (Bienfang, 1981) in the Ross Sea by Becquevort & Smith (2001), however they didn't report any negative sinking rates. This could be due to high abundance of *Phaeocystis sp.* in their sampling area. The mean sinking rates of both fast and slow sinking particles were used in the flux equations instead of assuming all particles settled at 9 m d^{-1}, which was assumed by Riley *et al.* (2012).

There was high variability of POC flux in the upper ocean in the Scotia Sea; where at half of the stations flux increased with depth for both slow and fast sinking particles (Fig. 2.8). In studies using sediment traps it is not possible to measure the flux of slow sinking particles separately. However in this study maximum values of fast and slow sinking POC flux were the same (Figs. 2.8 b & g). Interestingly all stations within the SIZ and MIZ had high export fluxes but in the SIZ, sampled at the end of the cruise, there was a large decrease in flux whereas in the MIZ (station 12) there was an increase in flux. This suggests the presence or absence of sea-ice may affect fluxes. This will be further discussed in section 2.5.5.

The total MSC-derived estimates of POC flux (2 - 140 mg C m^{-2} d^{-1}, Figs. 2.8 i & j) are consistent with other measurements in the region. For example, Ducklow *et al.* (2008) measured fluxes of 12 – 120 mg C m^{-2} d^{-1} using moored sediment traps at the Western Antarctic Peninsula, whilst Planchon *et al.* (2013) calculated fluxes of 11 – 61 mg C m^{-2} d^{-1} using the ^{234}Th method in the Atlantic Southern Ocean. Finally, Salter *et al.* (2007) measured fluxes of 28 – 46 mg C m^{-2} d^{-1} using the drifting sediment trap Particle Export measurement using LAGRAngian sediment traps (PELAGRA) at the Crozet Plateau. The comparability of MSC fluxes to those from other approaches indicates that the MSC is a robust method for estimating POC flux.

2.5.3 Export From the Mixed Layer

The ratio of the exported flux out of the mixed layer to primary production (PP) within the mixed layer (PE*eff*) is a useful tool to assess how efficiently particles are being exported. Highest values of PE*eff* were observed in the MIZ and SIZ (0.25 - 0.4, Figs. 2.9 a & c) rather than in the highly productive, opal-dominated blooms (Appendix Fig. A.1), which are often thought to be hot spots of carbon export in the SO (Korb *et al.*, 2012). This suggests that diatoms were not directly important for export flux, but they may have been important

indirectly following consumption by zooplankton and the subsequent production of zooplankton FPs. Station 43 is not included in this analysis as PE*eff* was > 1 for the fast sinking and total fluxes, which suggests more particles were exported than produced in the mixed layer.

Previously, high (< 0.3) values of PE*eff* were measured off the western Antarctic Peninsula by Buesseler *et al.* (2010). PE*eff* reached a maximum of 0.4 in this study (Fig. 2.9 c), which is similar to the maximum values reported by Henson *et al.* (2012). However, the total sinking mean value across the study region was much lower at 0.14 ($\pm$ 0.07 standard error of the mean). This shows these observations from the Scotia Sea do not conform to the generalisation that particle export efficiency is high across the SO (Armstrong *et al.*, 2002; Henson *et al.*, 2012).

Previous work has revealed a positive linear relationship between primary production and PE*eff* (Laws *et al.*, 2000). This data instead shows that a negative inverse relationship between primary production and PE*eff* was observed for both the fast sinking and total flux (Fig. 2.9), a pattern also recently reported by Maiti *et al.* (2013) in the SO. Maiti *et al.* (2013) observed a linear relationship between primary production and PE*eff*; however, in this study, a non-linear power function best fitted the data ($r = 0.75$, $p < 0.01$, $n = 18$; Fig. 2.10).

$$\mathrm{PE}eff = 538 * e^{-3.3LogPP} \tag{2.7}$$

An inverse relationship between PE*eff* and primary production means that a high fraction of primary production is exported when primary production is low. This could be due to temporal decoupling between primary production and export (Salter *et al.*, 2007), which may account for up to 60 % of the variability in the relationship between PE*eff* and primary production (Henson *et al.*, 2015). Alternatively, seasonal dynamics of the zooplankton community may explain this variation. For instance, many Calanoid copepods overwinter at depth and arrive in the surface layers in advance of the bloom (Tarling *et al.*, 2004), and the same may also apply to Antarctic krill (Kawaguchi *et al.*, 1986). Discarded moults, natural mortality, and predation mortality from this overwintering community will enhance POC levels independently of phytoplankton blooms (Kobari *et al.*, 2008). A further alternative proposed by Maiti *et al.* (2013) is that processes like zooplankton grazing, heavy remineralisation, and a large export of dissolved

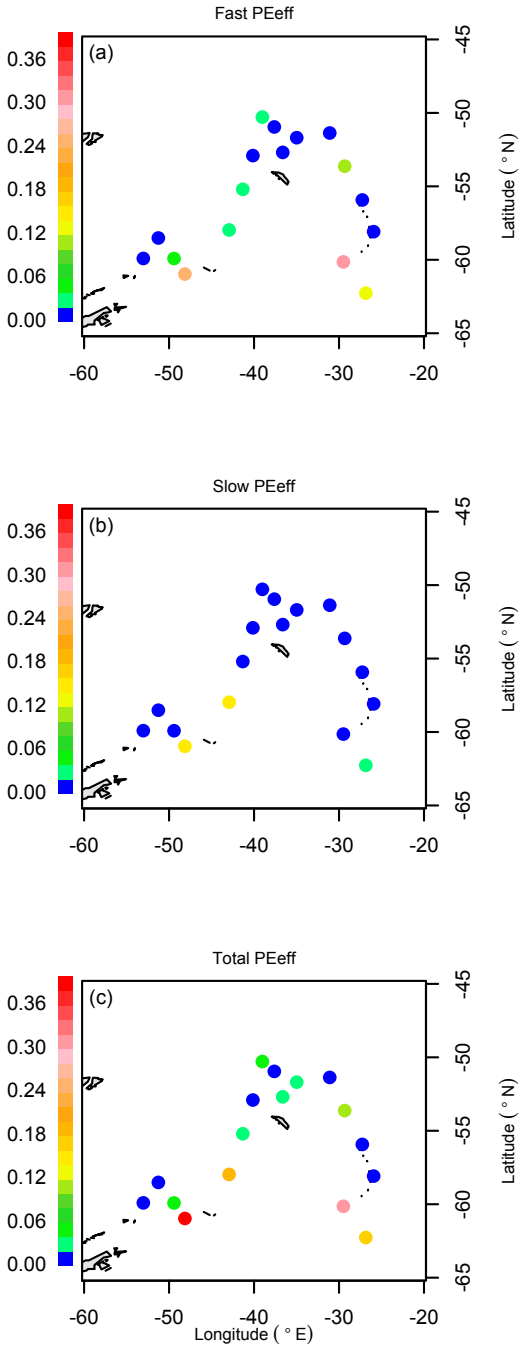

Figure 2.9: Geographical distribution of PE*eff* for a) fast b) slow sinking particles and c) the total sinking flux.

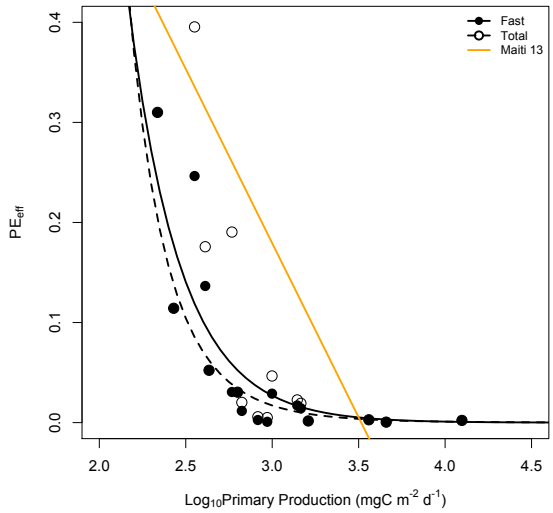

Figure 2.10: PE*eff* against the $\log_{10}$ of primary production (mg C m^{-2} d^{-1}). Solid circles and black line is fast sinking PE*eff* and open circles and dashed line is the total PE*eff*. Both black lines are a power law function and the orange line is the Maiti *et al.* (2013) regression. Slow sinking PE*eff* was not significantly related to primary production.

organic carbon all contribute collectively to produce this relationship.

Zooplankton grazing could be a significant factor due to the varying stability of phytoplankton growth in the SO. Primary production in the SIZ is stable, whereas further north in the open water seasonal variation is large. Here steep primary production gradients exist, which are caused by the influence of eddy-mediated cross frontal mixing, transporting nutrients and increasing chl *a* (Kahru *et al.*, 2007; Dulaiova *et al.*, 2009). Thus, zooplankton grazers can develop and graze down phytoplankton in the SIZ, whereas in the open water, the grazers do not develop quickly enough in response to a bloom to have a significant effect on primary production (Fig. 2.10). Therefore, to assess if the presence of zooplankton could further explain this relationship the residuals ($Residuals^2$) between the best fit line and the data points in Fig. 2.10 were calculated and compared with zooplankton abundance (Z). This showed that zooplankton abundance (equation 2.8 and Fig. 2.11) explained 40 % ($p < 0.01$) of the variance between primary productivity and PE*eff*.

$$Residuals^2 = 5 * Z^{-1.1} \tag{2.8}$$

Although grazing probably does not dictate the overall shape of the relationship between fast sinking PE*eff* and primary production, for the first time there

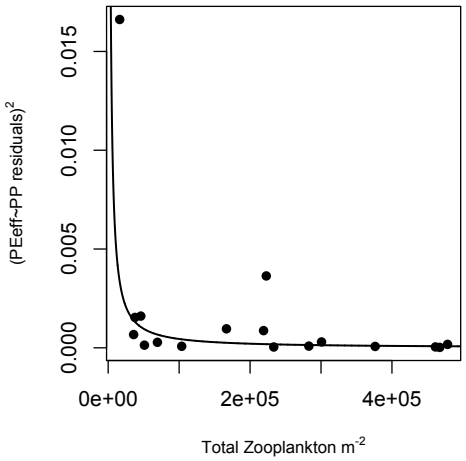

Figure 2.11: Residuals^2 from the regression of fast sinking PE*eff* *vs.* primary production (Fig. 2.10) against the total zooplankton abundance (ind m^{-2}). The data point with the highest residuals is the in the MIZ.

is clear evidence of its capacity to modulate this relationship and the importance of zooplankton in transferring organic carbon from the surface to the interior Southern Ocean.

2.5.4 POC Transfer Through the Upper Mesopelagic Zone

Once exported from the mixed layer, POC sinks into the ocean's interior where it is utilized by heterotrophs, reducing the size of the sinking flux with depth (Martin *et al.*, 1987; Steinberg *et al.*, 2008; Giering *et al.*, 2014). At six stations total sinking POC flux increased with depth, but this increased to almost 50 % of stations when separating fluxes into fast and slow sinking particles.

Therefore the power function of Martin *et al.* (1987) was fitted to the data to quantify the decrease in POC flux with depth, rather than z^*, so negative, non-dimensional b values represent increases in flux with depth. Negative z^* (m) values give the height of remineralisation of particles above the depth they were exported from, which may be into the atmosphere. Therefore using b makes much more sense in this context.

Fast sinking b ranged from -2.7 to 3 with a mean of 0.16 ($\pm$ 0.4) (Fig. 2.12 a). This implies an overall negligible attenuation of POC flux (and thus high (> 1) T*eff*) in the upper mesopelagic of the Scotia Sea, which only increased to 0.26 ($\pm$ 0.6) (Fig. 2.12 c) with the addition of the slow sinking fluxes (Fig. 2.12 b). Negative b values (increasing POC flux with depth) may be due to lateral advection at depth, flux integration time scales, or zooplankton DVM. Lateral

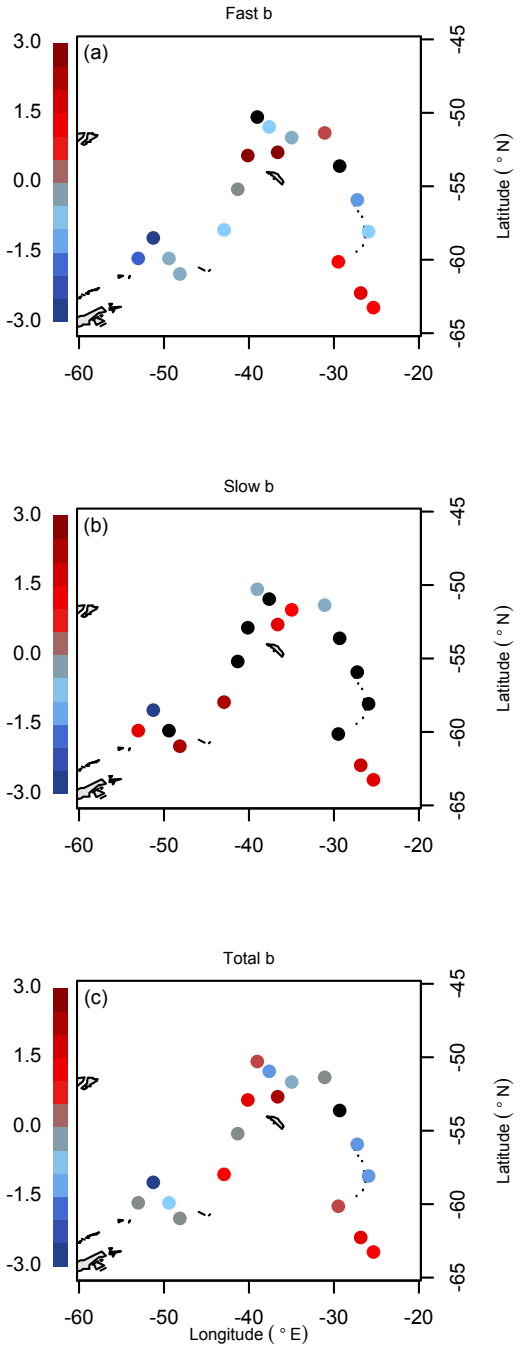

Figure 2.12: Geographical distribution of Martin's b for a) fast b) slow sinking particles and c) the total flux. Black points show areas where there was no quantified export flux.

advection is unlikely to have driven the observed increased fluxes at depth, as MSC deployments were < 175 m and therefore all within the single water mass classified as surface water by Heywood & King (2002), which occurs < 200 m between 45 and 65 ° S. Additionally, as FPs dominated the flux (see section 2.4.4), any pulse of flux in phytoplankton such as diatoms, which can occur in the SO (Salter *et al.*, 2012), would have had a limited effect on b. Therefore, it is assume that this interpretation of fluxes is correct, and possible controls of b, including DVM, are discussed in the following section.

2.5.5 Controls Over Mesopelagic Flux Attenuation

Mesopelagic POC attenuation is a key metric of the BCP (Buesseler & Boyd, 2009) and is linked to the amount of CO_2 stored in the interior by biological processes (Kwon *et al.*, 2009). b expresses the proportion of export flux that reaches the deep ocean. Unlike PE*eff* there was no significant effect of primary production on b (Pearson's product-moment correlation, $p > 0.05$, $n = 15$), suggesting that PP is unlikely to control variability in mesopelagic remineralisation. Given that flux was dominated by FPs (Figs. 2.8 c & d), and there is evidence from these results that the distribution of transfer efficiencies is linked to sea ice (a major distinguishing factor for ecosystems in the SO (Ward *et al.*, 2012*b*; Murphy *et al.*, 2013)), the hypothesis that zooplankton processes are involved was tested, and that these may change with sea ice cover. Sea ice retreat increases the vertical stability of the water column so phytoplankton can remain in the water column longer (Taylor *et al.*, 2013), and a pulse of flux often occurs after sea ice retreat (Ducklow *et al.*, 2008). The ratio of shallow FP flux to deep FP flux (the FP flux ratio) was calculated and plotted these against b (Fig. 2.13 a). The change in FP flux ratio is highly significantly related to the attenuation of POC (b) *via* an exponential regression ($r = 0.99$, $p < 0.001$):

$$\text{FP flux ratio} = -0.83 + 2.28e^{(1.1*b)} \tag{2.9}$$

No significant relationship exists between a similarly calculated PDA flux ratio and POC attenuation (b), again highlighting the important role of zooplankton in controlling the transfer of POC to depth in the Southern Ocean.

Zooplankton can cause depth variability in flux *via* the active transfer of organic carbon due to DVM (Wilson *et al.*, 2008). Zooplankton consume organic matter in the surface layer and then descend prior to releasing a fraction of it

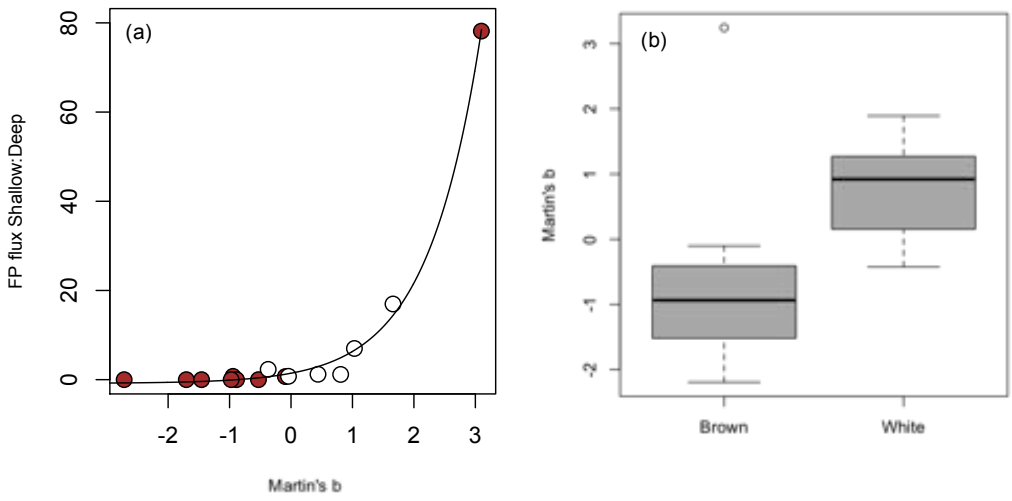

Figure 2.13: Zooplankton faecal pellet controls on *b*. a) Ratio of FP flux against *b* and b) the mean (bold line) and standard deviations (normal lines) of FP colour against *b*.

through respiration and defecation. Such DVM behaviour is well documented in our study area; for example, Atkinson *et al.* (1992) identified four copepod species near South Georgia migrating from a maximum daytime depth of 120 m (55 m above the deepest MSCs) to the surface layers at night. Similar effects of DVM on flux profiles have been postulated in the Arabian Sea (Wishner *et al.*, 2008).

The presence of sea ice may influence the extent to which DVM and active flux occur. The mixed layer depth was between 20 m and 30 m in the sea ice zone compared to $>$ 40 m in regions farther from the sea ice (Thorpe, 2014). The reduction of the upper mixed layer depth in the SIZ would mean that even zooplankton with less extensive DVMs are more likely to contribute to active flux than in 'deep' mixed layer depth conditions. Moreover, the level of active flux is enhanced by the reduced time required to migrate out the mixed layer. Sea ice will also have an effect on light levels as ice lowers the penetration of downwelling irradiance into the ocean (typically between 15 % and 90 %) through an increase in surface albedo and absorption (Grenfell & Maykut, 1977). The response to lowered light levels may be species specific; krill may reduce their DVM in the presence of ice as it protects them from their visual predators such as fur seals and macaroni penguins (Veit *et al.*, 1993); however, copepods may not as their predators, such as larval fish and chaetognaths (Froneman *et al.*, 1998; Turner, 2004), are less affected by ice. However, in the MIZ, FP flux increased with

depth, suggesting the presence of DVM, but in the SIZ, FP flux decreased (Figs. 2.8c & d), and these ice zones are likely dominated by krill, whereas copepods dominate in open water areas (Siegel *et al.*, 1992). Lancraft *et al.* (1991) also observed DVM by krill in the ice-covered Scotia Sea.

Taken together, the presence of sea ice and DVM can explain the broad geographical patterns of change in POC flux with depth. However, there are exceptions to these patterns, and diet may strongly link to the size of the active flux. White FPs indicate feeding on detritus, FPs, or transparent flagellates, whereas brown FPs indicate feeding on fresh phytoplankton (Wilson *et al.*, 2008). Data points on Fig. 2.13 b are coloured white or brown, indicating the dominant (> 70 % abundance) colour of FPs at each station. Where b was positive, most of the FPs were white, and where it was negative, most pellets were brown. The effect of the colour of FP on b was statistically significant (one-way analysis of variance, $F = 21.26$, $df = 13$, $p < 0.001$; Fig. 2.13 b; note that station 22 was an anomaly, where $b > 3$). The deviation to this rule was station 12 in the MIZ. This suggests that active transport is most pronounced where zooplankton were exclusively feeding on fresh phytoplankton, with zooplankton consuming detrital material in environments where the active flux, and hence T*eff* were low.

Including the slow sinking flux in this analysis (total b, Fig. 2.12 c) only slightly alters the b values but doesn't deviate away from the pattern of fast sinking b. From the parameters measured in this study (mixed layer temperature, nitrate, PP and zooplankton) none could explain the variation in slow sinking b. Therefore other processes may be more important such as the grazing rate of zooplankton (producing slow sinking particles by messy feeding (Mayor *et al.*, 2014)) and bacteria hydrolysis. For the total b though, where b increased the *in situ* water temperature increased, but only for the positive b values (exponential function, $p < 0.01$, $r = 0.57$). Marsay *et al.* (2015) showed a positive relationship between temperature and b over a much wider temperature range and using *in situ* sediment traps. Using their relationship and the mean *in situ* water temperature from the upper mesopelagic during this study (2.3 °C) then b should have been 0.45, when the mean total sinking b was actually 0.2. Further, the fact that there was no relationship when including the negative b values, which is almost half the data, one cannot conclude that temperature was ultimately a controlling factor on b in the Scotia Sea. This further demonstrates

that biological processes in the Southern Ocean do not conform to the global norm.

2.6 Summary

This was a unique collaborative study, which allowed sampling over large primary productivity ranges in the Southern Ocean. Estimating particle fluxes using the Marine Snow Catcher produced similar results to others sampling by different methods in the SO. The MSC was also used to estimate the speed of slow sinking particles. Although this had been done once previously, this is the first time net rising rates had been reported, suggesting that some plankton cells can control their buoyancy below the mixed layer.

Both fast and slow sinking particles could each produce POC fluxes of 90 mg C m^{-2} d^{-1}, which is an important result as it emphasises the key role of slow sinking particles in particle export. PE*eff* was lower than hypothesised and T*eff* was overall very high. Fast and total sinking PE*eff* in the Scotia Sea were inversely related to primary production, supporting the observations of Maiti *et al.* (2013). Further, zooplankton processes may be an important contributor to this relationship. The efficiency with which this exported material is transferred to the interior regulates the role ocean biological processes play in controlling atmospheric CO_2 levels. The upper mesopelagic element of this transfer was highly variable in the Scotia Sea, with zooplankton faecal pellets dominating flux. Active transport *via* surface ingestion and deep defecation linked to diel vertical migration is a key process involved in transferring material out of the euphotic zone, which appears to operate most strongly when zooplankton graze on fresh organic material and sea ice is present. Climate change may reduce crustaceous zooplankton abundance and change community structure (Atkinson *et al.*, 2004); any associated reduction in FP production will reduce the depth penetration of organic carbon, with long-term implications for atmospheric CO_2 and the SO carbon cycle.

Acknowledgements

I would like to acknowledge other participants in JR274 who collected data that contributed towards this study: Chris Daniels and Glaucia Fragoso for the primary production measurements, Mark Moore for chlorophyll *a* concentrations, Sophie Richier for the BSi concentrations and Geraint Tarling and Peter Ward for zooplankton abundance. Further thanks to other co-authors on the paper:

Richard Sanders, Fred Le Moigne and Alex Poulton, and to Annike Moje for running the POC samples.

Chapter 3

Remineralisation of organic carbon in a Pacific Oxygen Minimum Zone

Note, this chapter is in review in Nature Communications, although a more extensive analysis of the fast sinking particle sinking rates is included here.

3.1 Overview

In this chapter Marine Snow Catchers were used to collect fast and slow sinking particles in the upper mesopelagic zone of the Equatorial Tropical North Pacific (ETNP). Here persists an oxygen minimum zone between 50 and 950 m. Particulate organic carbon (POC) fluxes and microbial oxygen uptake from particles were measured. The latter was used to determine the lability and the magnitude of microbial degradation of particles in the ETNP. The observed attenuation of POC and that estimated by microbial degradation were compared to find the contribution of microbes to POC attenuation.

3.2 Introduction

It is well documented that a high fraction of the particulate organic carbon (POC) formed in the surface ocean during photosynthesis passes through oxygen minimum zones (OMZs) and sinks to the deep ocean (Martin *et al.*, 1987; Hartnett *et al.*, 1998; Keil & Cowie, 1999; Devol & Hartnett, 2001; Van Mooy *et al.*, 2002; Roullier *et al.*, 2014; Keil *et al.*, 2016). Consequently the transfer efficiency (T*eff*) of exported POC to depth is high. Another term to quantify the T*eff* is

the remineralisation length scale (RLS), which is the attenuation coefficient z^* from the exponential function determined by Boyd & Trull (2007). The RLS has a strong influence on atmospheric CO_2 level (Parekh *et al.*, 2006; Kwon *et al.*, 2009), such that an increase in the RLS of 100 m can decrease atmospheric CO_2 levels by ca. 50 ppm. Despite more than three decades of research, the reason for the large observed RLS in OMZs is still unclear.

Key hypotheses include: 1) changes in zooplankton behaviour e.g. reduced metabolism and vertical migration (Keil *et al.*, 2016); 2) low oxidation rate of sinking organic matter (Devol & Hartnett, 2001); 3) preferential consumption of nitrogen-rich organic matter over carbon (Van Mooy *et al.*, 2002); 4) the sinking material is more refractory, possibly due to phytoplankton community structure (Keil *et al.*, 2016) and finally 5) the addition of material in the mesopelagic zone *via* chemoautotrophy, such as anammox (Roullier *et al.*, 2014).

Oxygen minimum zones occur between 100 - 1000 m depth beneath productive waters (Lam, Doney, & Bishop, 2011). They persist due to high O_2 utilisation from the remineralisation of sinking organic particles and slow water ventilation (Wyrtki, 1964). Definitions of the upper limit of dissolved oxygen (DO) concentration for OMZs vary, however hypoxia is defined as < 0.2 mL O_2 L^{-1} (Kamykowski & Zentara, 1990). OMZs contribute to 20 - 40 % of the global oceanic N_2 loss even though they make up only 0.1 % of the global ocean volume (Codispoti, 1995; Gruber, 2004; Lam *et al.*, 2009). This is because they are key areas for the removal of fixed nitrogen *via* the microbial processes of denitrification and anammox (anaerobic ammonium oxidation (Mulder *et al.*, 1995)) (Paulmier & Ruiz-Pino, 2009).

OMZs have expanded over the past 50 years and are likely to expand further with global change due to increases in temperature and slowing down in ventilation (Stramma *et al.*, 2008; Cabré *et al.*, 2015). OMZs are common at eastern boundary upwelling systems, such as the Eastern Pacific and off the west coast of Africa, because the high productivity is supported by upwelling nutrient-rich waters. These productive areas are also areas of intense fishing activity that may reduce with decreasing biodiversity from expanding OMZs (Stramma *et al.*, 2010). The Pacific OMZs near the equator are the thickest and deepest globally, reaching depths of up to 3000 m. Understanding the biological processes in these OMZs is important so we may predict how the global carbon and nitrogen cycles

may change as they expand.

This study aimed at testing hypotheses 2 and 4, that lability (reactivity) and oxidation of sinking POC is reduced in OMZs and responsible for the high proportion of POC at depth. To do this fast and slow sinking particles were collected from the Eastern Tropical North Pacific OMZ to measure the lability or turnover of the POC by microbes within the OMZ, in collaboration with colleagues from Queen Mary University London. In parallel the POC concentration and sinking rates were measured to determine POC fluxes. This is the first time reactivity or carbon-specific respiration rate has been measured on slow sinking particles. Also a more sophisticated method for measuring fast sinking particle sinking rates using a FlowCAM was developed.

The hypothesis is that POC T*eff* and RLS will be high as commonly observed in OMZs and the lability/microbial turnover of POC will be reduced within the core OMZ. If the lability of particles is lower in OMZs, possibly due to more refractory particles being exported above OMZs, then degradation rates will be slower leading to a high RLS. Microbial turnover of POC may be reduced in the low oxygen conditions, reducing the degradation rate of POC, also leading to a high RLS.

3.3 Methods

3.3.1 Cruise location

Measurements were made in the Eastern Tropical North Pacific (ETNP) onboard the *RRS James Cook* from 28th December 2013 until 10th February 2014 (Fig. 3.1). Particles were collected from 6 stations moving from onshore to offshore (Appendix Table B.1). Onshore stations were defined as those where the bottom depth was < 600 m (stations 1 - 3) and offshore > 600 m (Kalvelage *et al.*, 2013) (stations 4 - 6). At each station a CTD was deployed with a fluorometer to identify the peak in fluorescence and an oxygen sensor to measure the dissolved O_2 concentrations.

3.3.2 Sampling the MSC for particle flux

Giant (300 L) Marine Snow Catchers (MSCs) were used to collect sinking particles from the upper mesopelagic zone (closed circles Fig. 3.1). These MSCs only differ from the smaller 95 L volume MSCs by having a larger diameter (40 cm) and height (2 m) and more taps along the length of the MSC, including one

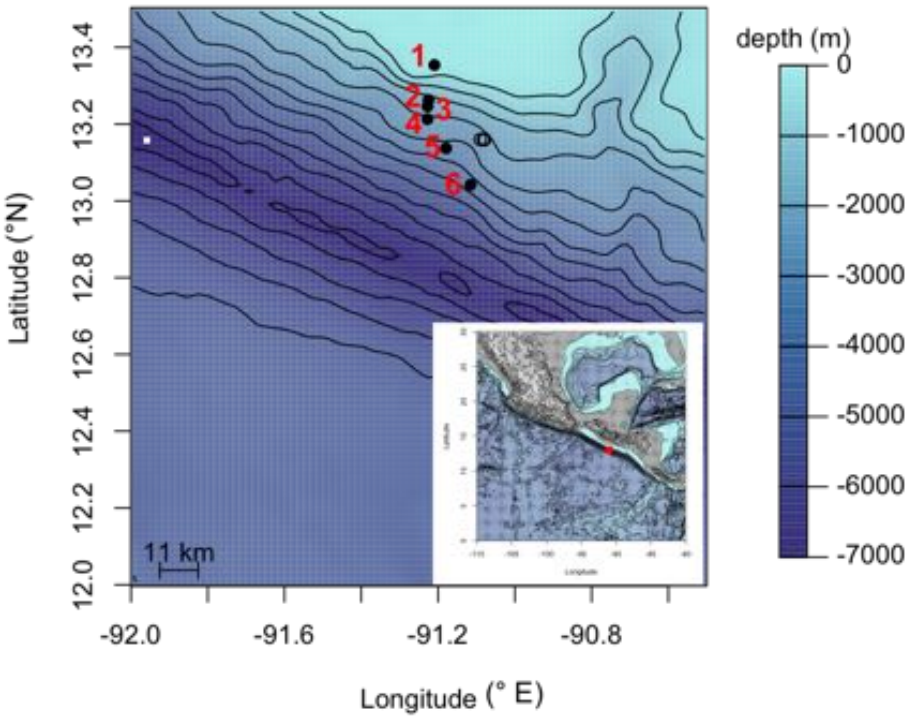

Figure 3.1: MSC sampling location in the ETNP. Colour contours are bathymetry from NOAA database. Closed circles and red station numbers are MSC deployments for POC flux measurements and open circles are MSC deployments for oxygen uptake incubations. Red dot on inset shows general station location in relation to the Pacific Guatemalan coast (grey).

on the base section. Deployment depths started from 10 m below the subsurface fluorescence maximum (as determined from prior fluorometer casts) to 350 m water depth.

The MSCs were left to settle for 2 hours before being sampled. Once the MSC reached the required depth it was closed by a messenger-release system and immediately returned to deck. On deck an initial 2 L sample of water was taken from the central tap on the top part of the MSC (*t0*), representing the homogeneous water column. After leaving the MSCs to settle for 2 h another 2 L of water was taken from the same central tap representing the suspended fraction of particles (*t2*) and 2 L from the base tap representing slow sinking and suspended particles (*b2*). Once the MSC had been emptied, a tray at the bottom of the MSC containing the fast sinking particles was removed. The base tray was taken inside the ship and any zooplankton swimmers removed using a plastic 2 mL pipette.

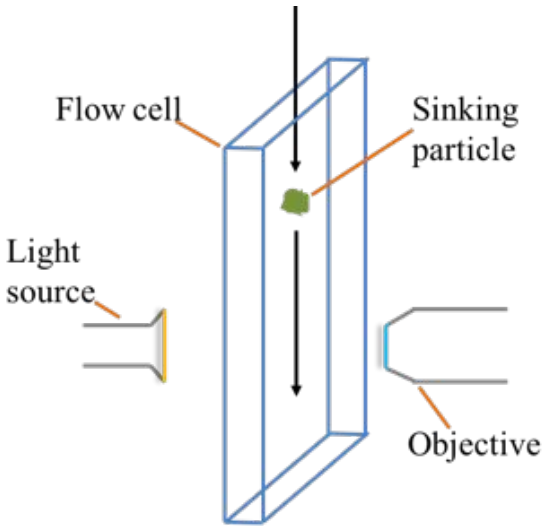

Figure 3.2: Schematic (not to scale) of FlowCAM set up for estimating sinking rates adapted from Bach *et al.* (2012).

Fast sinking particles

For fast sinking particles, photographs were systematically taken of the base tray using a Veho VMS-004 USB digital microscope at 20 x magnification. ImageJ64 was used to both identify particles and measure their area and an Olympus SZX16 microscope at 100 x magnification was used to manually classify particles as either phytodetrital aggregates or faecal pellets. The POC mass was estimated using the same method and conversion factors (Alldredge, 1998) as in Chapter 2.

Fast sinking particle sinking rates

Fast sinking particle sinking rates were estimated using a FlowCAM following a similar method to Bach *et al.* (2012). FlowCAMs allow for image particle analysis; particles (phytoplankton, zooplankton, aggregates e.t.c) in *in situ* water are usually syringed at a constant rate through a flow cell (cuvette) where high resolution photographs are taken and the corresponding software distinguishes between different particles (Sieracki *et al.*, 1998). These photographs allow high resolution measurements of abundance, size, shape plus particle identification

To analyse the sinking rate the FlowCAM setup was slightly modified so instead of particles being syringed in at a constant rate they sank into the flow cell at their natural *in situ* settling rate due to gravity (Bach *et al.*, 2012). To do this the syringe was replaced with a small funnel and the funnel/tube/flow cell filled with *in situ* water. Particles were then placed individually into the funnel and left to sink through the tube and flow cell. The tube was 4 inches

long allowing a large distance between the funnel and flow cell for the particles to settle at an undisturbed sinking rate (see Fig. 3.2 for similar set up by Bach *et al.* (2012)). The distance the particle sank before entering the flow cell is equivalent to a human crossing the lengths of two football fields.

The camera was set to take 7 photographs a second, meaning that more than one photograph was taken of each particle as they passed it's field of view (FOV). The time taken for particles to pass through the FOV (number of photographs taken of each individual particle at a rate of 0.12 seconds) was divided by the length of the field of view (2 mm) to estimate sinking rate.

Slow sinking particles

Slow sinking particles were collected and their sinking rates measured in the same way as in Chapter 2, section 2.3.4.

Particle flux

Fast and slow sinking POC fluxes were calculated following the same flux equation as in Chapter 2, equation 2.6.

3.3.3 Estimating the reactivity of particulate organic carbon by microbial oxygen uptake

Separate MSC deployments were made (open circles, Fig. 3.1) between 40 and 250 m to collect particles for microbial oxygen consumption using the same sampling method as for flux estimates. Swimmers and large (visible) organisms were removed from the base tray leaving only the particles and microbial organisms. 400 mL of water from the base (slow sinking and suspended particles) and the middle tap (suspended particles) were filtered through a GF/F (Whatman) for subsequent elemental analysis.

Figure 3.3: Unisense micro-respiration system setup for oxygen uptake of particles in a water bath.

A dedicated micro-respiration system (Unisense) was used with an eight-chamber rack secured in a water bath at 24 °C. Eight glass micro-respiration chambers (4 x 4 mL and 4 x 2 mL) were each fitted with a disc of fine mesh at their base to separate the underlying glass-coated magnetic stirrer from the fragile particles.

Fast sinking particles and their associated water from $\frac{3}{4}$ of the base tray, were transferred to four chambers (two 4 mL and two 2 mL); water collected from the base of the MSC (slow sinking and suspended particles) was placed in two chambers (one 4 mL and one 2 mL) and water from the middle tap (suspended particles) in the remaining two chambers (one 4 mL and one 2 mL). The chambers were sealed and placed in the water-bath to equilibrate to temperature (24 °C) for 20 minutes in the dark before the first measurements of oxygen were made. A rapid-response, micro-oxygen electrode (OX 20, Unisense) was then lowered through the capillary in the chamber lid and data logged in each chamber for 30 seconds, every 30 - 40 minutes for ca. 4 hours. The Unisense electrode had previously been calibrated using 0.1 M NaOH and ascorbic acid.

Rates of oxygen consumption, for each fraction (suspended, fast and slow sinking) in each chamber, were calculated using linear regression in R, where the rate is the fitted slope between oxygen uptake and time. Incubations with non-significant ($p > 0.05$) slopes were removed before continuing. Linear-mixed-effects-modelling (Zuur *et al.*, 2009) was used to characterise the overall rates of oxygen consumption in both the fast and slow sinking particles. Rates on slow sinking and suspended particles were indistinguishable so treated as one fraction. 'Time' and 'particle-fraction' were fitted as fixed effects, with random slopes and intercepts for both 'chamber' and 'MSC' where appropriate. Rates of consumption for slow sinking particles were subtracted from their respective parallel fast sinking fraction rates.

In total 88 measurements of oxygen consumption were made, 12 of which had non-significant t-values for their slope (rate) estimates. These 12 'non-significant' data-sets were used in a linear-mixed-effect model to give a best estimate for the limit of detection (LOD). Accordingly, the estimated LOD was -0.31 μM h^{-1} (s.e. 0.15, t = -1.99, p = 0.047) which, although marginally significant, is an order of magnitude lower than the mean rate for both fractions and an order of magnitude greater than that determined with an ultrasensitive STOX (switchable trace amount oxygen) sensor for raw, unadulterated, or non-concentrated, seawater of up to 0.085 μmol L^{-1} h^{-1} (Tiano *et al.*, 2014). Hence, only significant rates of oxygen consumption in seawater could be measured because the particles were concentrated by settling in the MSC.

At the end of each incubation all of the fast sinking particles were collected

from each chamber and frozen for elemental analysis. Upon return to the UK, the fast sinking particles were transferred directly to tin-cups, whereas the slow sinking and suspended filters were sub-sampled. The tin-cups were combusted at 1000 °C in an elemental analyser (Sercon Integra 2), along with respective standards and blanks to quantify the organic carbon content. Once normalized to their respective chamber volumes, the carbon-specific respiration constants were estimated: k (h^{-1}) = μmol O_2 $chamber^{-1}$ h^{-1} / μmol C $chamber^{-1}$. The data were examined for any effect of chamber volume or the initial oxygen concentrations on final estimates of k (Appendix Fig. B.3).

3.3.4 Modelling flux through the mesopelagic

To determine the extent of microbial turnover of POC in OMZs the attenuation of POC with depth by microbes (from estimates of k) was compared the measured POC attenuation (k). The exponential function (as outlined by Boyd & Trull (2007)) was used to calculate the remineralisation length scale (RLS; the exponent z*, equation 3.1):

$$F(z) = F(z_0) * e^{(z - z_0/z*)} \tag{3.1}$$

where *F(z)* is the flux at depth z, *F(z_0)* is the shallow reference flux at depth z_0 and z^* is the RLS or the depth (m) by which 63 % of the flux had been remineralised. One mean z^* was calculated for each sinking fraction onshore and offshore. Thus four flux profiles were made by taking the mean POC flux at each depth and fitting to equation 3.1, setting the shallowest observation to *F(z_0)*. To calculate z^* using microbial POC turnover or the k constants, the following equation was used:

$$z* = \frac{w}{k} \tag{3.2}$$

where w is the mean calculated sinking rates (m d^{-1}) for each profile and k is mean microbial carbon-specific respiration i.e. POC turnover (d^{-1}).

Temperature corrections

Both sinking rate and microbial oxygen uptake were measured at 24 °C, which is higher than the *in situ* water temperature the particles were collected from (10 - 20 °C). Therefore the effect of temperature was corrected for. For k the Q_{10} relationship where an increase in 10 °C increases respiration by a factor of 2.5 was used, which is equivalent to an activation energy of 0.65 eV (Yvon-Durocher

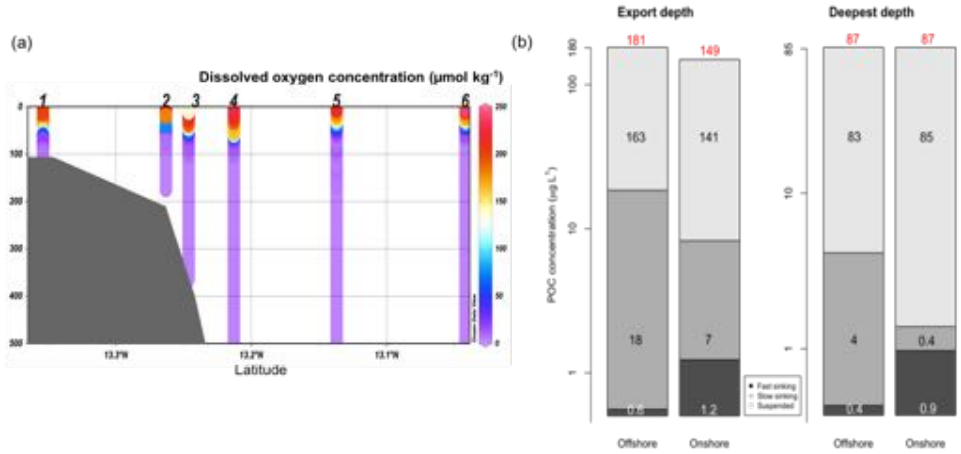

Figure 3.4: Concentrations of a) upper ocean dissolved O_2 (μmol kg^{-1}) across all stations and b) mean POC (μg L^{-1}) on- and offshore at the export depth (40 - 70 m) and the deepest depth sampled (220 - 350 m). Note the the grey polygon in a) is the bathymetry and the log y-axis in b). In b) the fast sinking particle concentrations are in dark grey, slow sinking in mid-grey and suspended in light grey. The numbers in black are mean concentrations for each fraction and in red the total mean of all fractions.

et al., 2012). For sinking rates an increase in 9 °C results in a 40 % increase in sinking rate (Bach *et al.*, 2012). These corrected values were used to model (equation 3.1) POC flux through the upper mesopelagic zone assuming microbial POC turnover was the only remineralisation pathway. All presented errors are one standard error of the mean.

3.4 Results and Discussion

3.4.1 Particulate organic carbon concentration in an oxygen minimum zone

Off the coast of Guatemala the Eastern Tropical North Pacific OMZ had a steep upper oxycline at 50 m (Fig. 3.4 a) and a lower oxycline at 950 m, below which dissolved oxygen (DO) concentrations increased. By 120 m in both the onshore (bottom depth $<$ 600 m) and offshore (bottom depth $>$ 600 m) regions (Kalvelage *et al.*, 2013), the DO concentrations were between 2 - 4 μmol kg^{-1}, with the lowest DO concentration (1.9 μmol kg^{-1} i.e. the limit of detection for the Seabird sensor) at station 4, at 350 m depth.

Total POC concentrations ranged from 65 to 214 μg L^{-1} (Appendix Table B.2) in the upper mesopelagic zone (40 - 350 m), with suspended particles consistently forming the largest fraction (Fig. 3.4b). Generally, concentrations of fast sinking particles were lowest apart from at depth onshore, where the concentra-

tion of fast sinking particles was 0.5 μg L^{-1} or 56 % larger than the slow sinking fraction. This is consistent with the findings of Riley *et al.* (2012), who used MSCs and observed that the majority of mesopelagic particles were suspended.

3.4.2 Estimated fast sinking rates using the FlowCAM

Using the FlowCAM to estimate fast particle sinking rates resulted in reasonable estimates. Sinking rates ranged from 5 to 745 m d^{-1}, with a mean of 116 ($\pm$ 0.18) m d^{-1}. In total 810 particle sinking rates were estimated using the FlowCAM, compared to the 161 particles measured in Chapter 2 using a measuring cylinder.

For each estimated particle sinking rate there is parallel information about the particle including equivalent spherical diameter (ESD), width, length, transparency and aspect ratio. These parameters are automatically assigned by the software. The photographs were used to identify the particle type such as phytodetrital aggregate, faecal pellet, pteropod, zooplankton exoskeleton e.t.c (see Chapter 4, section 4.4). Plus the depth and area (onshore or offshore) for each particle were known. The size (as ESD) of the particles ranged from 32 to 2424 μm, with an average ESD of 489 μm ($\pm$ 0.47 μm).

Slow sinking particles, by design, were also in the base tray water containing the fast sinking particles. Hence rates $<$ 20 m d^{-1} that are considered slow sinking (Riley *et al.*, 2012), were recorded by the FlowCAM. Estimates had a similar range as in Chapter 2 from the Southern Ocean but with a lower mean. Rates are also similar to those determined by observations elsewhere (Asper, 1987; Alldredge, 1998; Alonso-Gonzalez *et al.*, 2010; Riley *et al.*, 2012; Iversen & Ploug, 2013), with Alldredge (1998) estimating an extremely similar mean of 117 m d^{-1}. This consolidates that the FlowCAM can be a very efficient method of estimating reasonable particle sinking rates.

Applicability of the FlowCAM

Some of the main benefits of using the FlowCAM include the ease, speed and number of particles that can be measured. Another huge benefit compared to the previous method is that even small particles not visible to the naked eye are included in this analysis. Consequently a greater range of particle size was measured.

As with every method there were some disadvantages that with more time could be improved. For instance large particles could get stuck on the flow cell

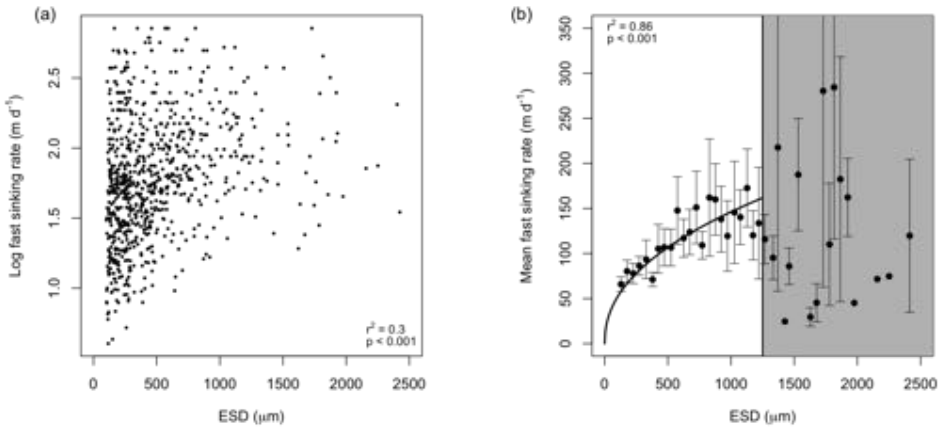

Figure 3.5: Estimated particle sinking rates (corrected for temperature) against size (ESD) for a) all estimates, note the log of the y-axis and b) the mean estimated sinking rate of particles in each ESD bin (50 μm). Error bars are standard error of the mean and the grey shaded area is where the relationship between sinking rate and ESD breaks down.

wall, slowing their sinking time through the cell. This could be overcome by using a flow cell with a larger depth (> 2 mm), however this may cause issues with smaller particles becoming unfocussed in the greater depth of the cell. Bach *et al.* (2012) only measured particles smaller than 400 μm in ESD, which is much smaller than the largest particle measured here. Additionally their highest sinking rate accurately measured was only 200 m d^{-1} as the short distance the particles sunk through the FOV made it hard to track very fast sinking particles, even at the highest frame rate (Bach *et al.*, 2012). However, in this study only 15 % of particles measured sank at speeds greater than 200 m d^{-1}, and only 10 % sank at rates greater than 250 m d^{-1}.

Another problem was that particles stuck to the inside wall of the tube before they entered the flow cell. This meant that other particles sinking behind them could stick to them forming a larger particle than naturally formed *in situ*. This could be improved by using a tube made of PTFE (Polytetrafluoroethylene) which has no electrical charge, thus the particles should not stick to the side of the tube.

Controls on sinking rates

All particle sinking rates were estimated at a temperature of 24 °C, however the *in situ* water temperature was lower and ranged from ca. 10 to 20 °C over the depth range the particles were sampled from. Temperature corrections were made as discussed in the methods section 3.3.4. Temperature corrected rates

ranged from 4 to 715 m d^{-1} with a mean of 100 ± 4.3 m d^{-1}. Therefore the *in situ* decrease of temperature caused a mean decrease in sinking rate of 16 m d^{-1}. Subsequent analysis only presents the corrected sinking rates.

One of the main factors believed to control particle sinking rates is particle size (Alldredge & Gotschalk, 1989; Guidi *et al.*, 2008; Alonso-Gonzalez *et al.*, 2010; Iversen & Ploug, 2010; McDonnell & Buesseler, 2010), with models using phytoplankton size class to determine subsequent particle sinking rate (Yool *et al.*, 2011; Aumont *et al.*, 2015). In the ETNP there was a weak effect of size (ESD μm) on sinking rates (Fig. 3.5 a, r = 0.3, $p < 0.001$, note the y-axis is log-scaled) when comparing the entire data set. For small particles (< 500 μm, Fig. 3.5 a) there was a large range in particle sinking rate however larger particles generally sank only at high rates, greater than 30 m d^{-1}. To reduce the scatter the ESD was binned into 50 μm width bins and the mean sinking rate calculated for each bin (Fig. 3.5 b). This showed that when particle size was small (ESD < 1250 μm) there was a highly significant relationship between size and sinking rate (w, r = 0.86, $p < 0.001$, white area of Fig. 3.5 b, equation 3.3).

$$ln(w)(md^{-1}) = 1.9 + (0.44 * ln(_{ESD})) \tag{3.3}$$

Above this size the relationship broke down (grey-shaded area of Fig. 3.5 b). This could be because the size of large particles was not enough to control sinking speed. However, fewer (37) particles were measured with ESDs > 1250 μm, with many more (773) measured with ESDs below 1250 μm. Thus the n-value might control this relationship and if more larger particles were measured the relationship between particle size and sinking rate may be extended to large particles. Non-linear binning by ESD, such that each bin was 1.5 x greater than the previous, continued the relationship between ESD and sinking rate even at ESDs larger than 1250 μm (Appendix Fig. B.1). Yet this reduced the n-value from 810 to just 8.

Using the relationship from equation 3.3 the sinking rate at 1250 μm is 157 m d^{-1}. This is close to the maximum rate of 200 m d^{-1} that Bach *et al.* (2012) found could produce reliable sinking rates. For the purpose of estimating carbon flux all sinking rates have been included, as particles *in situ* can sink much faster than 200 m d^{-1} (Alonso-Gonzalez *et al.*, 2010). To analyse what might be controlling sinking rate, only particles with a rate between 20 and 200 m d^{-1}

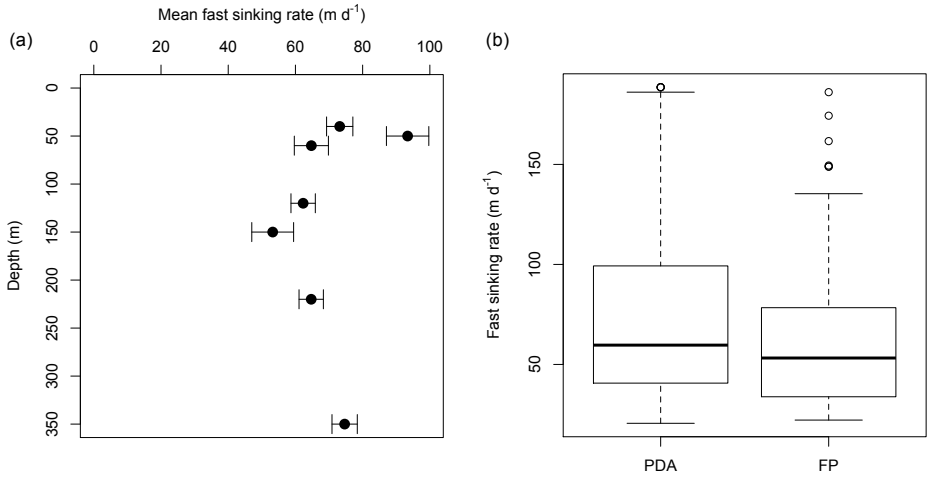

Figure 3.6: Mean estimated particle sinking rates, for particles sinking with a rate between 20 and 200 m d^{-1}, at a) each depth sampled where error bars are standard error of the mean and b) box and whisker plot of sinking rates for phytodetrital aggregates (PDAs) and faecal pellets (FPs).

have been used, giving a reduced mean of 70 $\pm$ 1.7 m d^{-1}.

There was no overall effect of sample depth on mean sinking rates (Fig. 3.6). Sinking rates generally declined from 40 m to 150 m and then increased with depth below this. To test other factors that may influence fast sinking rates analyses of variances (ANOVAs) were performed to test the effect of the type of particle, the area collected from (on/offshore) and the time of day (day/night). Sinking rates were log-transformed to fit a normal distribution for analyses. There was no individual effect of either the type of particle, sampling area or time of day on fast sinking rates ($p > 0.05$). Although comparing just particles that were PDAs or FPs (80 % all particles, Chapter 4) showed that PDAs sank significantly faster (61 m d^{-1}) than FPs (51 m d^{-1}, t=-2.32, df = 154, $p < 0.05$). This is similar to the result from the Southern Ocean where PDAs also sank significantly faster than FPs.

To summarise the FlowCAM was a useful tool to measure the sinking rates of 100s of particles without any limit on the size of particle. Particles could also be identified from the images and assigned individual sinking rates (Chapter 4). Sinking rates produced were of a similar range to other studies. Of the parameters tested, the size of particle had the greatest effect on sinking rate on particles smaller than 1250 μm. This is a method which I strongly recommend should be further developed and made part of the standard protocol in particle

Table 3.1: Mean sinking rates (w) and observed and estimated (by microbial O_2 uptake) remineralisation length scales (z^*'s) for fast and slow sinking particles. NA is where there was no net attenuation of POC flux with depth, as it actually increased at intermediate depths. Offshore the microbial z^* is close to that observed for the fast sinking particles but is much higher than the observed onshore.

	Fast sinking particles			**Slow sinking particles**		
Area	w (m d^{-1})	Observed z^* (m)	Microbial z^* (m)	w (m d^{-1})	Observed z^* (m)	Microbial z^* (m)
Onshore	171	76	874	4	NA	0.5
Offshore	104	357	532	9	27	1.3

flux studies at NOCS.

3.4.3 Fast and slow sinking particle fluxes

Fast sinking POC flux peaked onshore (78 - 350 mg C m^{-2} d^{-1}, compared to 37 - 122 mg C m^{-2} d^{-1} offshore) and decreased with depth both onshore and offshore (Fig. 3.7 a, Appendix Table B.3). Overall the mean fast flux was 116 ± 2.6 mg C m^{-2} d^{-1}. Fast sinking particles mostly comprised phytodetrital aggregates (PDAs) and faecal pellets (FPs), with PDAs forming the largest flux at the base of the mixed layer onshore (Appendix Fig. B.2). The composition of these particles is further discussed in Chapter 4.

The greatest attenuation of fast sinking POC flux occurred onshore with rapid attenuation in the upper 150 m of the water column. This gave a short mean RLS (z^*) of 76 m (Table 3.1) and a low mean (32 %) transfer efficiency (T*eff*). Offshore (Fig. 3.7 a), a higher proportion of POC was preserved with depth (T*eff* = 52 % and z^* = 357) thus this POC flux profile was similar to others observed in OMZs (Martin *et al.*, 1987; Hartnett *et al.*, 1998; Keil & Cowie, 1999; Devol & Hartnett, 2001; Van Mooy *et al.*, 2002; Roullier *et al.*, 2014; Keil *et al.*, 2016). This RLS is much longer than occurs in fully oxic waters of a similar temperature; the Marsay *et al.* (2015) function, ($z^* = x * T$) suggests that z^* in the ETNP should be ca. 100 m, close to the observed onshore z^* of 76 m. It is possible to conclude that the offshore environment is characterised by an efficient transfer of material through the midwater region, similar to that found in other anoxic regions, and different to that found in oxic waters.

Slow sinking POC flux was higher offshore (0 - 345 mg C m^{-2} d^{-1}) than onshore (0 - 168 mg C m^{-2} d^{-1}, Fig. 3.7 b, Appendix Table B.3), with an overall mean of 49 ± 2.2 mg C m^{-2} d^{-1}. As with fast sinking flux, the slow

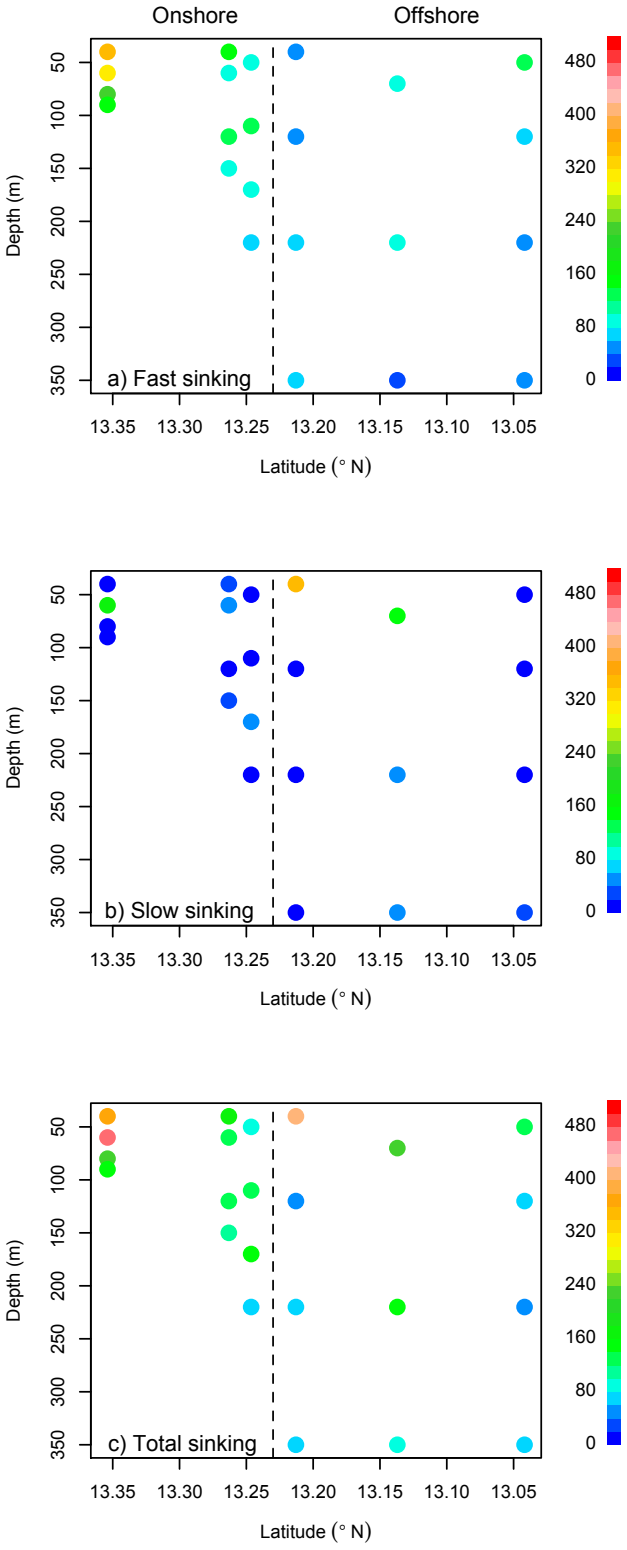

Figure 3.7: Particle fluxes (mg C m^{-2} d^{-1}) in the ETNP a) fast sinking, b) slow sinking and c) total sinking flux. Stations to the left of the vertical dashed line were classed as onshore and to the right offshore.

sinking flux decreased with depth offshore (Fig. 3.7 b, T*eff* = 16 %, z^* = 27 m, Table 3.1), whereas onshore, it increased at intermediate depths (T*eff* = 200 %, z^* = NA). Increases of POC flux at depth were either due to the *in situ* generation of small particles *via* the interior fragmentation of large, fast sinking particles or due to the resuspension of material from the seafloor.

Both fast and slow sinking particle fluxes peaked at 350 mg C m^{-2} d^{-1}, which is much higher than the maximum fluxes observed in the Southern Ocean in Chapter 2 (90 mg C m^{-2} d^{-1}). Here in the ETNP the total sinking flux (fast plus slow sinking) ranged from 35 to 478 mg C m^{-2} d^{-1} with a mean of 165 ± 3.4 mg C m^{-2} d^{-1} (Fig. 3.7 c, Appendix Table B.3). Van Mooy *et al.* (2002) measured reduced fluxes of ca. 48 to 120 mg C m^{-2} d^{-1} in the ETNP, possibly because their shallowest sampling depth was 130 m, 90 m deeper than where the high fluxes were found in this study. Keil *et al.* (2016) also observed lower fluxes of 3 to 36 mg C m^{-2} d^{-1} in the Arabian sea OMZ, while primary production rates were much higher (815 - 1380 mg C m^{-2} d^{-1} (Lee *et al.*, 1998)) than during this study, here estimated from satellite (483 - 629 mg C m^{-2} d^{-1}) (Behrenfeld & Falkowski, 1997). The higher fluxes observed here at sites with lower primary production rates also suggests an inverse relationship between primary production and export, as observed in the Southern Ocean. Unfortunately the primary productivity range is too small to test this hypothesis in this area. Both of the other studies used sediment traps, which likely underestimate slow sinking POC flux.

3.4.4 Microbial carbon specific turnover

Here the first direct measurements of oxygen consumption in two fractions of sinking organic particles from short incubations between 40 m and 200 m are presented. The water recovered with the particles from below 120 m was almost depleted (< 2 μmol kg^{-1}) in oxygen. There was a detectable and measurable change in oxygen in 76 out of 88 incubations (Fig. 3.8 a), down to 0.3 μM h^{-1}. To measure the microbial turnover of the particles, temperature and oxygen were kept constant. The incubations were not aerated to limit the disaggregation of particles, but the water would have become oxygenated during sampling. There was no effect of initial oxygen concentrations or chamber volume on k (carbon-specific respiration rates) for either the fast or slow sinking fractions (Appendix Fig. B.3).

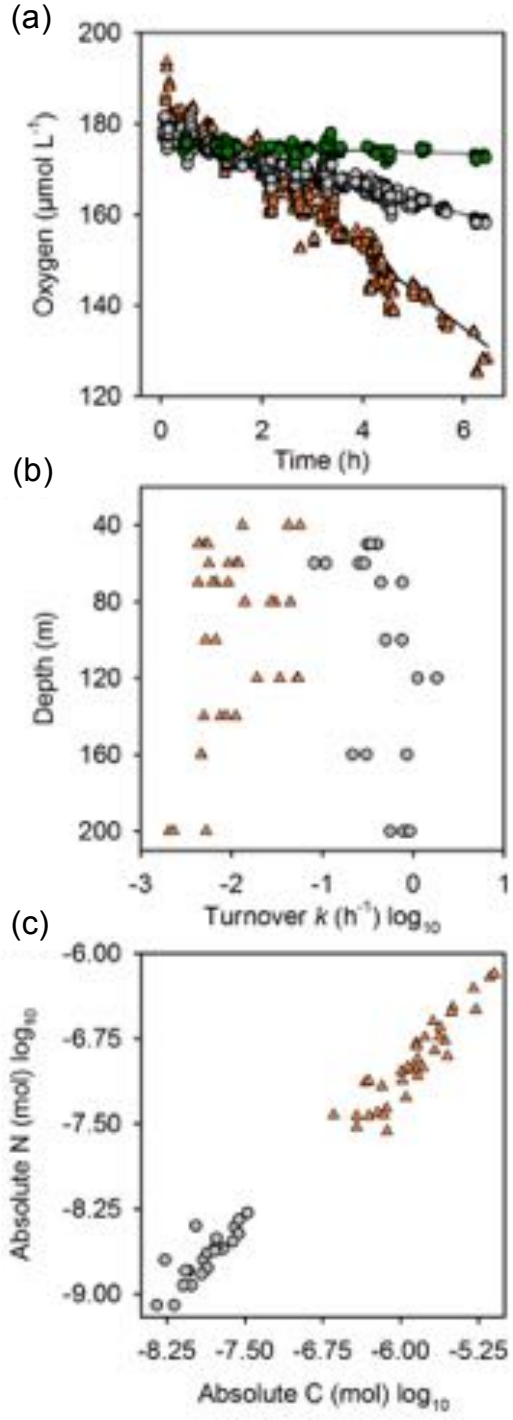

Figure 3.8: Oxygen consumption, turnover and stoichiometry of particles. Data and plots by Mark Trimmer. a) overall estimates for change in oxygen concentration with time. The data are standardised to account for the random intercept fitted to each MSC deployment and incubation chamber. The slope between the two fractions is significantly different to the LOD. b) k (Log_{10}, h^{-1}) calculated by normalising the oxygen uptake rates, prior to temperature corrections, by POC from c) the amounts of POC and PON (mol) in each incubation chamber. Orange triangles and grey circles are fast and slow sinking fractions respectively and green is the limit of detection (see Methods section 3.3.3).

Table 3.2: Overall estimates of k ($\log_{10}$, h^{-1}) prior to temperature corrections.

Coefficients	Estimate	s.e	t value	p
k h^{-1} Fast	-2.05	0.07	-27.53	$<$ 2e-16
Δ k h^{-1} Slow v Fast	1.70	0.12	13.97	$<$ 2e-16

There is some evidence that k (Table 3.2), measured at 24 °C, increased with depth (Fig. 3.8b) but this is most likely an artefact from measuring k at constant temperature, as temperature changes with depth. Further, the residuals from an ANCOVA (analysis of co-variance) testing the affect of depth should not show any obvious pattern (Appendix Fig. B.4 and Table. B.4). Therefore the results are interpreted assuming microbial POC turnover is constant with depth.

The mean temperature-corrected fast sinking k estimate (0.13 $\pm$ 0.01 d^{-1}, here reported in d^{-1} to allow for comparisons) is within the reported global (and oxic) literature range of 0.01 - 0.5 d^{-1} (Ploug & Grossart, 2000; Ploug *et al.*, 2008; Iversen & Ploug, 2010; Collins *et al.*, 2015; Mcdonnell *et al.*, 2015; Belcher *et al.*, 2016), and indistinguishable from those reported at a similar temperature by Iversen & Ploug (2013). Further, Van Mooy *et al.* (2002) also found that microbes degraded carbon at a similar rate in oxic and suboxic conditions and more recent work suggests heterotrophic bacteria biomass production and growth rates are not affected in OMZs (Piontek *et al.*, 2016).

However particles in OMZs are chemically reduced compared to those in the above oxygenated waters, which may affect these microbial respiration rates. Currently most, if not all, published studies have looked at the effect of changing oxidation states on remineralisation in the sediments; for instance oscillating redox which occurs in bioturbation of sediments by tubeworms. Aller (1994) exposed sediment over 28-days to oxic, anoxic or a combination of the both (anoxic with 2 or 3 2-day periods being oxic) and found the percentage of total carbon and nitrogen in the sediment was lowest under oxic conditions, increasing through the oxygen exposures with the highest percentage remaining under anoxic conditions. This suggests introducing reduced particles to oxic waters may increase the degradation of organic carbon, thus our results may overestimate carbon-specific respiration rates. However, the results by Aller (1994) were not significantly different between conditions at the 95 % level.

Over a longer time period (2 years) (Reimers *et al.*, 2013) found oscillating

redox environments did not produce different degradation rates of organic matter in sediments and rates of electron fluxes were similar over the two year experiment. Our introduction of particles to oxygen was on a much shorter timescale (< 0.5 days) than these studies and this may be where the effect of increasing oxygen is greatest. Nonetheless, particles were collected from 40 - 250 m in this study and 'normal' oxygen levels persisted in the upper 100 m. Yet there was no significant change on carbon-specific respiration rates with depth. If the exposure to oxygen was likely to have a large effect on these results then particles where oxygen was at the limit of detection or absent (> 120 m) should have a significantly higher carbon-specific respiration rate than those in the upper oxygenated waters. Additionally, our measured rates were corrected for changes in temperature, reducing mean fast sinking k by over half and the mean slow sinking k by one order of magnitude. Thus when using the k value to estimate microbial degradation of POC in the OMZ the rates used are vastly lower than those measured. As mentioned, the effect of oxidation state on particle remineralisation has only been studied in the sediments, yet is equally important in the water column in OMZs; particularly areas with seasonal OMZs where oscillating redox environments may alter degradation rates of organic matter.

The novel estimates of slow sinking POC turnover were much more rapid (mean temperature-corrected $k = 5 \pm 0.4$ d^{-1}). There was at least a one-order of magnitude difference in the rate at which the two fractions were potentially turned over (Table 3.2); with the carbon in the slow sinking particles potentially being completely remineralised in less than a day, whilst the fast sinking fraction could take up to 8 days to be remineralised. These are the first ever observations of respiration rates on slow sinking particles - previously k has only been measured on large, fast sinking particles, and often on laboratory-produced aggregates (Ploug & Grossart, 2000; Ploug *et al.*, 2008; Iversen & Ploug, 2010, 2013). These elevated rates likely result from the higher surface area to volume ratio of slow sinking particles, which allow their rapid colonization by free-living bacteria. For instance it is estimated the concentrations of particle-attached bacteria are 100 - 1000 x higher than free-living bacteria, even though only 10 - 15 % of the population are generally attached (Fenchel *et al.*, 1998; Herndl & Reinthaler, 2013).

The extremely high turnover rates, coupled to the observation that reactivity

is constant with depth, suggest that slow sinking particles in the mesopelagic zone (100 - 1000 m) are generated there (they are respired too fast and sink too slowly to be surface-derived). For instance, if a particle sinking at 5 m d^{-1} is turned over at a rate of 5 d^{-1}, it would only sink 1 m before the carbon was completely remineralised. A suggested mechanism for their production is *via* the fragmentation of larger, fast sinking particles (Alldredge *et al.*, 1990; Mayor *et al.*, 2014). Recent work suggests that in temperate, oxic waters zooplankton fragment around 50 % of the sinking particles prior to their consumption by microbes (Giering *et al.*, 2014). This fragmentation likely produces the observed bimodal distribution of sinking velocities with the bulk of the material either sinking fast (> 100 m d^{-1}) or slow (< 10 m d^{-1}). Evidence of this is seen by the conservation of the POC:PON ratio (Fig. 3.8 c) between fast and slow sinking particles. Currently in biogeochemical models slow sinking particles are only formed in the upper ocean from small phytoplankton, with no fragmentation pathway (Yool *et al.*, 2011).

3.4.5 Microbial vs. non-microbial remineralisation

Coupling these turnover rates to sinking rates predicts an offshore profile of fast and slow sinking loss close to that observed (Figs 3.9 a & b), with microbial turnover of the fast sinking fraction, be it aerobic or anaerobic, explaining 70 % of the observed reduction in downward flux, with a more minor role for disaggregation.

This situation differs considerably from that in temperate (Giering *et al.*, 2014) and polar (Chapter 2) oxic waters where the main sink for fast sinking particles is zooplankton mediated consumption or disaggregation. Wishner *et al.* (2013) show that zooplankton are almost entirely absent from offshore OMZ waters and Williams *et al.* (2014) suggest that the few zooplankton that are there feed on surface-derived material. Further, zooplankton metabolic processes, such as respiration and excretion, are reduced in low dissolved oxygen concentrations (Kiko *et al.*, 2016). These factors account for the high proportion of fast sinking POC at depth observed, with the minor fraction of particle loss not attributable to microbial remineralisation being caused by abiotic fragmentation.

Onshore, the fraction of fast sinking POC loss attributable to microbial turnover is much lower (ca. 10 %), consistent with the lower RLS. Therefore, either both zooplankton fragmentation and behaviour in the dynamic near shore

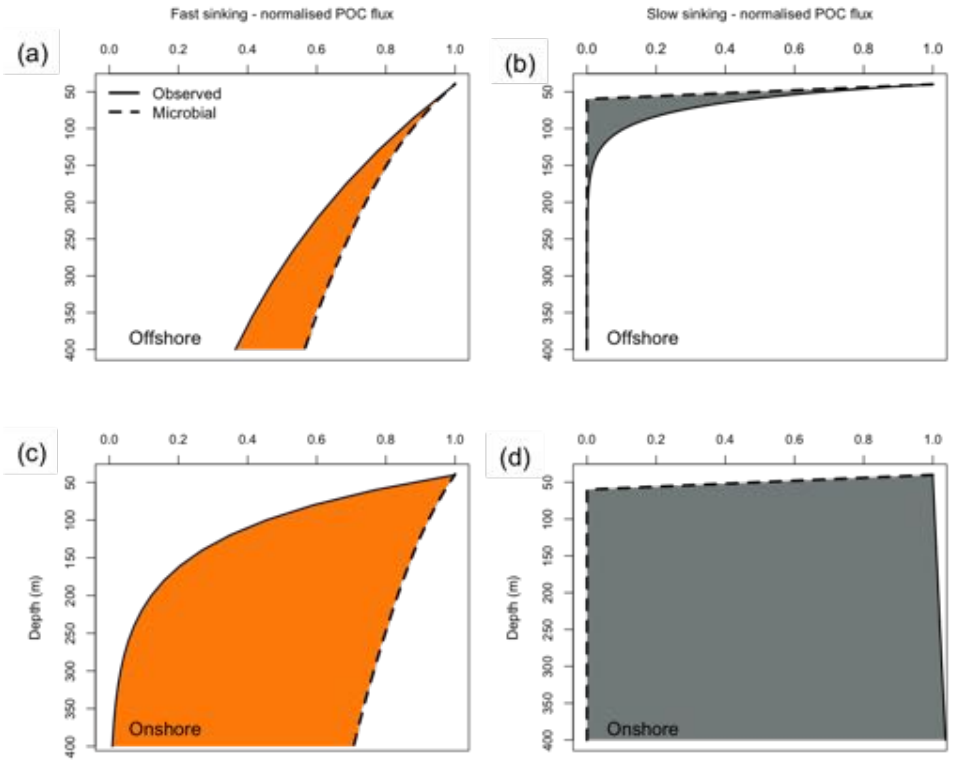

Figure 3.9: Observed (solid line) and predicted, assuming constant k estimated from microbial O_2 uptake (dashed line), normalised POC flux profiles through the upper mesopelagic zone offshore for a) fast sinking (orange shading) and b) slow sinking particles (grey shading) and onshore for c) fast sinking and d) slow sinking particles. The shading highlights the difference between the two flux profiles, with a larger shaded area indicating greater discrepancy between the two profiles.

environment are less impacted by low oxygen concentrations or the more energetic environment of the shelf leads to higher levels of abiotic disaggregation, with the latter being more plausible. In this area the predicted slow sinking flux did not match the observed flux, likely due to high resuspension of slow sinking particles from the seafloor in this upwelling region (Fiedler *et al.*, 1991).

Heterotrophic microbes can include nanoflagellates, ciliates, bacteria, dinoflagellates and some small (< 200 μm) metazoans (Olson & Daly, 2013). They have an integral role in the cycling of elements *via* the microbial loop (Azam *et al.*, 1983), where organisms tend to utilise particles or other organisms one order of magnitude smaller than themselves, thus organic matter is inefficiently returned to the main food web. To be able to metabolise at such low oxygen concentrations in the OMZ the microbes must be highly adapted (Wright *et al.*, 2012). For instance, in the Equatorial Tropical South Pacific the bacterial community was much more diverse in the OMZ than at the oxic surface (Stevens & Ulloa, 2008) and only a small number of macrobiota could exist in the OMZ (Ulloa & Pantoja, 2009). It is often thought that small phytoplankton/particles are only recycled in the microbial loop and not exported; however, here smaller, slowly sinking particles are exported and form an important part of the flux (Richardson & Jackson, 2007). Further, microbes are remineralising even the larger fast sinking particles and offshore are responsible for the majority of POC remineralisation.

This study has shown that potential microbial remineralisation of POC is not reduced in OMZs (hypothesis 2), that the lability of POC is not reduced, is constant with depth and consistent with measurements from fully oxygenated waters (hypothesis 3) and finally that nitrogen-rich material is not preferentially consumed as the POC:PON (8.3) ratio was similar to the Redfield ratio (Redfield, 1934) of 6.6 (hypothesis 4). This leaves hypotheses 1 and 5, the changes in zooplankton behaviour or the addition of material *via* chemoautotrophy, as possible explanations for a high RLS in OMZs.

One chemolithoautotropic process is the use of oxidants to detoxify hydrogen sulphide leading to carbon fixation. Schunck *et al.* (2013) observed a sulphide plume in the Eastern Tropical South Pacific (ETSP) which produced high rates of carbon fixation, up to 30 % of photoautotrophic carbon fixation. However these rates occur only if a hydrogen sulphide plume persists which are sporadic, thus unlikely to explain the consistent pattern of high proportions of surface-produced

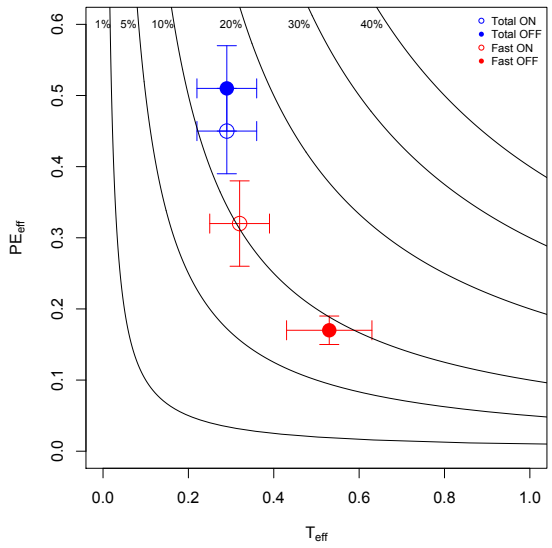

Figure 3.10: BCP*eff* for the fast particles (closed circles) and total sinking particles (open circles) offshore (red) and onshore; estimated by plotting T*eff* against PE*eff*. Contours represent the BCP*eff* (proportion of mixed layer primary production at depth) and error bars standard error of the mean.

POC through OMZs. Another chemolithoautotrophic process, anammox, is elevated in onshore shelf OMZs in the ETNP compared to offshore OMZs and occurs at nanomolar rates (< 225 nM d^{-1}) (Kalvelage *et al.*, 2013), thus is unlikely to be solely responsible for the high RLS observed offshore. Löscher *et al.* (2016) also observed that fixation of nitrogen and carbon in OMZ eddies was higher onshore in young coastal waters in the ETSP.

Thus changes in zooplankton behaviour (hypothesis 1), mostly the reduced daytime depth of the diel vertical migrators (Bianchi *et al.*, 2013) and the low resident populations in the OMZ core (Wishner *et al.*, 2013), are responsible for the high proportion of surface-produced POC at depth in OMZs. Evidence for this is given for the high proportion of degradation attributed to microbes through the OMZ.

3.4.6 Biological carbon pump efficiency

The efficiency of the biological carbon pump (BCP), BCP*eff*, is the fraction of primary production (PP) that reaches the deep ocean (Buesseler & Boyd, 2009), here the sea floor onshore and 350 m offshore. Comparing PE*eff* and T*eff* is a useful tool in assessing BCP*eff* as shown in Fig. 3.10, where the contours represent BCP*eff*. BCP*eff* was similar for fast sinking particles onshore and offshore at 10 %. Offshore there was a high T*eff* where > 50 % of exported material

made it to the deep ocean, however a low PE*eff* of < 20 %. This is as predicted by Henson *et al.* (2012) and other authors for low latitude environments, where a small amount of PP is exported but a large proportion of this reaches the interior ocean. Onshore more fast sinking particles were exported but less reached the deep ocean (Fig. 3.10, closed circles).

When including the slow sinking as well, providing the total sinking flux, the BCP*eff* increases to ca. 15 %, due to increases in PE*eff* both onshore and offshore (Fig. 3.10, open circles). The total sinking T*eff* onshore is similar to the fast sinking but including the slow sinking offshore decreases T*eff* by ca. 20 %. This is because slow sinking particles are exported but remineralised quickly so BCP*eff* is rarely greater than 40 %. So a high T*eff* may not be that important in sequestering POC to the deep ocean at equatorial OMZs. However the majority (78 %) of field data from the meta-analysis by Buesseler & Boyd (2009) had lower BCP*effs* than in the ETNP, with the closest stations to 15 % being K2 in the North Pacific (2005) and station KIWI in the Pacific Southern Ocean (1997). Both these sites are at high latitudes, with very different oceanic systems to the ETNP.

3.5 Summary

Sinking rates, fluxes and microbial turnover of fast and slow sinking POC have been combined to understand the processes which lead to a high transfer efficiency of POC in OMZs, and to test the efficiency of the biological carbon pump. The FlowCAM is an extremely useful way of measuring the sinking rates of particles and showed the size of the particles influenced sinking rate.

The importance of collecting and measuring the flux of slow sinking particles, which are often ignored (Herndl & Reinthaler, 2013), is shown. Slow sinking particles represented ca. 40 % of the exported flux and increased PE*eff* and overall the efficiency of the biological carbon pump, but reduced T*eff* because they are turned over so rapidly by microbes.

Microbes dominated remineralisation of fast sinking particles resulting in a high proportion of POC passing through the OMZ, likely due to the absence of large heterotrophs from the core OMZ waters. This absence reduces the fragmentation of large to small particles and thus indirectly reduces remineralisation. The role of zooplankton in the biological carbon pump will become increasingly reduced with further expanding OMZs under a changing climate, leading to an

even higher proportion of POC at depth. Numerical models suggest that this is associated with increased carbon storage, hence expanding OMZs will likely cause ocean biological processes to play an enhanced role in storing carbon in the ocean, away from the atmosphere. This represents a negative feedback on climate change that numerical models, which typically simulate remineralisation rather poorly, need to incorporate into future structures.

Acknowledgements

Thanks to all the participants on JC097, including the crew and the Master. Thanks particularly to Mark Trimmer who was the PI on this cruise and his then PhD student Felicity Shelley who oversaw the incubations of particles for oxygen uptake. Mark Trimmer then analysed the raw data from these incubations, summarised in Figure 3.10 and shown in some appendix figures. It was Mike Zubkov who suggested I used the FlowCAM to measure the sinking rates of particles for which I shall be forever grateful! Also thanks to Annike Moje in Bremen for again measuring the POC content of the particles for flux analyses.

Chapter 4

Particle composition in the Eastern Tropical North Pacific

4.1 Overview

In this chapter the composition of particles from the Equatorial Tropical North Pacific (Chapter 3) are determined. This is done first morphologically using images and then biochemically using lipids as biomarkers. Particle lipids are used to: compare the composition of mixed layer and exported particles; to infer how particles are formed; assess how the lability of particles changes with depth and determine if zooplankton diel vertical migration is influencing particle composition.

4.2 Introduction

A high proportion of surface-produced organic carbon reaches the deep ocean in OMZs (Van Mooy *et al.*, 2002; Keil *et al.*, 2016) including in the Eastern Tropical North Pacific (ETNP, Chapter 3). Coupling particulate organic carbon measurements with microbial oxygen uptake measurements showed that offshore in the ETNP microbial organisms, adapted to the low O_2 environment, were largely responsible for the attenuation of particle flux. Crustaceous zooplankton have a limited role in reworking particles in the mesopelagic zone (100 - 1000 m) in the ETNP as vertical migration is reduced in oxygen minimum zones (OMZs) (Bianchi *et al.*, 2013). Thus the hypothesis is that the high proportion of flux through OMZs globally is due to a large reduction in zooplankton processing in the biological carbon pump (BCP) compared to oxygenated waters (Fig. 4.1).

Moreover the finding that slow sinking particles are turned over so rapidly (<

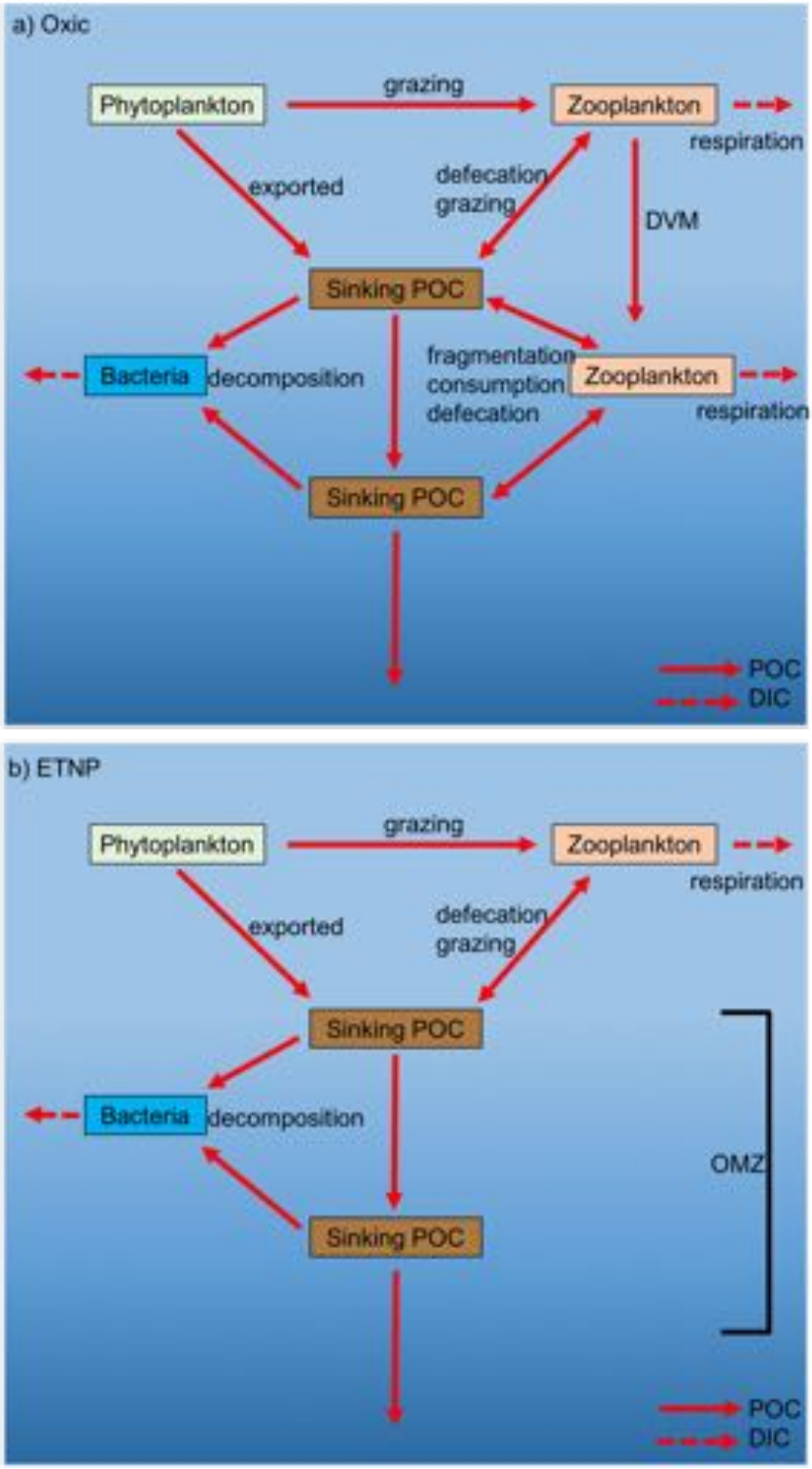

Figure 4.1: Oxic (a) and OMZ (b) biological carbon pump. Solid red arrows represent flows of POC and dashed red arrows remineralisation to DIC. In the oxic BCP zooplankton interact with particles at the surface and deeper in the water column. In the ETNP where an OMZ exists in the mid-water column zooplankton only interact with particles in the upper oxic waters.

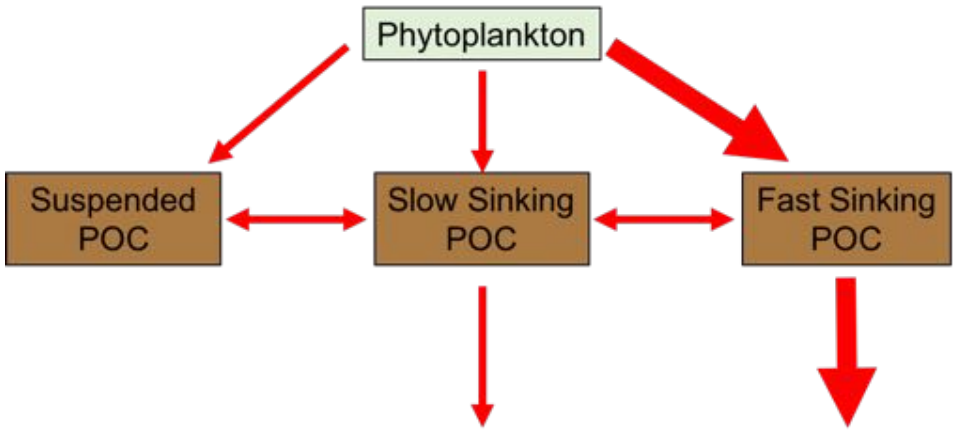

Figure 4.2: Interactions between sinking particulate organic carbon (POC). Specifically shown are transformation pathways for fragmentation from fast to slow sinking and slow sinking to suspended particles, plus aggregation. The large red arrows show the dominant route of export and flux in temperate and polar latitudes *via* fast sinking particles.

1 day) but are present at depth (> 100 m) shows they must be produced at depth *via* disaggregation (Alldredge *et al.*, 1990) or fragmentation (Lampitt *et al.*, 1990) from larger fast sinking particles (Chapter 3). Models often do not include the fragmentation of fast sinking particles (Yool *et al.*, 2013). At temperate latitudes particles form in the upper ocean from the aggregation of phytoplankton cells, possibly from the production of sticky transparent exopolymer particles (Riley *et al.*, 2012), and rapidly sink out of the mixed layer (Billett *et al.*, 1983; Lampitt *et al.*, 1993). This classical view for particle formation is shown in Fig. 4.2 with the addition of the formation of slow sinking particles from fast sinking particles.

Particle composition can be used to gain an even greater understanding of processes affecting organic particles in the ETNP OMZ. The composition of particles (e.g. phytodetrital aggregates or faecal pellets) can affect their sinking rates, organic carbon content, mineral ballast and lability. These factors indirectly influence the rate and depth of particle remineralisation, and hence atmospheric CO_2 levels (Parekh *et al.*, 2006; Kwon *et al.*, 2009). Knowledge of particle composition can also help elucidate processes associated with the BCP, such as particle formation or the influence of zooplankton diel vertical migration on particle flux.

Determining the composition of exported fast (> 20 m d^{-1}) sinking particles can be achieved using a microscope because they are generally large enough (> 200 μm) to be viewed. In this thesis fast sinking particles have been categorised simply as either zooplankton faecal pellets (FPs) or phytodetrital aggregates

(PDAs). Whilst this information can be extremely useful, it does not give any information on the original source of organic carbon, for instance the specific phytoplankton composition. Phytodetritus is often amorphous, making it difficult to determine the dominant exported phytoplankton species through microscopy.

Additionally, microscopy and imaging are not useful in classifying small ($<$ 50 μm), slow ($<$ 20 m d^{-1}) sinking particles, as even with a high magnification or resolution the particles often appear as homogeneous detritus. Previous work at NOCS has estimated that only 5 % of measured particulate organic carbon (POC) could be identified using microscopy (Riley J., pers. comm.). Therefore using chemical biomarkers, such as lipids, can give more information on the composition of particles and allow comparisons between slow and fast sinking pools using the same method.

Lipids are rich in carbon and can form up to 85 % of POC (Wakeham *et al.*, 2009) in the Mediterranean Sea. They have a large range in reactivity such that long-chain saturated fatty acids are relatively refractory and unsaturated fatty acids (with a C-C double bond) are more labile (reactive) (Jeffreys *et al.*, 2009). Many particle flux studies use lipids as biomarkers (Wakeham & Lee, 1989; Wolff *et al.*, 2011; Hernandez-Sanchez *et al.*, 2012) as they can be specific to their source (Wakeham & Canuel, 1988). Lipid biomarkers include fatty acids, sterols, alkenones and alcohols (Hernandez-Sanchez *et al.*, 2012).

In this chapter lipids were extracted from particles collected from the Eastern Tropical North Pacific (ETNP) oxygen minimum zone (OMZ) (Chapter 3). Images of fast sinking particles taken using a FlowCAM are used to identify the main types of large ($>$ 50 μm), fast sinking particles. They are then be compared with the biochemical composition of fast sinking, slow sinking and suspended particles. Lipid biomarkers are used to test the following hypotheses:

1. The composition of exported fast sinking particles is similar to those in the mixed layer (Fig. 4.2)

2. Slow sinking particles can be produced by the fragmentation of fast sinking particles (Fig. 4.2 and Chapter 3)

3. Diel vertical migration is reduced and not an important process in the biological carbon pump of OMZs (Chapter 3 and (Bianchi *et al.*, 2013))

4. The oxygen uptake (inferred lability) of particles is constant with depth

(Chapter 3).

4.3 Methods

Particles were collected from the ETNP oxygen minimum zone. Niskin bottles mounted on a Rosette were used to collect unconcentrated particles from the mixed layer (< 30 m) and Marine Snow Catchers (MSCs) were used to collect and concentrate exported particles (> 40 m). For details on the particle collection protocol and use of the FlowCAM see Chapter 3. Lipid samples were collected from the mesopelagic zone during day and night, but only from the mixed layer during the day. Fast sinking particles were collected from $\frac{1}{4}$ (600 mL) of the base tray and 2 L of suspended and slow sinking particles were filtered through GF/F filters, which were then dried and frozen at -80 °C onboard. Lipids were extracted at the University of Liverpool.

4.3.1 Lipid extractions

The frozen filters were freeze-dried (24 h) and stored (-20 °C). Extraction followed the method of Jeffreys *et al.* (2009). Whole filters were cut into small (approximately 5 mm width) pieces and placed in centrifuge tubes. The filters were spiked with 5 μL of 5αH-cholestane (101.42 ng L^{-1}), an internal quantification standard and the solvent mixture of dichloromethane (DCM):methanol (9:1, 3 mL). The centrifuge tubes were sonificated (30 mins) and centrifuged (5 mins, at 2500 rpm, 15 °C). This was repeated twice more, the extracts combined and the solvent evaporated using a rotary evaporator. The total lipid extract (TLE) was transferred to Reacti-vials by redissolving in approximately 3 mL of the 9:1 solvent mixture. The sample was transmethylated using methanol, previously cooled in an ice bath, and acetylchloride:methanol (1:40, 1 mL) added dropwise and then kept at 45 °C in the dark overnight (Christie, 1982). The methanol was removed under a stream of N_2 and once dry, the sample was neutralised by using DCM to transfer the sample from the Reacti-vials through a potassium carbonate column (Pasteur pipette). The remaining DCM was blown down with N_2 and 0.25 μL of BSTFA (*bis*-trimethylsilyl-trifluoroacetamide) was added to each sample and kept on a heating block for 1 hour at 60 °C. The samples were then stored in a freezer at - 20 °C until analysis.

The samples were redissolved in DCM and analysed firstly on a gas chromatograph (GC) to check their quality and then on a gas chromatograph mass spectrometer (GCMS). Aliquots of the TLE of samples were injected onto a Trace

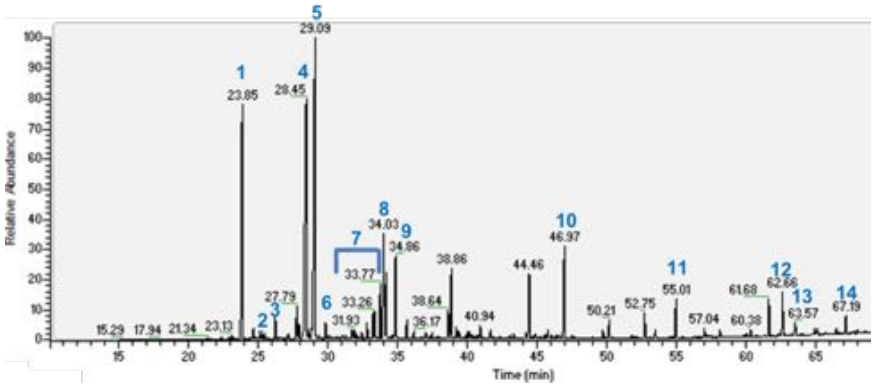

Figure 4.3: Chromatogram from a GCMS. This sample was from 50 m at night. The numbers above each peak represent the compounds identified: 1 = C14:0, 2 = *a*-C15:0 and *i*-C15:0, 3 = C15:0, 4 = C16:1, 5 = C16:0, 6 = C17:0, 7 = C18:1-4, 8 = C18:0, 9 = C18OH, 10 = a phthalate, 11 = Cholestane (internal standard), 12 = Cholesterol, 13 = Brassicasterol and 14 = Sitosterol. See appendix Table C.1 for more details on all lipid compounds identified.

2000 Series GC fitted with an on-column injector and a fused high-temperature silica column (60 m 0.25 mm i.d.; film: (5 % phenyl-methylpolysiloxane; DB5-HT equivalent; JW)) with helium as the carrier gas (ca. 1.6 mL min^{-1}). A retention gap of deactivated fused silica (1 m 0.32 mm i.d.) was used at the front of the column. The oven was programmed from 60 to 170 °C at 6 °C min^{-1} after 1 min, then to 315 °C at 2.5 °C min^{-1} and held for 10 min. The GC column was fed directly into the EI source of a Thermoquest Finnigan TSQ7000 mass spectrometer (ionisation potential 70 eV; source temperature 315 °C; trap current 300 μA), operated in Full Data Acquisition mode (50–600 Thompsons cycled every second). Xcalibur software was used to receive and process the data. Compounds were quantified by comparison of the peak areas of the internal standard (5αH-cholestane) with the peak areas of the compound and corrected for by their relative response factors (Kiriakoulakis *et al.*, 2004).

4.3.2 Compound quantification

Fatty acids (saturated, branched and unsaturated), alcohols and sterol compounds were identified and quantified. Fig. 4.3 shows a typical chromatogram, from a sample taken at 50 m at night offshore. Fatty acid notation is conventionally C#:#, with the first number representing the number of carbon atoms and the second the number of double bonds. Hence the notation of a saturated acid with 16 C atoms is C16:0 and for a unsaturated fatty acid with one double bond C16:1. Lower molecular weight compounds elute earlier on the chromatogram,

Table 4.1: Lipid biomarkers assigned to ecological groups. Biomarkers denoted by * are those assigned to detrital phytoplankton in Figs 4.13 and 4.15, although these can also be present in live phytoplankton cells.

Group	Biomarker	Reference
Zooplankton	C27D2,55, Cholesterol	(Jeffreys *et al.*, 2009)
Bacteria	*a*-C15:0, *i*-C15:0, *a*-C17:0, *i*-C17:0	(Jeffreys *et al.*, 2009)
Phytoplankton	C14:0, C16:0, C16:1, C18:0*, C18:1*, C18:2, C18:4	(Wakeham & Lee, 1989) (Tolosa *et al.*, 2013)
Terrestrial	C22:0, C24:0	(Holtvoeth *et al.*, 2010)

hence sterols with 27 - 29 C atoms appear towards the end (e.g. cholesterol and sitosterol). Short (< 20 C atoms) chains and double bonds indicate labile compounds and long-chain compounds with few or no double bonds are more refractory. Phthlates are plastic compounds that have entered the sample during sampling or lipid extraction. Cholestane is the internal standard.

Lipid mass (ng) was converted to concentration by dividing by the volume of water filtered. Concentrations were also normalised to POC to determine the percentage contribution of lipids to POC. Slow sinking particle lipids by definition include suspended particles. Multivariate analyses such as ANOSIM (analysis of similarities) were done using the program PRIMER-6. A Bray-curtis dissilimarity matrix was used and prior to analyses all data were log-transformed to best fit a Draftsman plot. ANOSIM compares the variation in sample composition in terms of a grouping factor such as, in this study, depth or time of day. All errors presented are one standard error of the mean.

16 compounds thought to specifically represent either phytoplankton (labile and/or detrital), zooplankton, bacteria and terrestrial higher (vascular) plants were used to identify the dominant group of biomarkers (Table 4.1).

4.4 Morphological composition: Results and Discussion

As discussed in Chapter 3, the FlowCAM was used to measure sinking rates of fast (> 20 m d^{-1}) sinking particles from the ETNP oxygen minimum zone. A by-product of this is a vast library of images of each particle, which was used to classify the particles.

Of the 810 particles measured, 759 were identifiable (Table 4.2). Phytoplank-

Table 4.2: Number of different exported particle types and mean sinking rates. Rates in parentheses are one standard error of the mean. Exoskeleton refers to zooplankton exoskeletons.

Particle type	n	Sinking rate (m d^{-1})
PDA	530	104 (9)
FP	114	90 (15)
Vascular plant	33	65 (16)
Zooplankton	32	120 (41)
Exoskeleton	17	86 (29)
Diatom cell	11	46 (14)
Gelatinous plankton	11	120 (73)
Pollen	7	159 (36)
Pteropod	4	296 (123)
Unidentified	51	65 (31)

ton detrital aggregates (PDAs) were the most abundant, followed by faecal pellets (FPs). Together these particles comprised 80 % of the fast sinking particle pool in the ETNP. The largest particle found was a PDA (Fig. 4.4) with an equivalent spherical diameter (ESD) of 2.4 mm. However there was a large size range of PDAs and the smallest particle was also a PDA at 32 μm ESD.

Some of the PDAs and FPs aggregated together as shown in Fig. 4.4 f, where at least 2 FPs can be seen protruding out of the PDA. This aggregation could be caused by transparent exopolymer particles (TEP) that are produced by phytoplankton and thought to enhance aggregation (Engel *et al.*, 2015). This gelatinous material could be responsible for forming the PDA in Fig. 4.4 d, where many PDA particles appear to be attached to one gelatinous object. Another type of gelatinous particle are discarded appendicularian houses (Alldredge, 1976), which are shed by the organism as the filters clog.

FPs are generally much more regular in shape than PDAs as shown by Fig. 4.5, although some were more degraded than others. For instance Fig. 4.5 a is less dense (lighter in colour) than Fig. 4.5 b and is less well defined. These FPs are likely from copepods, which are common in the ETNP (Wishner *et al.*, 2013). Also copepods tend to produce individual FPs as observed here, whereas krill produce FPs in long chains (Chapter 2).

Sinking zooplankton were observed, which would only happen if they were deceased as otherwise they would swim and be unlikely to enter the flow cell where the images were taken. However it is difficult to determine if the zooplankton died naturally in the water column or because of sampling by the MSC

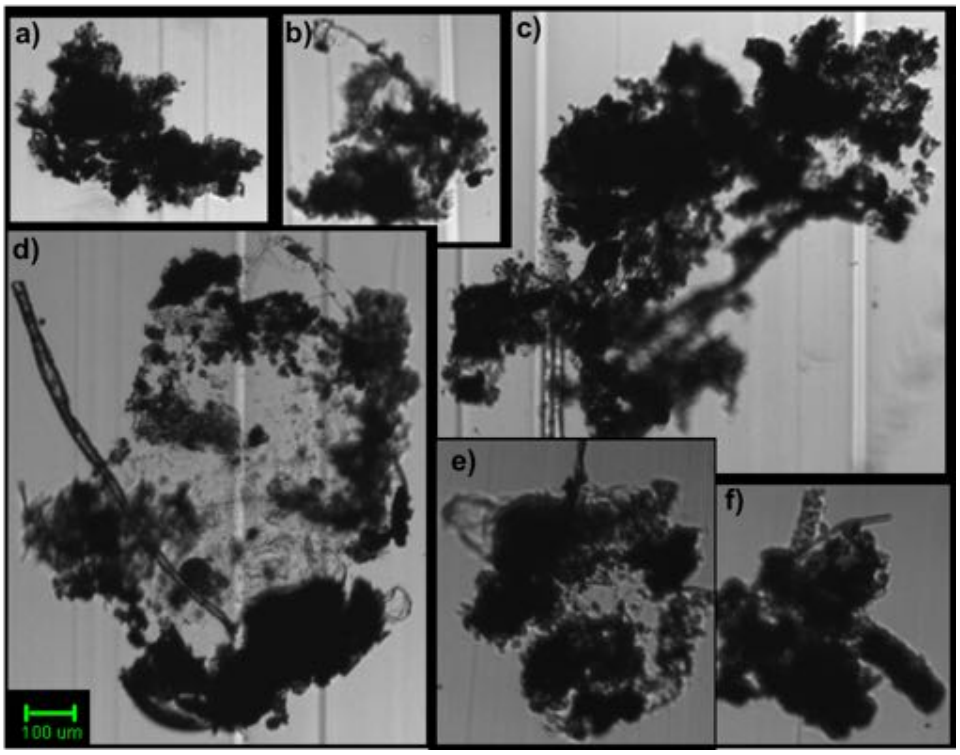

Figure 4.4: Phytodetrital aggregates. Gelatinous particles present in d) e) and faecal pellets in f). Green scale bar = 100 μm.

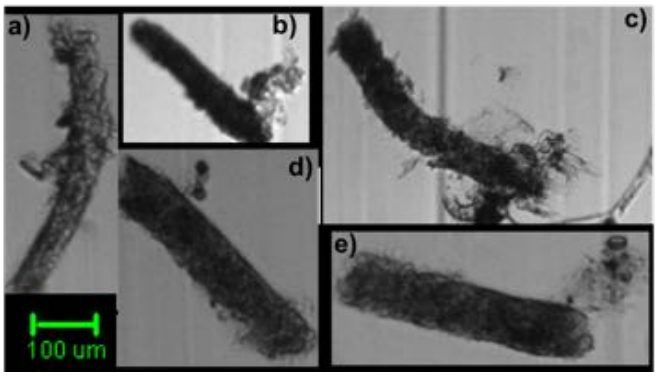

Figure 4.5: Faecal pellets. Green scale bar = 100 μm.

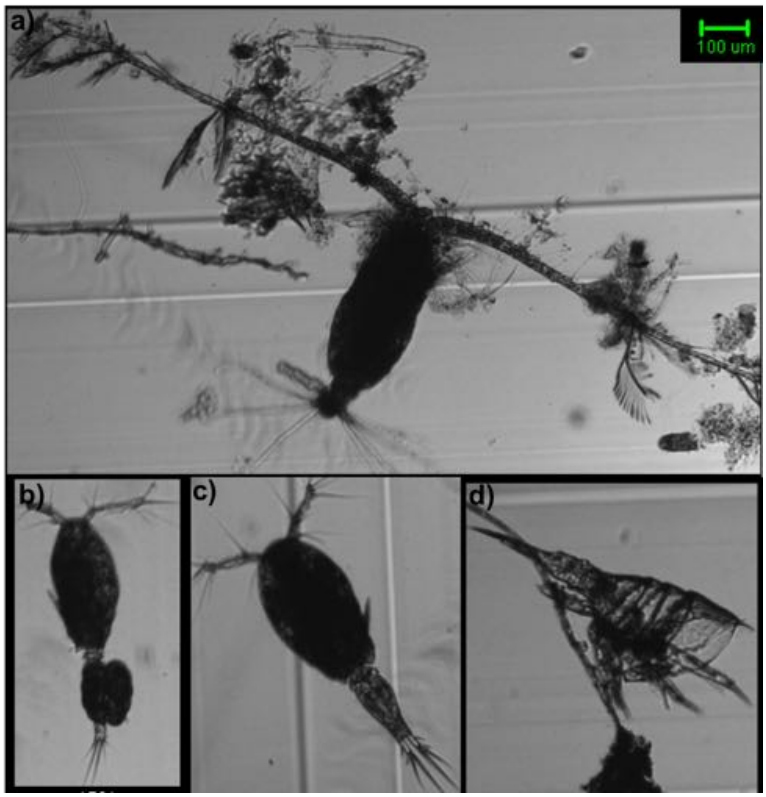

Figure 4.6: Sinking zooplankton: a) *Calanus* copepod, b) and c) *Oncaea* copepods and d) *Calanus* copepod exoskeleton. Green scale bar = 100 μm.

and processing in the ship's laboratories. The zooplankton in Fig. 4.6 are all copepods. The *Calanus* copepod in Fig. 4.6 a has many PDAs attached to its antenna, suggesting it had died prior to entering the MSC. However, the *Oncaea* copepod in Fig. 4.6 b has egg sacs on its abdomen and is not covered in detritus, suggesting it died because of sampling. Fig. 4.6 d shows a copepod exoskeleton; these are shed as zooplankton grow and are known to contribute to particle flux (Fowler, 1977).

Other less common particles were identified such as parts of vascular plants (Fig. 4.7 a), pollen (Fig. 4.7 b), pteropods (Figs. 4.7 c & d), diatom cells (Fig. 4.7 e) and gelatinous plankton (Fig. 4.6 f). Pteropods are free-living gastropods that occasionally form a large part of particle flux, either from their feeding nets or empty shells (Bathmann *et al.*, 1991).

4.4.1 Summary

These images are useful to identify the different types of large, fast sinking particles sinking through the mesopelagic zone. Phytodetrital aggregates dominated particle composition. This consolidates that zooplankton contribute a relatively small amount to particle flux compared with other oceanic areas, such

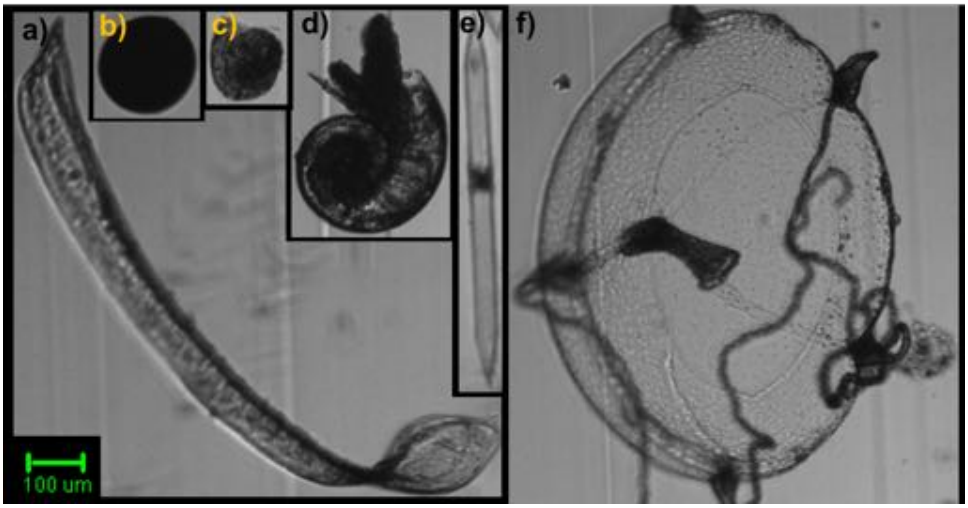

Figure 4.7: Other types of particles; a) vascular plant, b) pollen c) and d) pteropod, e) diatom and f) gelatinous plankton. Green scale bar = 100 μm.

as the Southern Ocean (Chapter 2).

4.5 Biochemical composition: Results and discussion

4.5.1 Total lipid concentration

Lipids were extracted from 90 particulate samples from the ETNP oxygen minimum zone. 11 of these were from Niskin bottle samples in the mixed layer, with the remainder from concentrated particles collected by the MSC that had been exported below the mixed layer.

Total (sum) particulate lipid concentrations ranged from 0.1 to 15.7 μg L^{-1}, with a mean of 2.4 ($\pm$ 0.3) μg L^{-1}, similar to those observed by Wakeham & Canuel (1988) in the ETNP OMZ ($< 3\mu$g L^{-1}). Saturated fatty acids (SFAs) were the largest and most abundant lipid group (Table 4.3), followed by labile poly-unsaturated fatty acids (PUFAs). Branched fatty acids were the least abundant compound class. Alcohols were not included in analyses presented as in 43 % of the samples alcohols were not present, possibly because they were below the detection limit. Lipids constituted on average (mean) 1.4 % ($\pm$ 0.01 %) of POC, with a range of 0.04 - 10 %. These results suggest particle lipid concentration and contribution to POC were relatively low in the ETNP. By contrast a study in the Northeast Atlantic showed lipid concentrations ranged from 36 to 135 μg L^{-1} (Mayzaud *et al.*, 2014) and in the Mediterranean lipid content was up to 27

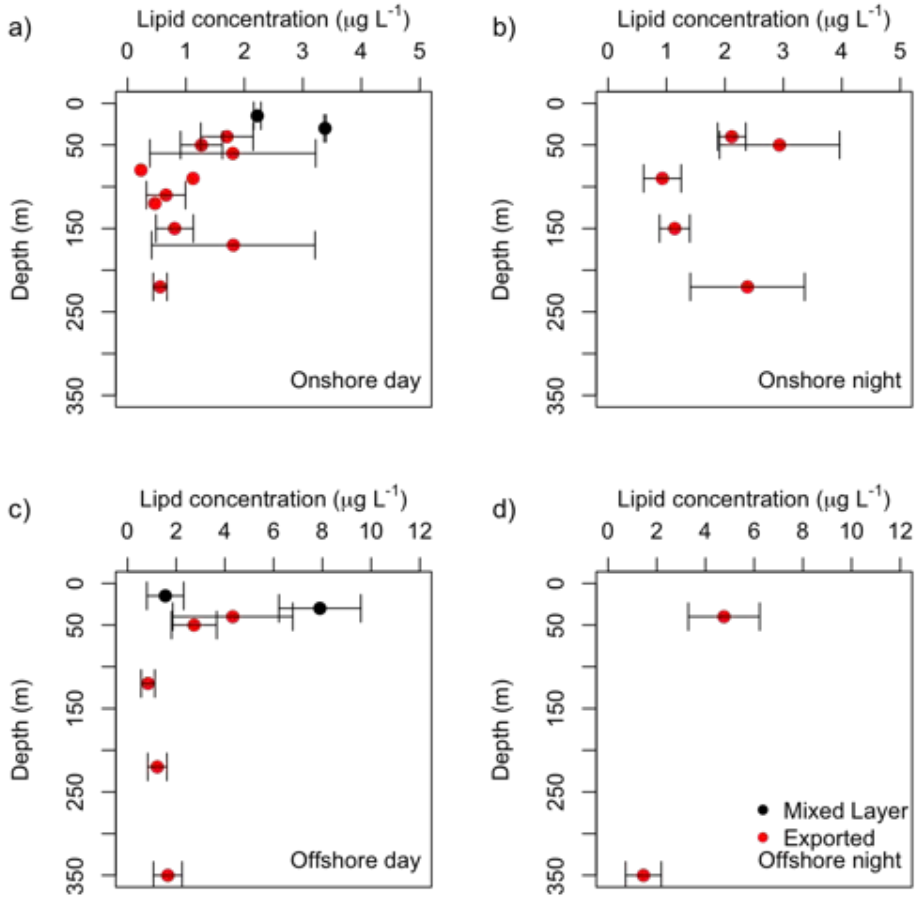

Figure 4.8: Total mean particle lipid concentration (μg L^{-1}) with depth for all particles a) onshore in the day, b) onshore at night, c) offshore in the day, d) offshore at night. Black points are particles collected using Niskin bottles in the mixed layer and red points from exported particles collected using the MSC. All points are means with one standard error shown by the error bars.

% of POC in sinking particles (Giani *et al.*, 2012). In the ETNP the remainder of the POC could be formed of carbohydrates from gelatinous substances (Engel *et al.*, 2015), which were seen in some the images of PDAs (section 4.4).

Both total lipid concentration and percentage of POC decreased with depth during the day (Figs. 4.8 & 4.9). Particles in the mixed layer (black points) generally had a higher lipid content than exported particles (red points). Particulate lipid concentrations were significantly ($p < 0.05$, $t = -2.4$, $df = 55$) higher offshore (mean = 3.1 $\pm$ 0.5 μg L^{-1}) than onshore (mean = 1.6 $\pm$ 0.3 μg L^{-1}), however there was no significant difference in the contribution of lipids to total POC on- and offshore. Lipid concentrations decreased considerably below 50 m in the upper mesopelagic zone where remineralisation is most intense (Martin

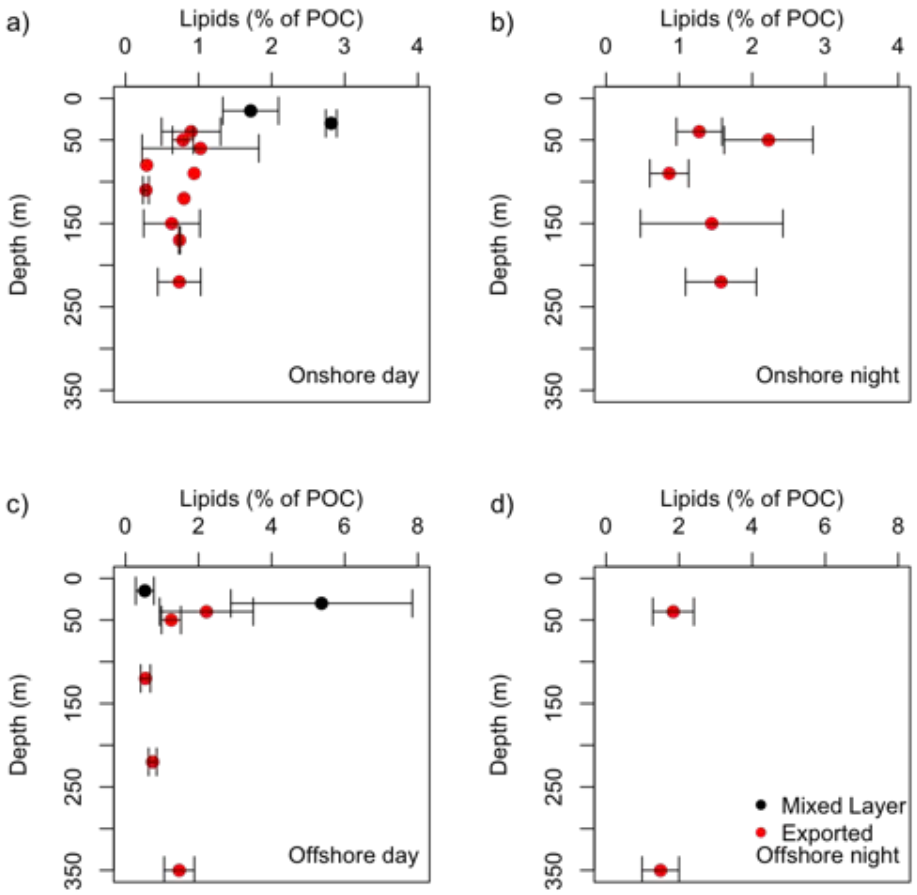

Figure 4.9: Total meant particle lipid percentage of POC) with depth for all particles a) onshore in the day, b) onshore at night, c) offshore in the day, d) offshore at night. Black points are particles collected using Niskin bottles in the mixed layer and red points from exported particles collected using the MSC. All points are means with standard error one shown by the error bars.

Table 4.3: Mean particle lipid concentrations with depth for mixed layer (ML) and exported particles (EXP). All concentrations are in μg L^{-1}. Numbers in parentheses are one standard error of the mean. SFA = saturated fatty acid, FA = fatty acid, MUFA = mono-unsaturated fatty acid and PUFA = poly-unsaturated fatty acid.

Fraction	Depth	Total lipids	SFA	Branched FA	MUFA	PUFA	Sterols
ML	15	1.89	0.94	0.01	0.64	0.22	0.01
		(0.37)	(0.20)	(0.003)	(0.18)	(0.07)	(0.01)
	30	6.09	3.47	0.03	1.32	0.79	0.10
		(1.44)	(0.85)	(0.01)	(0.43)	(0.17)	(0.1)
EXP	40	3.19	1.62	0.01	0.45	0.57	0.04
		(0.64)	(0.41)	(0.004)	(0.17)	(0.09)	(0.01)
	50	4.5	1.95	0.02	1.24	0.64	0.07
		(1.54)	(0.65)	(0.01)	(0.68)	(0.16)	(0.03)
	60	1.80	0.77	0.001	0.17	0.41	0.04
		(1.41)	(0.58)	(0.001)	(0.15)	(0.32)	(0.04)
	90	0.99	0.60	0.01	0.04	0.19	0.01
		(0.20)	(0.22)	(0.01)	(0.04)	(0.12)	(0.01)
	120	0.78	0.24	0.00	0.04	0.23	0.04
		(0.23)	(0.04)	(0.00)	(0.03)	(0.09)	(0.03)
	220	1.34	0.65	0.0004	0.07	0.28	0.01
		(0.33)	(0.14)	(0.0003)	(0.03)	(0.08)	(0.01)
	350	1.56	0.65	0.0004	0.07	0.28	0.01
		(0.44)	(0.19)	(0.002)	(0.04)	(0.20)	(0.02)

et al., 1987) during the day, but were fairly constant at night. Although few depths were measured at night and no mixed layer samples were taken. The decrease in POC lipid content with depth suggests lipids can be a preferred energy source of heterotrophic organisms, particularly labile short-chain SFAs, MUFAs (mono-unsaturated) and PUFAs (Holtvoeth *et al.*, 2010).

45 different lipid compounds were identified (Appendix Table C.1). The SFA C16:0 had the highest concentration and was present in all 90 samples, with a mean concentration of 0.6 ($\pm$ 0.008) μg L^{-1}, followed by the MUFA C16:1 (0.3 $\pm$ 0.007 μg L^{-1}). The C18 SFA, MUFAs and PUFAs were also abundant. The PUFAs eicosapentaenoic acid (EPA) and docosahexaenoic acid (DHA), biomarkers of the phytoplankton groups diatoms and dinoflagellates respectively, (Okuyama *et al.*, 2008) were absent from all samples. These two lipids are often abundant in ocean particles (Fileman *et al.*, 1998) and because of their high lability, their concentrations rapidly decline with depth (Mayor *et al.*, 2014). This suggests a different phytoplankton group may have dominated the phytoplankton community, such as cyanobacteria, which are high in C16:0 and C16:1 (Wakeham, 1995), and abundant (up to 160 x 10^6 cells L^{-1}) in the ETNP (Goericke *et al.*, 2000).

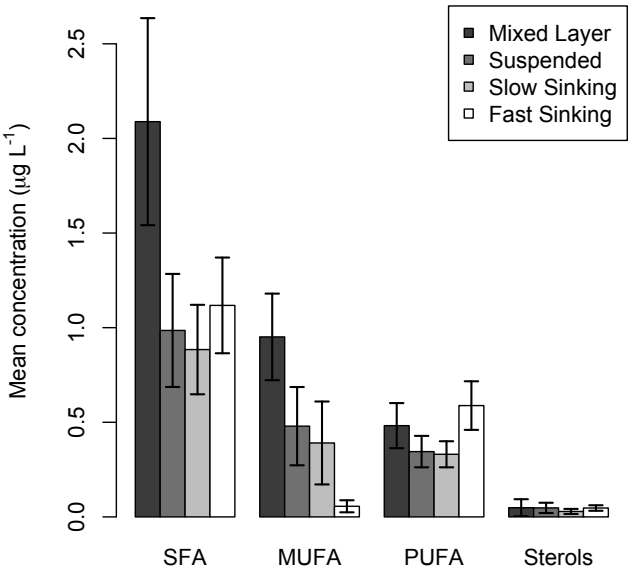

Figure 4.10: Fatty acid concentrations across particle fractions. SFA = saturated fatty acids, MUFA = mono-unsaturated fatty acid, PUFA = poly-unsaturated fatty acid. Error bars are standard error of the mean.

C16.1 made a significantly higher contribution ($p < 0.05$, $t = -2.4$, $df = 12$) to mixed layer particles (0.7 μg L^{-1}) than exported particles (0.2 μg L^{-1}). Moreover, ANOVA (analysis of variance) results show C16.1 concentrations were significantly lower in the fast sinking fraction ($F_{3,86} = 3.5$, $p < 0.05$) than the suspended and slow sinking fraction. C16.1 contributed the most to the total MUFA concentration and Fig. 4.10 highlights the difference in MUFA concentration across the different particle fractions.

Cholesterol, a biomarker for heterotrophy (Cavagna *et al.*, 2013), was the most abundant sterol, with a mean of concentration of 0.2 ($\pm$ 0.01) μg L^{-1}. The sterol representing autotrophy, brassicasterol (Cavagna *et al.*, 2013), was less abundant and in low concentration (mean = 0.06 $\pm$ 0.0006 μg L^{-1}).

4.5.2 Particle composition

Using lipids as biomarkers allowed comparisons between all three particle fractions: suspended, slow sinking and fast sinking and between particles from the mixed layer and those exported.

Multivariate analyses were used to examine differences in particle lipid composition between samples using the following factors: day *vs.* night, onshore *vs.* offshore, sampling depth and particle fraction. The data were log-transformed to

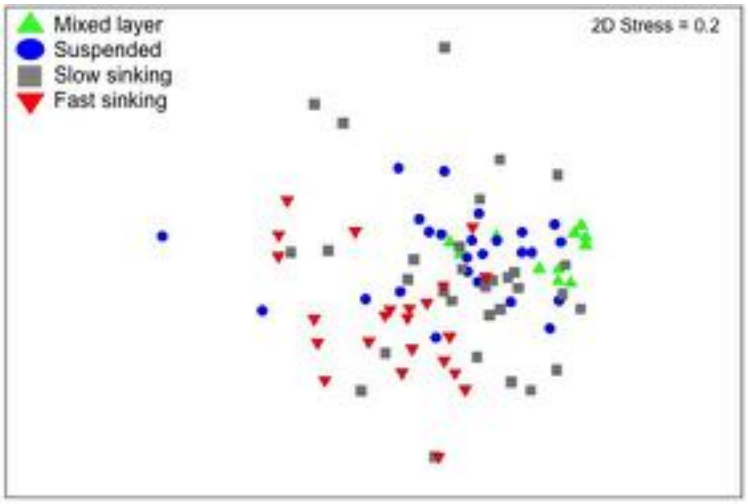

Figure 4.11: Multi-dimensional scaling (MDS) plot of all lipid samples by fraction. Green triangles = mixed layer particles, blue circles = suspended particles, grey squares = slow sinking (and suspended) particles and red inverted triangles = fast sinking particles. 2D stress = 0.2.

produce a normal distribution. An analysis of similarities (ANOSIM) was used to test for differences in lipid composition (using all compounds except the alcohols, new n = 33) and showed that there was no significant difference in particle composition due to the time of day, area or depth. The ANOSIM result showed that lipid composition was actually statistically similar with depth ($p < 0.01$ and $R = 0.12$). R values close to 1 indicate a very different composition and R values close to 0 a very similar composition.

There was a significant difference in lipid composition between the different particle fractions. The greatest difference was between mixed layer and exported fast sinking particles ($p < 0.001$ and $R = 0.55$). Particle composition increased in similarity as sinking speed increased, such that the similarity between suspended and fast sinking particles was $R = 0.33$ ($p < 0.01$) and between slow sinking and fast sinking particles $R = 0.13$ ($p < 0.01$). The multi-dimensional scaling plot (Fig. 4.11) emphasises this as only two fast sinking samples overlap with those from the mixed layer. There are few lipid studies on particles of different settling velocities and none in the ETNP. One study used an indented rotating sphere trap (Chapter 1) in the Mediterranean to show sinking velocity had little effect on particle lipid concentration or composition (Wakeham *et al.*, 2009). However only exported particles were sampled.

According to SIMPER (similarity percentages) analysis the most abundant

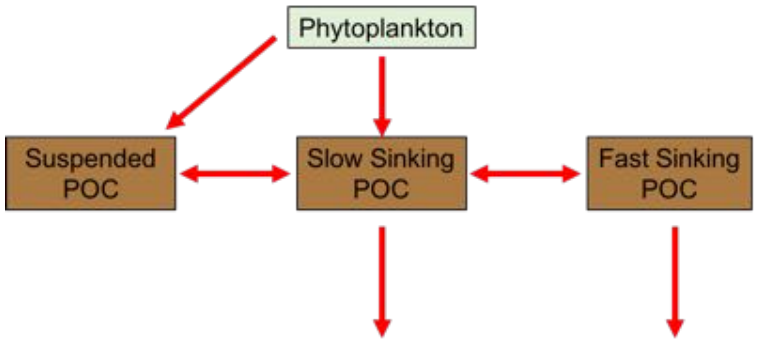

Figure 4.12: Revised interactions between sinking POC for the ETNP. In low latitude environments dominated by small phytoplankton, large fast sinking particles are formed from aggregation of slow sinking particles, not directly from fresh phytoplankton.

(cumulative abundance of 50 % of total) lipid compounds in the mixed layer were short-chain labile compounds: C16:0, C16:1, C18:0 and C18:1. For the fast sinking particles C16:1 was not abundant forming < 2 % of total lipid composition, but cholesterol was (18 %). The difference between mixed layer and fast sinking particles could be because exported particles are reworked extensively, hence their composition no long represents those of fresh particles in the mixed layer. However the microbial respiration rates presented in Chapter 3 show slow sinking particles are turned over much more rapidly than fast sinking in the OMZ, yet their lipid composition was not different from those in the mixed layer ($p > 0.05$, ANOSIM). Further zooplankton reworking of particles is likely low in OMZs (Chapter 3). Therefore the observed difference in composition suggests fast sinking particles are not formed from fresh phytoplankton in the ETNP.

This result challenges the hypothesis that fast sinking particles are produced in the mixed layer by phytoplankton, as shown in temperate regions (Billett *et al.*, 1983) and suggests, at least in the ETNP, fast sinking particles are a product of smaller, slow sinking particles aggregating. In tropical, low latitude oceanic environments small phytoplankton, possibly here cyanobacteria (< 2 μm diameter), dominate the phytoplankton community. This further alters our understanding of particle formation, suggesting that in the tropical oceans fast sinking particles are likely formed from the aggregation of smaller, slower sinking

particles (Fig. 4.12). This rejects the first hypotheses; that the composition of exported fast sinking particles is similar to particles in the mixed layer. The second hypothesis (slow sinking particles can be produced by the fragmentation of fast sinking particles) is confirmed by the significant similarity of the slow and fast sinking particles. This was also shown by the conservation of the C:N in both sinking pools (Chapter 3). Small, slow sinking parties have previously been found at depth (< 500 m) by Durkin *et al.* (2015) but the authors could not give a conclusive reason as to why. Results presented in this thesis suggest the continuous aggregation and disaggregation of particles. Much earlier work has documented the continuous aggregation and disaggregation of particles (Cochran *et al.*, 1993), however these processes are often not parametrised in ecological models.

4.5.3 Ecological groups

Certain lipid biomarkers can be diagnostic of different ecological groups (see section 4.3.2). Here 16 different compounds that represent either marine phytoplankton, marine zooplankton, bacteria or terrestrial plants were used. The phytoplankton group was split into labile and detrital. Assigning lipids in this way is complex as some lipids can represent both labile and detrital phytoplankton, hence phytoplankton are represented as one group with a possible distinction detrital and labile (Fig. 4.13).

Phytoplankton lipids biomarkers dominated the lipid composition, comprising over 80 % in the mixed layer (15 - 30 m, Fig. 4.13), which reduced to about 60 % in the mesopelagic zone and OMZ (> 50 m, Fig. 4.13). This decrease was either due to decreases in the relative amounts of phytoplankton biomarkers or increases in zooplankton biomarkers. Labile phytoplankton biomarkers such as PUFAs decrease rapidly with depth as they are preferentially metabolised by zooplankton (Lampitt *et al.*, 1990; Mayor *et al.*, 2014). In this study PUFAs (C18) from the exported particles were lower in concentration than those in the mixed layer (Fig. 4.14) and mostly decreased with depth. These results concur with those from the morphological analysis (section 4.4) that phytoplankton-derived particles dominated flux.

Crustaceous zooplankton are low in abundance in OMZs and have little interaction with particles at depth (Wishner *et al.*, 2013; Williams *et al.*, 2014). However gelatinous zooplankton such as jellyfish and salps that thrive in warm

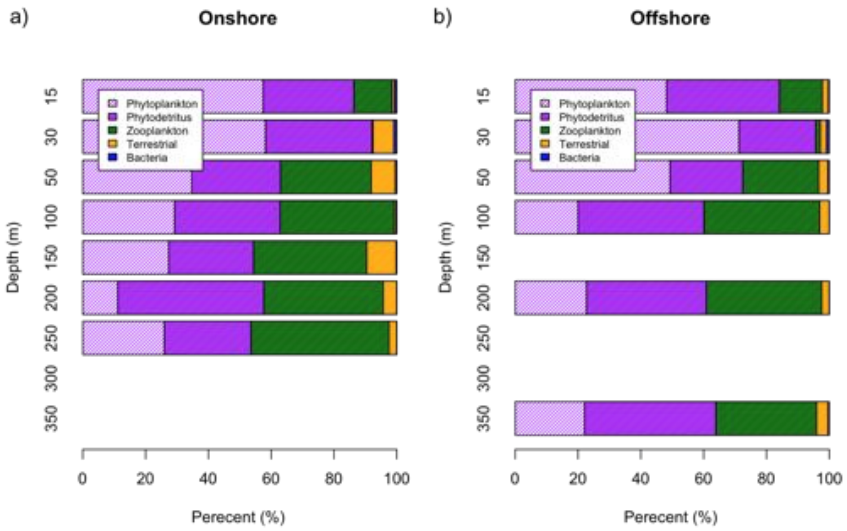

Figure 4.13: Lipid composition with depth separated by site, a) onshore and b) offshore. The percentage contribution of each group at each depth is averaged over all corresponding samples so n is on average 3 - 4 samples per depth. Samples at depths 15 and 30 m are from the mixed layer and those below are exported particles. The purple bars show phytoplankton biomarkers, with a possible distinction between fresh or detritus, see text for more details.

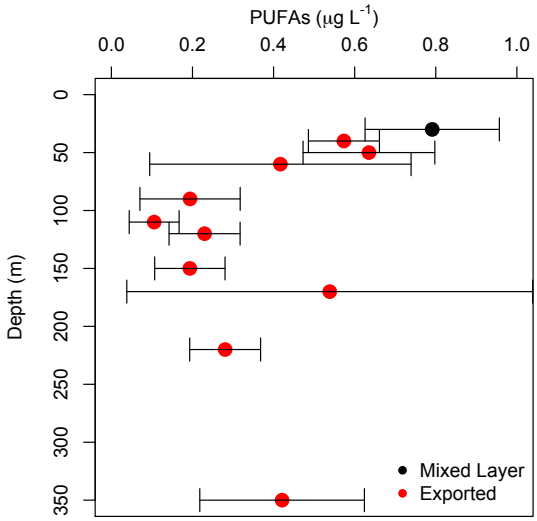

Figure 4.14: Particle poly-unsaturated fatty acid concentration (μg L^{-1}). Solid black circles are from particles sampled in the day and open circles from particles sampled at night. All points are means with standard error shown by the error bars.

waters (Richardson, 2008), could be responsible for an increase in the zooplankton biomarkers. Although salps were not sampled, they are abundant in this region and many were seen in the surface waters from the ship and some became attached to the outside of the MSCs. The largest (by concentration) biomarker assigned to the zooplankton group was cholesterol, the sterol that represents heterotrophy. The zooplankton signal is similar with depth, suggesting zooplankton (crustaceous and/or gelatinous) rework the particles after they've been exported from 50 m, where the dissolved O_2 concentration is 160 μmol kg^{-1}, and the signal remains in the particles as it sinks through the oxygen minimum zone. Any further heterotrophy at depth in low O_2 regions is either by salps or microbial organisms.

The sampling stations were close (50 - 60 nautical miles) to the coast of Guatemala, hence terrestrial higher (vascular) plants formed up to 20 % of lipid composition. Bacteria biomarkers were the smallest group, although the biomarkers that represent bacteria (branched SFAs) are always in low abundance relative to straight-chain SFAs, so using lipids might not be the best method to compare bacteria with zooplankton or phytoplankton (Wakeham, 1995). Particularly as bacteria are known to be in high concentrations on particles (Alldredge & Youngbluth, 1985), which is not represented by these results.

As the particle fraction (mixed layer and exported suspended, slow or fast sinking particles) significantly influenced the lipid composition (ANOSIM results) the ecological groups were separated for each fraction (Fig. 4.15). Mixed layer composition can be seen in Fig. 4.13 at 15 and 30 m. This further consolidates the view that the greatest difference in composition is between the mixed layer and all exported particles (Fig. 4.15). Slow sinking lipids comprised mostly heterotrophic zooplankton biomarkers at 350 m, whereas fast sinking lipids comprised mostly phytoplankton at the same depth. This may be explained by the extremely rapid reworking of slow sinking cells by heterotrophic microbes compared to fast sinking cells (Chapter 3). Phytoplankton biomarkers remained the highest component of lipid composition across all mixed layer and exported particles.

4.5.4 Ecological processes

Lipid biomarkers can be used to assess whether some ecological processes are occurring. The following analyses only use concentrated exported particles,

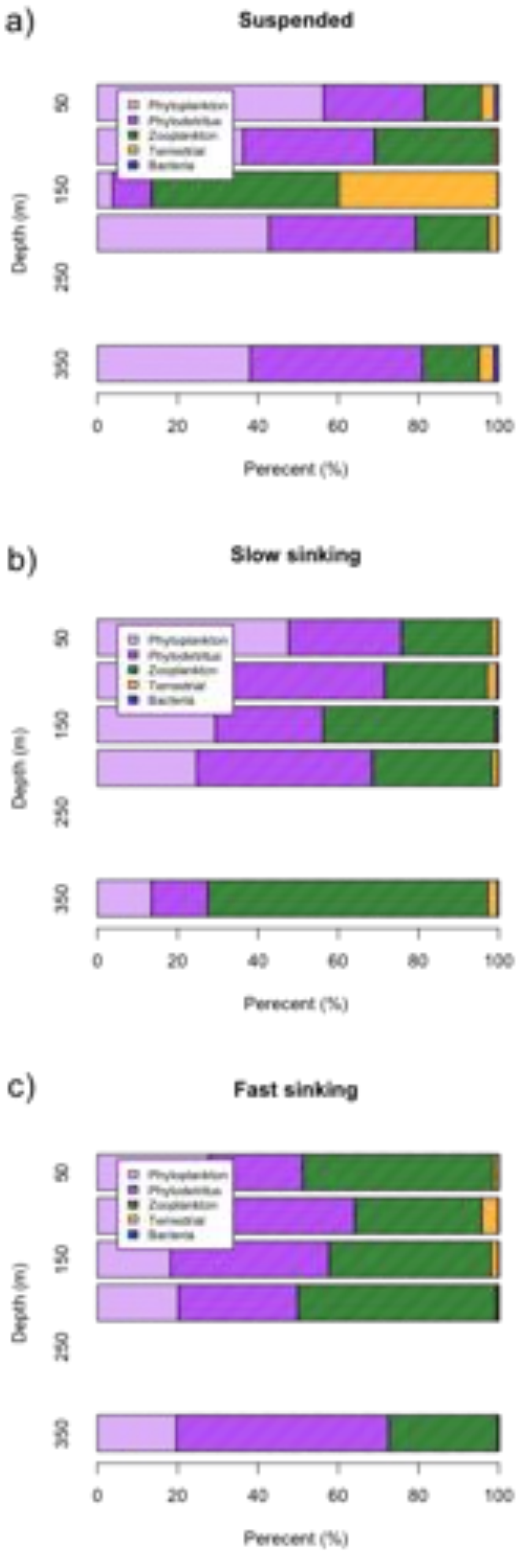

Figure 4.15: Particle lipid composition with depth separated by fraction, a) suspended, b) slow sinking and c) fast sinking particles. The percentage contribution of each group at each depth is averaged over all corresponding samples so n is on average 5 samples per depth. The purple bars show phytoplankton biomarkers, with a possible distinction between fresh or detritus, see text for more details.

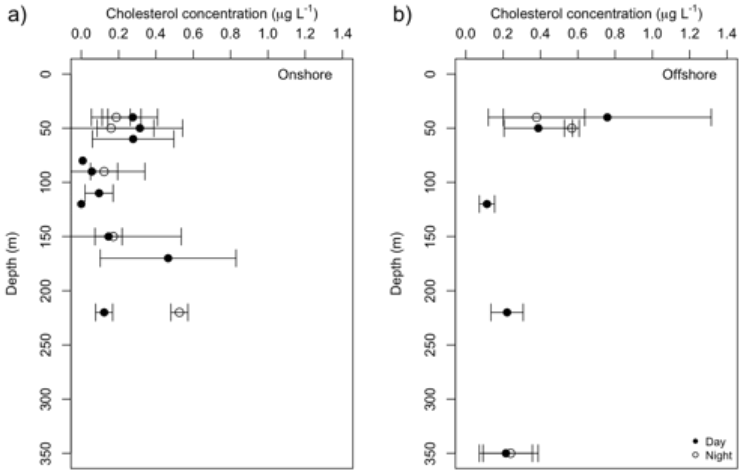

Figure 4.16: Cholesterol concentrations (μg L^{-1}) with depth for evidence of particle reworking by vertically migrating heterotrophic organisms; a) onshore b) offshore. Solid black circles are from particles sampled in the day and open circles from particles sampled at night. All points are means with standard error shown by the error bars.

not those from the mixed layer. One useful tool is the heterotrophic biomarker cholesterol to determine if zooplankton diel vertical migration occurs and influences particle flux (hypothesis 3). Although DVM by crustaceous zooplankton is thought to be limited in OMZs (Bianchi *et al.*, 2013; Wishner *et al.*, 2013), salps also undergo DVM, and may affect POC fluxes through the mesopelagic zone (Wiebe *et al.*, 1979).

If DVM was occurring in the ETNP and organisms were feeding at the surface at night, concentrations of cholesterol would be expected to be higher in the upper water column at night than in the day. Fig. 4.16 shows that both onshore and offshore there was no significant difference (t-test, $p > 0.05$) in particulate cholesterol concentration between day (solid circles) and night (open circles). Cholesterol concentration was marginally higher at the surface in the day *vs.* night in both areas suggesting DVM is not a prominent process in this region as hypothesised. Further there was no significant relationship (linear regression, $p > 0.05$) between cholesterol and the fast sinking, aggregate or faecal pellet flux. Zooplankton DVM is more likely to be limited in OMZs compared to temperate or polar waters where it strongly influences the particle flux (Steinberg *et al.*, 2008).

Another useful ecological index is the lability or reactivity of particles. This was measured using microbial oxygen uptake in Chapter 3, where it was con-

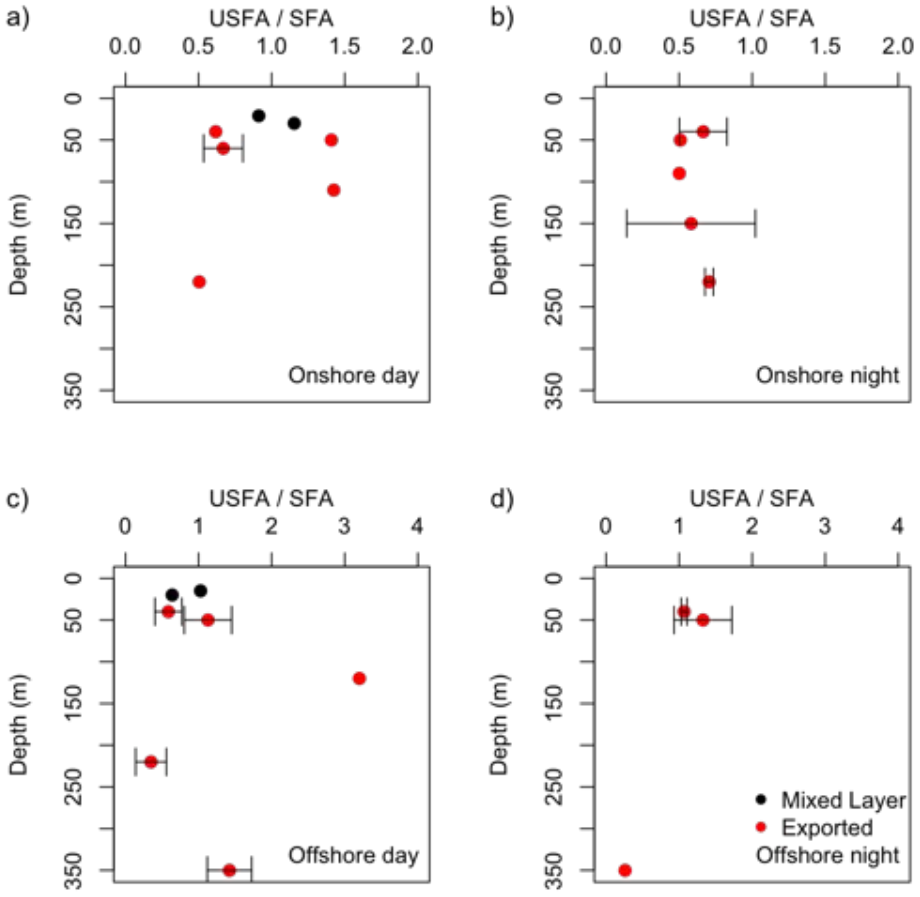

Figure 4.17: Lability index with depth (USFA/SFA); a) onshore in the day, b) onshore at night, c) offshore in the day, d) offshore at night. Black points are particles collected using Niskin bottles in the mixed layer and red points from exported particles collected using the MSC. All points are means with standard error shown by the error bars. USFA = unsaturated fatty acids and SFA = saturated fatty acids.

cluded that lability was constant with depth. Here the lability index (Jeffreys *et al.*, 2009) (the ratio of unsaturated (mono and poly) fatty acids (USFAs) to saturated fatty acids (SFAs)) was used to test if the estimate of a constant lability with depth was correct (hypothesis 4). Unsaturated fatty acids have C-C double bonds, which are relatively more reactive than C-C single bonds, thus USFAs are classified as labile and reactive compounds (Sun *et al.*, 1997). Saturated fatty acids do not have any double bonds and so are more refractory compounds. Therefore a USFA:SFA greater than one suggests particles are labile and a USFA:SFA less than one suggests particles are more refractory.

There was no clear pattern of particle lability with depth in the ETNP, reiterating the results from Chapter 3 (Fig. 4.17). Onshore lability decreased from day to night. Particles from the mixed layer were not more labile than the those which were exported, even though the mixed layer should have fresher, more labile phytoplankton than the mesopelagic zone, where photoautotrophy cannot occur. The lability index mostly ranged from 0.5 - 1.5 suggesting the particles were neither very labile nor very refractory, but they were generally more labile than at the Pakistan Margin OMZ (lability index < 1) (Jeffreys *et al.*, 2009).

4.6 Summary

Both the morphological and biochemical analyses of particle composition show phytoplankton-derived particles dominated flux. This shows how lipids can be useful biomarkers for otherwise amorphous material. The most important finding was that exported fast sinking particles were most dissimilar to mixed layer particles. This suggests that in the ETNP, and likely other low latitude, tropical environments dominated by smaller phytoplankton, fast sinking particles are formed from the aggregation of small, slowly sinking particles. Particles in the ocean are continuously aggregating and disaggregating, changing size, sinking rate and density. Often particles are thought to be either fast or slow sinking, large or small. While this may be the simplest and most robust way to model particle fluxes, it is important to appreciate that the natural environment is much more complex. It is probable that models may need to be enhanced, to fully replicate the complex and continuous cycling between particles of different sizes and sinking speeds. This will be discussed more fully in Chapter 5.

Acknowledgements

Thanks to George Wolff and Anu Thompson at the University of Liverpool for accommodating me and all of their help with lipid extractions. Without it this chapter would not have been possible. Thanks also to Rachel Jeffreys for her advice on the interpretation of the lipid biomarker results.

Chapter 5

The role of zooplankton in determining the efficiency of the biological carbon pump

5.1 Overview

In this chapter POC fluxes calculated for the Southern Ocean (Chapter 2) and the equatorial Pacific (Chapter 3), were combined with previously undescribed data from the North Atlantic and compared with an ecosystem model output. Zooplankton processes are poorly parameterised in the model, with the only interactions being the production of faecal pellets or grazing on slow sinking particles. Fragmentation, active flux and grazing on fast sinking particles are not parameterised. Therefore any differences between the observations and model are highly likely to be driven by zooplankton.

5.2 Introduction

The biological carbon pump plays an important role in regulating atmospheric carbon dioxide levels (Parekh *et al.*, 2006; Kwon *et al.*, 2009). Phytoplankton in the surface ocean fix inorganic carbon during photosynthesis to particulate organic carbon (POC), a fraction of which is then exported out of the upper ocean. As particles sink through the interior ocean they are subjected to remineralisation by heterotrophs, such that only a small proportion of surface produced POC reaches the deep ocean (Martin *et al.*, 1987). The efficiency of the biological carbon pump (BCP*eff*; defined as the proportion of surface primary production that is transferred to the interior ocean) therefore affects the air-sea partitioning

of CO_2 (Kwon *et al.*, 2009). Greater understanding of the controls of BCP*eff* may result in more accurate assessments of the BCP's role in the global carbon cycle.

One approach to determine BCP*eff* over long time scales (millennia) is to use the fraction of a nutrient (either nitrate or phosphate) from upwelling waters that is removed from surface waters by biological uptake (Hilting *et al.*, 2008). However to assess BCP*eff* over much shorter timescales (days to weeks) the definition by Buesseler & Boyd (2009) is used where BCP*eff* is the product of particle export efficiency (PE*eff*, the ratio of exported flux to mixed layer primary production) and transfer efficiency (T*eff*, the ratio of deep flux to exported flux). Using these two parameters together allows a more in-depth analysis of the biological processes involved and thus the assessment of the role of zooplankton in setting BCP*eff*. Additionally the attenuation coefficients Martin's b (Martin *et al.*, 1987) and z^* (Boyd & Trull, 2007) are useful to deduce how much exported POC is remineralised in the mesopelagic zone.

PE*eff* varies proportionally to primary production, although discrepancies exist as to whether the relationship is inverse or positive (Aksnes & Wassmann, 1993; Laws *et al.*, 2000; Maiti *et al.*, 2013; Henson *et al.*, 2015; Le Moigne *et al.*, 2016). Potential controls on PE*eff* include temperature (Laws *et al.*, 2000; Henson *et al.*, 2015), zooplankton grazing (Chapter 2), microbial cycling (Le Moigne *et al.*, 2016), mineral ballasting (Armstrong *et al.*, 2002; François *et al.*, 2002; Le Moigne *et al.*, 2014) or export of dissolved organic carbon (Maiti *et al.*, 2013). T*eff* and POC attenuation coefficients describe how much of the exported POC reaches the deep ocean and how much of it is remineralised. The attenuation of POC with depth is influenced by the sinking rates of particles and how rapidly the POC is turned over (Boyd & Trull, 2007). However, these factors themselves are controlled by various other environmental factors such as ballasting by minerals (François *et al.*, 2002; Le Moigne *et al.*, 2012), epipelagic community structure (Lam *et al.*, 2011), temperature (Marsay *et al.*, 2015), lability of the particles (Keil *et al.*, 2016) or zooplankton diel vertical migration (Chapter 2). Therefore it is unlikely that any single factor controls BCP*eff*.

The role of zooplankton in controlling the efficiency of the BCP is overlooked, with greater focus on factors such as biominerals for ballasting (De La Rocha & Passow, 2007), or microbial respiration (Herndl & Reinthaler, 2013). Nevertheless

zooplankton are an important part of the biological carbon pump as they can consume and completely transform particles (Lampitt *et al.*, 1990). Grazing by zooplankton results in POC either passing through the gut and being egested as a faecal pellet, being respired as CO_2 or fragmented into smaller particles through messy feeding (Lampitt *et al.*, 1990). Some zooplankton also undergo diel vertical migration (DVM), feeding on particles at night in the surface and egesting them at depth during the day (Wilson *et al.*, 2013). Consequently a significant proportion of POC may escape remineralisation in the upper mesopelagic zone where recycling of POC is most intense (Martin *et al.*, 1987).

In this chapter observations and model output are combined to investigate the role of zooplankton in setting the efficiency of the biological carbon pump in three contrasting oceanic regions. These are: the Atlantic sector of the Southern Ocean (SO), the Porcupine Abyssal Plain (PAP) site in the temperate North Atlantic and the Equatorial Tropical North Pacific (ETNP) oxygen minimum zone. The ecosystem model used here, MEDUSA (Yool *et al.*, 2013), was chosen as it separates particle fluxes into slow and fast sinking. Additionally the only interactions between zooplankton and particles in MEDUSA are through the production of particles (faecal pellets) and by grazing on slow sinking particles. Here various parameters of BCP*eff* are compared between the observations and model output to infer the role of zooplankton in controlling BCP*eff* and to determine if zooplankton processes should be enhanced in models.

5.3 Methods

5.3.1 Site description

The three sites used in this study were: the Atlantic sector of the Southern Ocean (Chapter 2), the temperate North Atlantic (49 °N, 16.5 °W) and the Equatorial Pacific oxygen minimum zone (Chapter 3) as shown in Fig. 5.1. The Southern Ocean (SO) accounts for 20 % of the global ocean CO_2 uptake (Takahashi *et al.*, 2002; Park *et al.*, 2010) and is a large high-nutrient-low-chlorophyll region, likely due to limited iron availability (Martin, 1990). Nevertheless, iron from oceanic islands and melting sea ice can cause intense phytoplankton blooms, which may lead to high POC export (Pollard *et al.*, 2009). In the temperate North Atlantic seasonality is high, with phytoplankton blooms occurring in spring and summer (Lampitt *et al.*, 2001). Here the Porcupine Abyssal Plain (PAP) observatory was sampled in the Northeast Atlantic, a region which contributes

disproportionally to global export with 5 – 18 % of the annual global export occurring here (Sanders *et al.*, 2014). In the equatorial tropical north Pacific (ETNP) region, a strong oxygen minimum persists between 50 and 950 m where dissolved oxygen concentrations fall below 2 μmol kg^{-1} (Paulmier & Ruiz-Pino, 2009). In OMZs the low oxygen concentrations lead to a high transfer efficiency of POC (Hartnett *et al.*, 1998; Devol & Hartnett, 2001; Van Mooy *et al.*, 2002; Keil *et al.*, 2016).

5.3.2 Observations

Particles were collected using Marine Snow Catchers (MSCs) from the 3 different oceanic sites. In total 27 stations were sampled, 18 in the SO, 5 at PAP and 4 in the ETNP (Appendix Table D.1). MSCs were deployed below the mixed layer depth (MLD), which was determined subjectively as the depth with the steepest gradient of salinity and temperature, between 20 and 70 m. The shallowest MSC was deployed 10 m below the MLD and another 100 m deeper than this for the Southern Ocean and the PAP site. In the ETNP MSCs were also deployed deeper into the water column to a maximum depth of 220 m. Primary production (PP) was estimated from satellite-derived data using the Vertically Generalised Productivity Model applied to MODIS data (Behrenfeld & Falkowski, 1997).

POC fluxes in the SO and ETNP have already been described in Chapters 2 and 3 respectively. This chapter includes new *in situ* data from the PAP site, however the sampling protocol and methods were the same as in Chapter 2.

5.3.3 Model output

The ecosystem model MEDUSA (Yool *et al.*, 2013) was used as it distinguishes detrital fluxes into two pools, fast and slow sinking. In the model fast sinking particles sink quicker than one time-step of the model and are remineralised instantaneously at all depths with the flux profile determined by a ballast model (Armstrong *et al.*, 2002). Slow sinking particles sink at 3 m d^{-1} and remineralisation is temperature dependant, with zooplankton grazing on slow sinking particles but not on the fast sinking particles. Zooplankton DVM is not parameterised. Primary production is modelled as non-diatom and diatom production, which is summed to give the total depth-integrated primary production. The model was run in hindcast mode at $\frac{1}{4}^{\circ}$ spatial resolution and output saved with a 5-day temporal resolution. The model output was extracted at the same locations as the observations were made and averaged over 12 years (1994 - 2006)

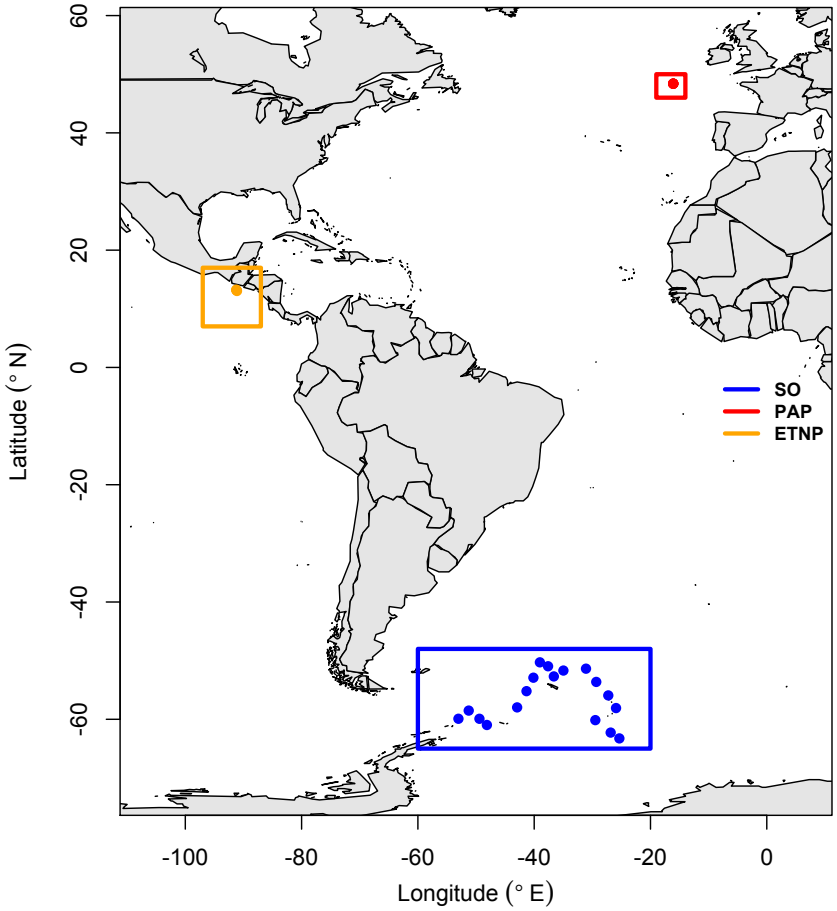

Figure 5.1: Map of ocean sites sampled. Blue rectangle shows the area in Scotia Sea sampled, the red square the Porucpine Abyssal Plain and the orange square the Equatorial Tropical North Pacific. Points show individual sampling stations.

to give the climatological seasonal cycle. The model outputs fluxes of particulate organic nitrogen (mg N m^{-2} d^{-1}) which were converted to POC (mg C m^{-2} d^{-1}) using the Redfield ratio (Redfield 1934).

5.3.4 Data manipulation

For both the observations and the model outputs the fast and slow sinking fluxes were summed to calculate the total sinking POC flux. Model output was available at fixed depths of 100 and 200 m, which introduces an offset with our at-sea observations (Appendix Table D.1). Therefore this study is assessing the role of zooplankton on the upper ocean BCP*eff*. Parameters calculated to test the efficiency of the biological carbon pump were the percentage contribution of fast and slow sinking particles to the total sinking flux, particle export efficiency (PE*eff*), the attenuation of flux with depth expressed as b and z^* and transfer efficiency (T*eff*).

PE*eff* is the proportion of surface produced primary production that is exported out of the mixed layer (observations) or at 100 m (model) and is calculated by dividing the exported flux by primary production. To estimate the attenuation of flux over the upper mesopelagic zone the exponents b and z^* were calculated following the functions of Martin *et al.* (1987) & Boyd & Trull (2007) respectively. The b exponent is dimensionless and generally ranges from 0 to 1.5 with low values indicating low attenuation, thus low remineralisation, and higher values representing high attenuation and remineralisation. The z^* (m) exponent is the remineralisation length scale, or the depth by which only 37 % of the reference flux (here at the export depth) remains. Thus a long z^* suggests low attenuation and low remineralisation of the particle flux. The T*eff* is another parameter that represents the proportion of flux that reaches the deeper ocean and thus is not remineralised. This is simply calculated by dividing the deep flux (here ca. 200 m, see Appendix Table D.1) by the export flux. All indexes are dimensionless apart from the proportion of slow and fast sinking flux which is expressed as a percentage and z^* which is in metres.

5.4 Results and Discussion

5.4.1 Comparison of fluxes

The aim of this study is to determine the role of zooplankton on the BCP efficiency using observations and a model output with few zooplankton interactions

on particles; both methods separate particles into fast and slow sinking. Initially it is important to assess how well the observations and model fluxes compare, such as primary production (PP) and the POC export and deep (150 - 220 m) fluxes (Fig. 5.2). Overall primary production is well reproduced in the model when compared to satellite-derived estimates, with a strong positive correlation between the two ($p < 0.001$, $r = 0.84$, Fig. 5.2 a), although the model slightly overestimates PP. When comparing the total (fast + slow) sinking export fluxes and total deep fluxes, most points lie below the 1:1 line, suggesting that the model is overestimating fluxes (Figs. 5.2 b & c).

5.4.2 Export production

The traditional view on export production is that as primary production increases, so does the percentage of PP exported (Laws *et al.*, 2000). However more recent analyses from the Southern Ocean suggest this is not always the case and that an inverse relationship between PE*eff* and PP exists (Maiti *et al.*, 2013; Le Moigne *et al.*, 2016). For fast sinking particles the model shows PE*eff* increases with PP (Fig. 5.2 d) according to a power law function ($p < 0.001$, $r = 0.6$) and the observations show an inverse relationship (logarithmic function, $p < 0.001$, $r = 0.4$). The inverse relationship was also seen using just data from the Southern Ocean and the primary control thought to be zooplankton grazing (Chapter 2).

However, for the slow sinking particles the model shows an inverse relationship between PP and PE*eff*, similar to that seen in the observations for the fast sinking particles (power law function, $p < 0.001$, $r = 0.97$, Fig. 5.2 e). Potential reasons for an inverse relationship include the temporal decoupling between primary production and export (Salter *et al.*, 2007), seasonal dynamics of the zooplankton community (Tarling *et al.*, 2004) or grazing by zooplankton (Maiti *et al.*, 2013; Le Moigne *et al.*, 2016). As previously mentioned one of the differences between the fast and slow sinking detrital pools in the model is that slow sinking particles are grazed on by zooplankton and fast sinking are not. Thus when zooplankton graze on particles in the model an inverse relationship between PE*eff* and PP exists and when zooplankton grazing is not accounted for, the opposite occurs. This highlights the importance of zooplankton in determining the efficiency of the BCP.

The observed slow sinking PE*eff* were generally very low (< 0.05) thus slow

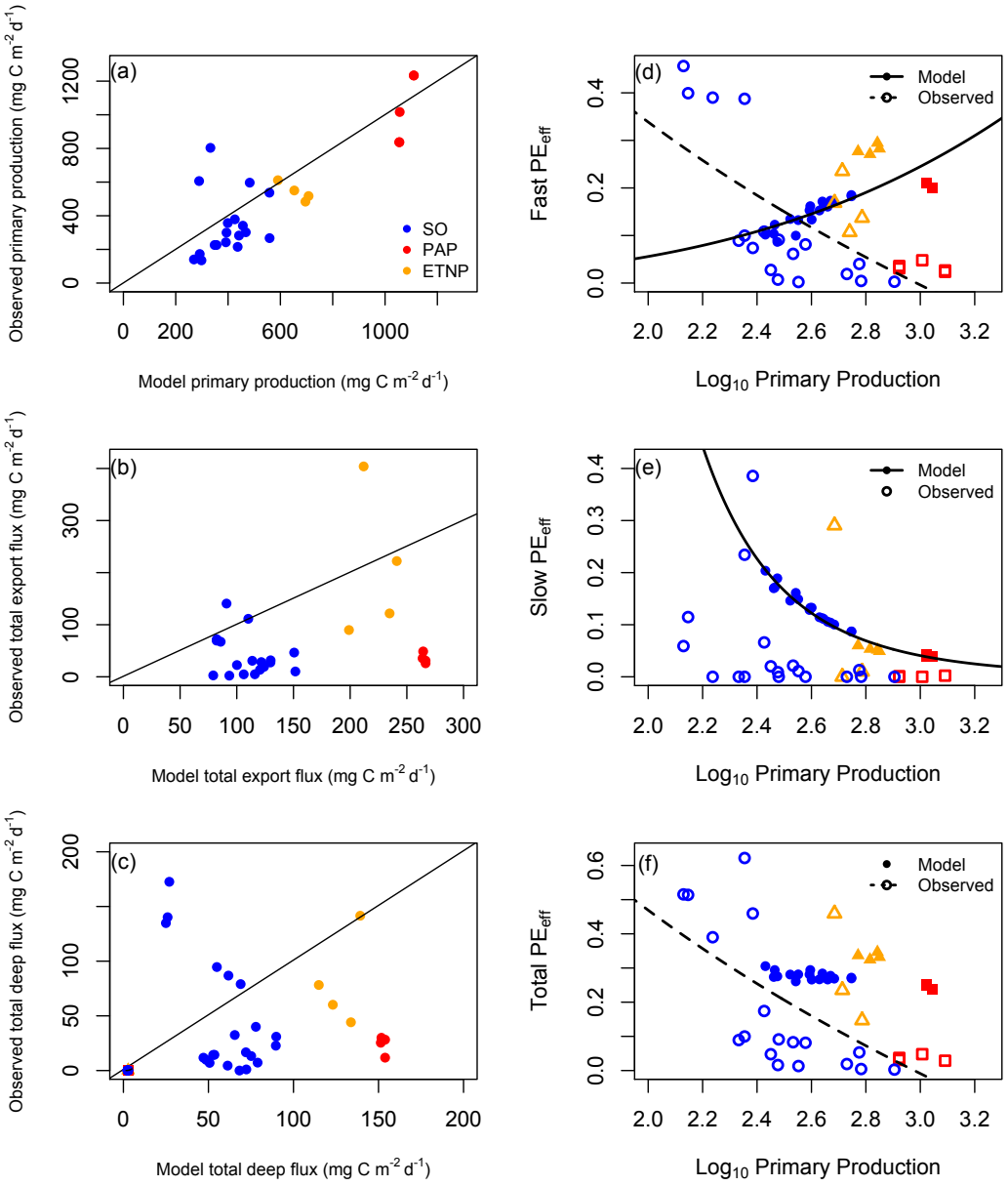

Figure 5.2: Primary production and export. Comparisons between observations and model output a) primary production, b) export flux and c) deep flux and PE*eff* with primary production for d) fast, e) slow and f) total sinking particles. Black lines in a - c are 1:1 lines and in d - f are fitted regressions. Only significant regressions are shown in d - f, solid black line and solid points are model output and dashed black line and open points are observations. See text for more details.

sinking PE*eff* had little influence on the total PE*eff*, which was also non-linearly inverse ($p < 0.001$, $r = 0.4$, Fig. 5.2 f) to PP. It is important to note that high values of PP (> 1000 mg C m^{-2} d^{-1}) were only present at PAP and the SO had the greatest range of PP thus is responsible for driving a large part of the inverse relationship. Therefore measuring PE*eff* in other regions with large PP ranges is fundamental to see if this relationship holds outside the sites from this study.

5.4.3 Contribution of fast and slow sinking POC fluxes

Particles naturally sink at different rates with slow sinking particles assumed to sink at < 20 m d^{-1} and fast sinking particles at > 20 m d^{-1} (Chapter 3). Most sediment traps cannot separately measure fluxes of fast and slow sinking particles and are unlikely to capture much of the slow sinking flux due to to their deployment in the lower mesopelagic and bathypelagic zones (Buesseler *et al.*, 2007*b*; Lampitt *et al.*, 2008). Slow sinking particles sink too slowly and are remineralised too quickly (Chapter 3) to reach the deep ocean unless they are formed there. Hence the MSC is a useful tool to analyse the two sinking fluxes separately.

In both the model output and the observations, the slow sinking flux was consistently smaller than the fast sinking flux and generally only contributed 20 % or less of the total flux (Fig. 5.3). The major difference is that in the model the proportion of slow sinking flux always decreases with depth (Figs. 5.3 a - c) whereas observations at the PAP site show the proportion of slow sinking fluxes increasing with depth (Figs. 5.3 e). Increases in slow sinking particles with depth must be either from the temporal decoupling of samples or fragmentation of larger fast sinking particles either abiotically (Alldredge *et al.*, 1990) or from sloppy feeding by zooplankton (Lampitt *et al.*, 1990). Sloppy feeding results in zooplankton fragmenting particles into smaller particles, resulting in a larger surface area to volume ratio increasing colonization by microbes and thus remineralisation (Mayor *et al.*, 2014). Zooplankton do not graze on fast sinking particles in the model thus sloppy feeding is not represented, nor is abiotic fragmentation (Yool *et al.*, 2013). This is likely why the contribution of slow sinking particles can only decrease with depth in the model but not in the observations.

5.4.4 Attenuation of POC with depth

The attenuation of POC through the water column describes how quickly sinking POC is remineralised, with a high attenuation suggesting high POC

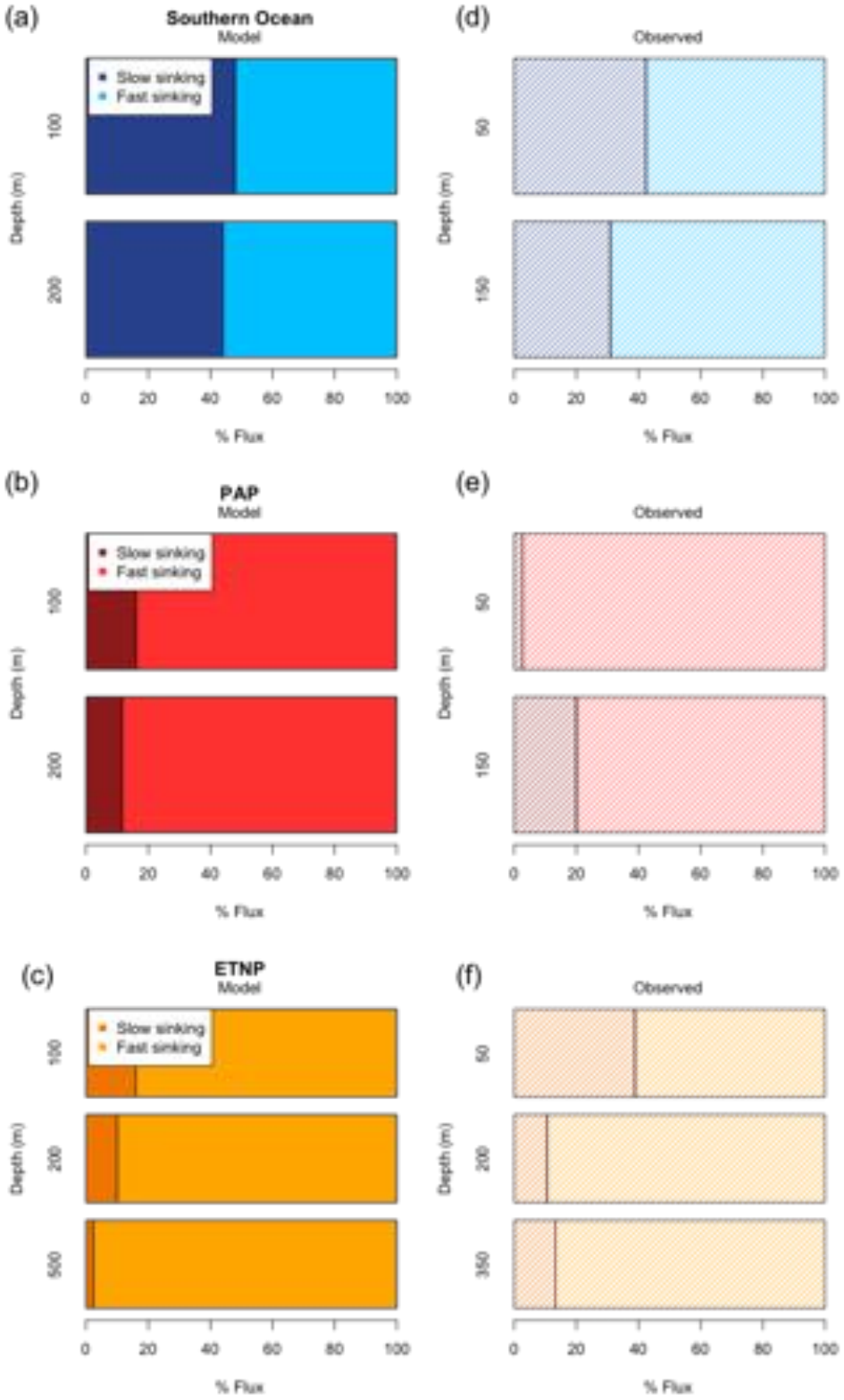

Figure 5.3: Proportion of fast and slow sinking particles to total flux from the model (a - c) and observations (d - f) from the Southern Ocean (blue), Porcupine Abyssal Plain (red) and equatorial Pacific (orange).

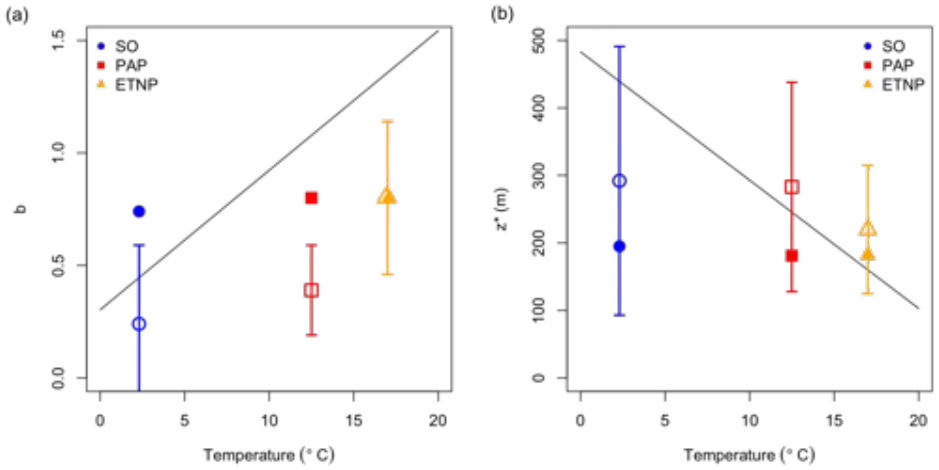

Figure 5.4: Total (fast + slow) mean attenuation of flux with *in situ* (mean over sampling depth) temperature; a) b and b) z^*. Solid points are model outputs and open points from observations. Error bars are standard error of the mean. The error was too low from the model output to plot error bars. Blue circles are SO, red squares PAP and orange triangles ETNP. The black lines are the Marsay *et al.* (2015) regressions.

remineralisation. The parameters b (Martin *et al.*, 1987) and z^* (Boyd & Trull, 2007) were used to describe the attenuation of flux with depth. A recent study suggests POC remineralisation is temperature dependent (Marsay *et al.*, 2015), hence the attenuation coefficients with temperature were compared. Total (fast + slow) sinking mean b and z^* values from the model were similar at all sites (Figs. 5.4 a & b) with no correspondence with temperature, even though slow sinking particles are remineralised as a function of temperature in the model. Hence modelled slow sinking b and z^* increase and decrease respectively with temperature (Table 5.1). The observations show a non-linear relationship with temperature that deviates away from the Marsay *et al.* (2015) regression, such that remineralisation increases (high attenuation) rapidly at temperatures greater than 13 °C. The variability is much greater in the observations than the model, a feature that is consistent across all indices (Fig. 5.4 a & b). Apart from at the ETNP where the model and observations agree, the observations consistently conserve POC with depth compared to the model. This could be due to diel vertical migration (DVM) of zooplankton that actively transfer POC to depth (Wilson *et al.*, 2008). Chapter 2 showed the high Southern Ocean b values were a result of DVM, a process not parameterised in the MEDUSA model. Active transfer *via* DVM is a complex process that is difficult to model, but it is potentially important as it has been shown to account for 27 % of the total flux

Table 5.1: Fast and slow sinking mean b and z^* at each site. NA shows sites where the range was too large (> 1000 m) and n too small (< 5) to produce an accurate mean. ' - ' depicts where mean z^* values were negative because of higher fluxes at depth.

		b		*z* (m)*	
Sinking fraction	**Site**	**Model**	**Observed**	**Model**	**Observed**
Fast	SO	0.63	0.47	229	-
	PAP	0.72	0.57	199	329
	ETNP	0.70	0.24	207	-
Slow	SO	0.87	1.13	166	-
	PAP	1.27	NA	113	169
	ETNP	1.47	NA	98	33

in the North Atlantic (Hansen & Visser, 2016).

The strong alignment of the model and observed attenuation at the ETNP is likely because of the lack of particle processing by zooplankton in the model and naturally in oxygen minimum zones (OMZs). The daytime depth of vertically migrating zooplankton is reduced in OMZs due to low dissolved oxygen concentrations (Bianchi *et al.*, 2013), which at the ETNP reach < 2 μmol kg^{-1} by 120 m. Further, the population of zooplankton below this depth is almost non-existent in OMZs (Wishner *et al.*, 2013) and those that are there feed on surface particles, not those in the OMZ core (Williams *et al.*, 2014). Thus zooplankton consumption and manipulation of particles is greatly reduced naturally in OMZs and in the MEDUSA model.

5.4.5 Efficiency of the biological carbon pump

The BCP*eff* (proportion of mixed layer primary production found at depth, here 150 - 300 m) plots of Buesseler & Boyd (2009) have been replicated by plotting PE*eff* against transfer efficiency (T*eff*); for fast, slow and total sinking particles (Fig. 5.5 a - c). According to the observations, the SO had the highest total BCP*eff* at 40 % (Fig. 5.5 c), similar to the maximum observed by Buesseler & Boyd (2009) in the North Atlantic. For the Southern Ocean the observations showed a higher BCP*eff* than the model by about 10 % across all sinking fluxes (Fig. 5.5). This difference was largely due to a very high T*eff* estimated from observations (> 1). This implies fluxes increased at depth, likely due to active fluxes by vertically migrating zooplankton (Chapter 2). Active fluxes could account for high observed T*eff* in the slow sinking particles, as well as fragmentation of larger particles at depth (Mayor *et al.*, 2014).

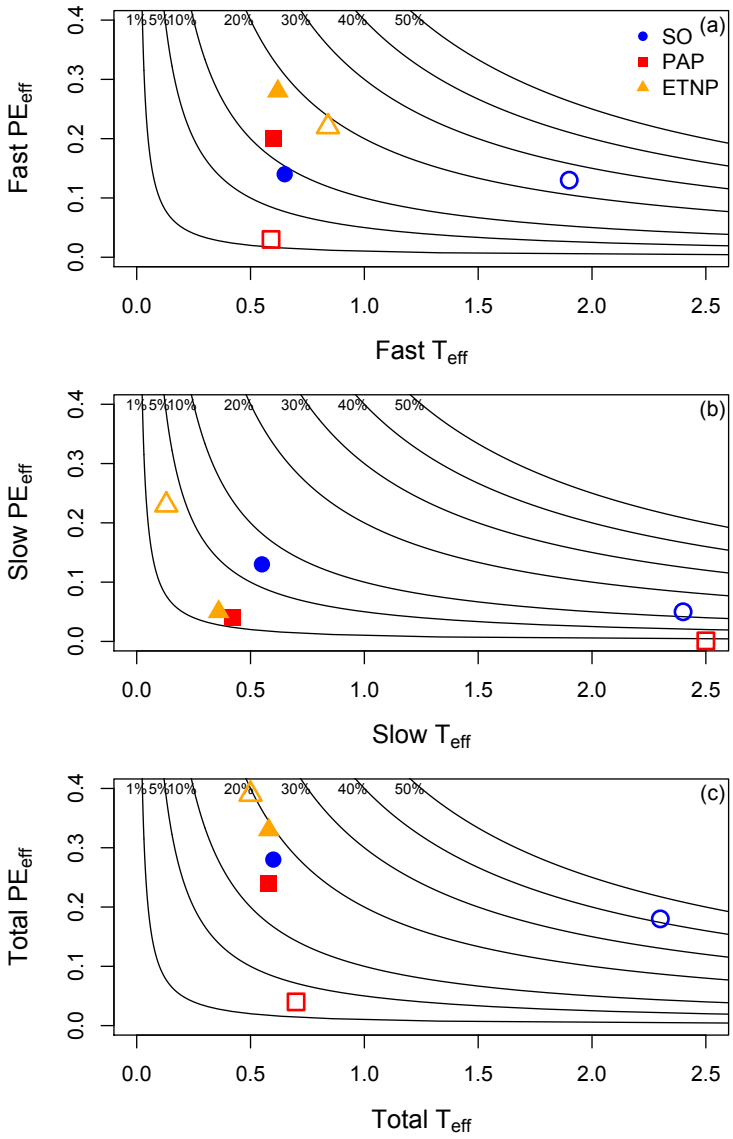

Figure 5.5: Efficiency of the biological carbon pump for a) fast, b) slow and c) total sinking particles. Particle export efficiency (PE*eff*) is plotted against transfer efficiency (T*eff*). Contours represent BCP*eff* (proportion of primary production at depth). Blue circles are Southern Ocean, red squares PAP and orange triangles equatorial Pacific. Closed points show model output and open points are observations.

Even though the PAP site had the highest PP, the BCP*eff* was lowest (< 15 %). There were also large differences (up to 15 %) in the BCP*eff* between the model and the observations at the PAP site driven by large discrepancies in PE*eff*. Observations of fast sinking PE*eff* were much lower than predicted by the model (Fig. 5.5 a), which could result from active grazing and fragmentation of large particles by zooplankton. T*eff* of fast sinking particles were low and consistent with model predictions suggesting that active transfer *via* DVM (not parameterised in the model) plays a relatively minor role at the PAP site. Therefore mineral ballasting (Armstrong *et al.*, 2002; François *et al.*, 2002), that drives T*eff* in the model, may be the main driver of T*eff* at PAP. The slow sinking BCP*eff* was similar at PAP (ca. 1 %) despite a large difference in T*eff* (Fig. 5.5 b). Fragmentation of fast to slow sinking particles at depth could explain the difference in slow sinking T*eff*.

Finally the BCP*eff* for the ETNP is very similar between the model and observations for all sinking fluxes (Fig. 5.5). The similarity in the BCP*eff* here echoes the similarity shown for POC attenuation with depth. This reiterates the finding that the observations and model agree on BCP*eff* only in areas of the global ocean where processing of particles by zooplankton is reduced due to very low dissolved oxygen concentrations.

5.5 Summary

Observations and model output from the upper mesopelagic zone in three contrasting oceanic regions were used to assess how zooplankton may affect the efficiency of the biological carbon pump. Fast and slow sinking particles were collected separately *in situ*, which are also separated into discrete classes in the MEDUSA model. The model has limited processing of particles by zooplankton with only slow sinking particles being grazed upon.

The results highlight the crucial role zooplankton play in regulating the efficiency of the biological carbon pump through: 1) controlling particle export by grazing, 2) fragmenting large, fast sinking particles into smaller, slower sinking particles and 3) active transfer of POC to depth. Comparisons of the model and observations in an oxygen minimum zone provide strong evidence of the importance of zooplankton in regulating the BCP. Here extremely low dissolved oxygen concentrations at depth reduce the abundance of zooplankton in the mid-water column and their metabolism. Thus the role of zooplankton on degrading or

repackaging particles is vastly reduced in OMZs, so here the model, with limited zooplankton interaction with particles, shows the strongest agreement with observations.

It is recommended that grazing on large, fast sinking particles and the fragmentation of fast to slow sinking particles (either *via* zooplankton or abiotically) is introduced into global biogeochemical models, with the aim of also incorporating active transfer. Future changes in climate such as the expansion of OMZs may decrease the role of zooplankton in the biological carbon pump globally thus increasing its efficiency.

Acknowledgements

I would like to thank all participants and crew on cruises JR274, JC087, JC097. Thanks to Anna Belcher for collecting samples from the PAP site on JC087 and to Annike Moje for running all POC samples in Bremen, Germany. Thanks also to Andrew Yool for producing the MEDUSA model output and for Stephanie Henson for her help with this work.

Chapter 6

Conclusions and further work

The aim of this thesis was to further our understanding of the biological carbon pump by looking at two key processes:

1. The export of particles out of the mixed layer

2. The transfer and degradation of particles in the mesopelagic zone.

These processes were studied in detail using observations made in the Southern Ocean and Equatorial Pacific, then coupled with observations from the North Atlantic to globally assess the efficiency of organic carbon cycling in the ocean. This work was unique due to the analysis of fast and slow sinking particles separately, as slow sinking particles are rarely collected separately in particle flux studies.

6.1 Key findings

This work produced three major findings:

1. Particle export efficiency is inversely related to primary production (Chapters 2 and 5)

2. The process of formation and disaggregation of suspended, slow sinking and fast sinking particles is more complex than previously thought (Chapters 3 and 4)

3. The magnitude of particulate organic carbon remineralisation in the mesopelagic zone is controlled by zooplankton (Chapters 2, 3 and 5).

6.1.1 Particle export efficiency and primary production

The classical view of the biological carbon pump is that organic carbon is produced during primary production in the surface ocean and that a fraction of this is exported. Thus the higher the primary production, the greater the proportion that is exported. In the last three years this long standing assumption has been overturned; for instance in the Southern Ocean the higher the primary production, the lower the efficiency at which the particles are exported. However, this relationship holds when including data from the equatorial Pacific and Northeast Atlantic, suggesting this may be a global phenomenon.

Using *in situ* data from the Southern Ocean showed that grazing by zooplankton could be an important top down control on particle export. Grazing could lower measured primary production, but increase the measured export flux due to high fluxes of zooplankton faecal pellets. When using the MEDUSA ecosystem model to study this relationship, an inverse relationship between particle export efficiency and primary production was only reproduced in the model when zooplankton grazed on particles.

6.1.2 Formation and disaggregation of particles

It is generally thought, and thus modelled (see section 1.4.2), that small phytoplankton cells become incorporated into slow sinking detritus and large phytoplankton cells become incorporated into fast sinking detritus, with little or no interaction between particles at depth. This suggests that once particles have been exported they either sink quickly to the deep ocean, undergoing little remineralisation as seen in the Northeast Atlantic (Billett *et al.*, 1983), or they sink slowly and are remineralised rapidly.

Work from this thesis in the Equatorial Tropical North Pacific showed that slow sinking particles are indeed remineralised rapidly, but the rate is so quick that slow sinking particles found at depth must be produced there. This is most likely from the disaggregation of fast sinking particles, which using lipid biomarkers, were shown to have a significantly similar composition to slow sinking particles.

Phytoplankton community structure does not directly affect the size of particle flux, however, it may have a strong influence on the type of particles and how they are formed. For instance in areas where large phytoplankton dominate such as the Southern Ocean, these may rapidly aggregate and sink to the deep

ocean or support larger zooplankton communities that produce large sinking faecal pellets. However, in tropical areas such as the equatorial Pacific, where small phytoplankton occur, large fast sinking aggregates may only be formed through the aggregation of smaller particles or flocculation with gelatinous particles. This was shown by the significant dissimilarity in lipid composition of mixed layer and exported fast sinking particles. Adjusting models to take these findings into account may result in increased accuracy when compared to observations.

6.1.3 Remineralisation in the mesopelagic zone by zooplankton

The role of zooplankton in the biological carbon pump is complicated, as they can both enhance and decrease particle flux. In the Southern Ocean zooplankton, mostly krill, enhanced flux at depth by producing faecal pellets, thus the attenuation of flux (or remineralisation) with depth was low. Conversely, in the Equatorial Pacific the overall effect of zooplankton was to decrease flux to depth *via* respiration and fragmentation of particulate organic carbon; because decreased interactions between zooplankton and particles actually increased flux to depth.

The MEDUSA model was also used to examine the influence of zooplankton on mesoepelagic particle flux. In the Southern Ocean the model underestimated the transfer of POC to depth, as it does not parameterise diel vertical migration and its contribution to particle flux. However, in the Equatorial Pacific the model matched well with observations as here low oxygen concentrations drastically reduce zooplankton processing on particles. Therefore the reduced zooplankton paramterisations in the model means it best represents environments where zooplankton abundance and metabolism, thus reworking of particles, is low.

Modelling zooplankton is complex and thus produces some uncertainties in these conclusions. For instance zooplankton can be herbivores, detritivores and bacteriovores with different feeding techniques (Fasham *et al.*, 1990). Yet when modelled often only one or two zooplankton groups are parameterised and so parameters representing one particular group of zooplankton are chosen to be represented, e.g. a copepod herbivore (Fasham *et al.*, 1990). Additionally the relationship between grazing rate and food supply is often expressed as a Michaelis-Menton relationship which saturates. However if a different relationship is used that does not saturate this effects the output of zooplankton in the model (Franks,

2002).

In modelling there is a trade-off between the complexity of a model and performance. Increasing parameterisations likely leads to the model best representing an ecosystem, however this also increases some uncertainties and is computationally expensive. A review of ecological models recommended that simple 'minimum-realistic' models are used over a single 'ultimate' ecosystem model (Fulton *et al.*, 2003). The MEDUSA model by Yool *et al.* (2013) is more complex than many ecosystem biogeochemical models as it includes two state boxes for phytoplankton, zooplankton and detritus, although obviously it does not represent all processes in the natural environment as we understand them. Thus it is possible other parameterisations other than zooplankton may explain some of the mis-matches between these observations and the model output.

For instance sinking speed of detritus has been shown to influence modelled zooplankton stocks, producing more zooplankton and higher sinking speeds (Fasham *et al.*, 1990). In the model detrital sinking speed is constant yet mean rates differ between areas in the observations by > 100 m d^{-1}. Also grazing rates are not expressed as a function of temperature in MEDUSA as they are in other studies (Schartau & Oschlies, 2003; Chen *et al.*, 2012), but this has been flagged as an area of development for MEDUSA (Yool *et al.*, 2013). Further the remineralisation rate in MEDUSA (0.01 d^{-1}) is much lower than the mean turnover of fast sinking detrital carbon in this thesis (0.13 d^{-1}) and that used in other modelling studies (0.1 d^{-1} (Fasham *et al.*, 1990; Doney, 1999)). To test if zooplankton parameterisation is the main reason for differences in observational and modelled attenuation of POC the MEDUSA model should be ran with zooplankton removed at mesopelagic depths (see section 6.3.3).

6.2 Major finding

The key theme running through these chapters has been that zooplankton are key regulators of the biological carbon pump. Their presence can increase particle flux to depth *via* production of faecal pellets and decrease it through fragmentation and respiration. Thus their influence on efficiency of the biological carbon pump is variable but important. A hypothesis is that when small phytoplankton (thus small zooplankton) dominate the plankton community, the zooplankton produce smaller, slower sinking faecal pellets, lowering the effect of any active transfer. Consequently in these areas the net role of zooplankton is

that they decrease particle flux due to the larger signals of fragmentation and respiration of particles. These environments often occur at low latitudes, where in some areas oxygen minimum zones exist. Hence, in oxygen minimum zones the absence of zooplankton leads to increased flux to the deep ocean. Conversely, in environments where large phytoplankton (so large zooplankton dominate), zooplankton increase flux to depth *via* the production of larger, faster sinking faecal pellets that contribute to active transfer. Capturing these complex dynamics mathematically is difficult, but is important so that models can estimate how changes in future climate will affect our ocean biology, thus our atmosphere.

6.3 Future work

6.3.1 Extended measurements of PE*eff* and primary production

This thesis showed that particle export efficiency can be inversely linked to primary production, a phenomena not regularly discussed or appreciated prior to Maiti *et al.* (2013). An inverse relationship has also be observed by Le Moigne *et al.* (2016) and other unpublished work being undertaken at NOCS. To determine the spatial and temporal extent of this relationship it is important to calculate it with a greater primary productivity range and in different areas to those observed in this thesis. The implications would change the general consensus of biological carbon pump processes and thus lead to alterations in the way particles are parameterised in models.

6.3.2 Develop sinking rate experiments using the FlowCAM

The FlowCAM proved to be a very useful tool for measuring the sinking rates of larger (100 - 2500 μm) particles. As well as providing data from which sinking rates could be calculated it also provide data on size, transparency, aspect ratio and the images were used to identify each particle. I would recommend using a FlowCAM to measure particle sinking rates in a laboratory setting. The FlowCAM could be used to test the relationship between size and sinking rate of particles in areas outside the ETNP (this thesis) and more faster sinking particles. The aim would be to test if the relationship observed here persists, where sinking rate increases non-linearly with particle size. If this relationship holds, the average sinking rates of particles could easily be estimated just by knowing the size (to the nearest 50 μm) of the particle. This would allow many more

particle sinking rates to be estimated and the use of autonomous instruments where particles do not need to be collected, such as a video plankton recorder.

6.3.3 Remove zooplankton from models

One of the main findings of this thesis was that zooplankton have a prominent role in the biological carbon pump and setting its efficiency. This could be tested using models. For instance taking the model produced by Giering *et al.* (2014) in the North Atlantic and running it at two depths, firstly at the mixed layer depth (e.g. 50 m) not altering the model and at 200 m below this simulating an oxygen minimum zone by removing zooplankton from the model. Here one would expect to see an increase in particle flux to depth from the lack of respiration and fragmentation by zooplankton. The model would likely need to be further altered to completely represent the tropical OMZ and not the North Atlantic. For example setting pico-phytoplankton as the dominant plankton and altering the pathways for aggregation such that slow sinking particles produced fast sinking particles and they are not formed from pico-phytoplankton directly. This work would consolidate the theory that the absence of zooplankton interacting with particles in oxygen minimum zones is the main driver of the high remineralisation length scales observed in OMZs.

6.3.4 Improve zooplankton parameterisation in models

One of the main observations throughout each study in this thesis was the importance of zooplankton in setting the efficiency of processes within the biological carbon pump (e.g. particle formation, particle export and transfer efficiencies). However, many biogeochemical models (NASA, MEDUSA, PISCES) have have fewer interactions between zooplankton and organic particles than we know about. For instance diel vertical migration (active transfer) is rarely ever parameterised and often fragmentation by zooplankton is not either. Improving models to include as many known particle processing by zooplankton would hopefully improve fidelity between modelled and observed particle flux data. Using models that represent particle processing to the best of our current knowledge is important so that the models can be used to predict with a great degree of certainty how atmospheric climate change will alter our oceans. A recent study compared the changes in export production of four marine ecosystem models under the RCP forcing 8.5 (business-as-usual) over the next 100 years (Laufkötter *et al.*, 2015). This study showed there was large discrepancy between all four models

and further research was needed on plankton community structure, particle composition and sinking behaviour, particle aggregation rates, ballasting effects and grazing to support further model development (Laufkötter *et al.*, 2015). Some of these elements were studied during this thesis, but still uncertainties of how processes will change with space and time is uncertain.

This thesis has furthered our understanding of the biological carbon pump, both on a regional and global level. It has highlighted the important role zooplankton play in indirectly regulating atmospheric carbon dioxide levels. How the biological processing of carbon in the ocean will be affected by global climate change is still unknown and this should be a focus for future research.

Appendix A

Particle flux in the Southern Ocean

Table A.1: Sampling locations and dates.

Station ID	**Date**	**Latitude** °N	**Longitude** °E
6	15-01-2013	-59.91	-53.03
8	16-01-2013	-58.52	-51.26
10	17-01-2013	-59.91	-49.42
12	18-01-2013	-60.97	-48.14
16	20-01-2013	-57.97	-42.93
19	21-01-2013	-55.20	-41.32
22	22-01-2013	-52.91	-40.14
25	23-01-2013	-50.29	-39.02
27	24-01-2013	-50.961	-37.62
29	25-01-2013	-52.61	-36.62
32	28-01-2013	-51.69	-34.98
34	29-01-2013	-51.37	-31.09
36	30-01-2013	-53.63	-29.33
38	31-01-2013	-55.93	-27.26
40	01-02-2013	-58.09	-25.93
43	03-02-2013	-63.26	-25.35
44	04-02-2013	-62.27	-26.85
46	05-02-2013	-60.14	-29.49

Table A.2: MSC_{Ex} POC concentrations for the fast sinking, slow sinking and suspended particles and the total POC.

Station ID	**Depth** (m)	**Fast** (μg L^{-1})	**Slow** (μg L^{-1})	**Susp** (μg L^{-1})	**Total** (μg L^{-1})
6	50	0.001	3.47	161.39	164.86
8	50	0.004	5.58	156.47	162.06
10	25	0.04	0.00	162.98	163.02
12	75	0.15	15.76	93.17	109.07
16	50	0.03	26.08	104.93	131.04
19	50	0.03	29.71	146.61	176.35
22	75	0.05	0.00	193.01	193.06
25	75	0.05	12.21	47.64	59.90
27	50	0.02	3.27	254.86	258.15
29	75	0.01	2.77	75.11	77.90
32	50	0.04	8.49	184.18	192.71
34	50	0.04	11.44	142.22	153.69
36	50	0.05	6.27	156.39	162.72
38	50	0.08	0.00	190.86	190.94
40	50	0.01	8.91	237.64	246.56
43	50	0.10	4.63	70.23	74.97
44	50	0.10	8.46	99.37	107.93
46	25	0.12	6.80	97.56	104.48

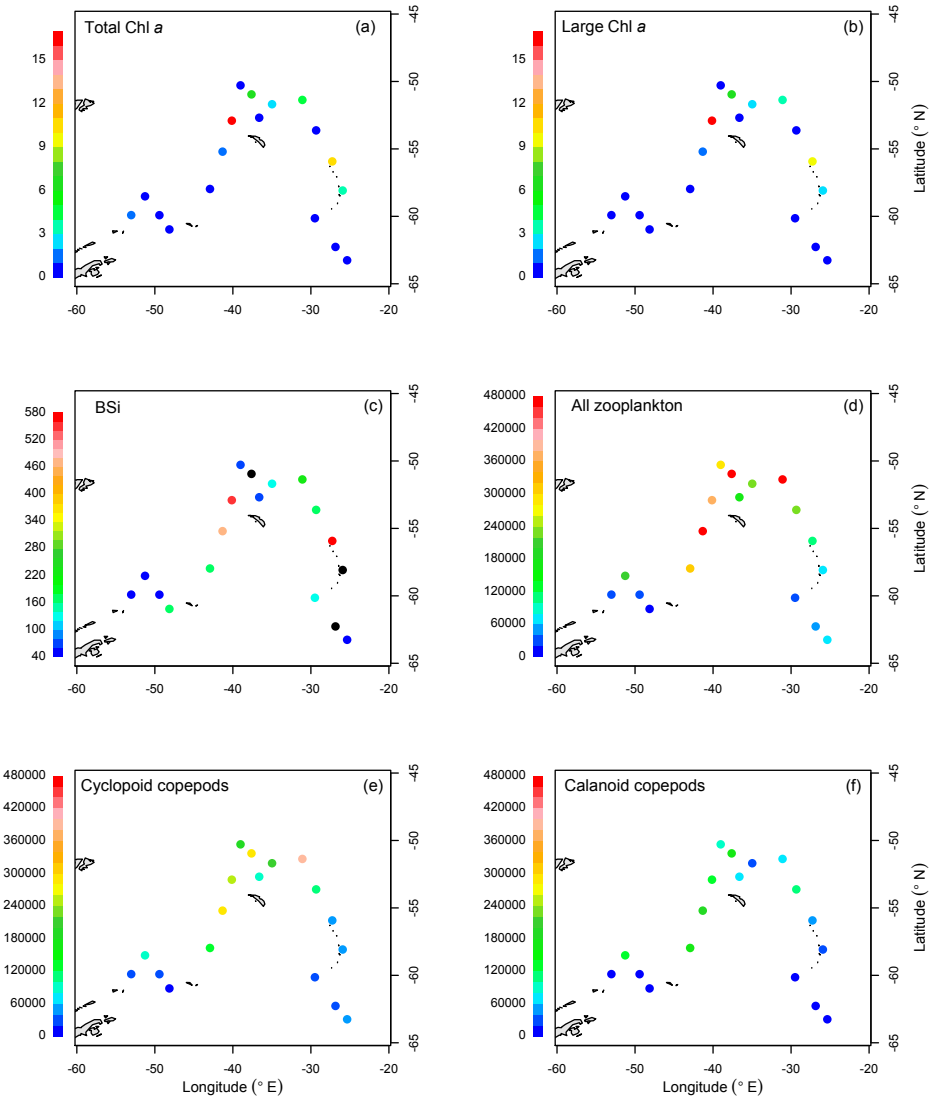

Figure A.1: Chlorophyll *a*, BSi and Zooplankton; a) Total (> 0.7 μm) and b) large (> 10 μm) Chl *a* and c) Biogenic silica concentrations averaged over the mixed layer, d) Total zooplankton, e) Cyclopoid copepod and f) Calanus copepod abundance (individuals m^{-2}) over the upper 200 m.

Table A.3: MSC_D POC concentrations for the fast sinking, slow sinking and suspended particles and the total POC.

Station ID	**Depth** (m)	**Fast** (μg L^{-1})	**Slow** (μg L^{-1})	**Susp** (μg L^{-1})	**Total** (μg L^{-1})
6	150	0.006	0.95	55.37	56.33
8	150	0.04	11.66	43.23	54.94
10	125	0.05	12.20	29.49	41.74
12	175	0.15	2.50	54.39	57.04
16	150	0.05	4.79	128.15	133.00
19	150	0.02	4.14	35.39	39.56
22	175	0.006	7.40	1106.78	114.19
25	175	0.00	7.02	47.04	54.07
27	150	0.04	6.77	110.22	117.02
29	175	0.00	0.00	69.88	69.88
32	150	0.06	5.35	72.55	77.97
34	150	0.01	4.01	61.18	65.20
36	150	0.00	0.00	57.36	57.36
38	150	0.02	7.09	350.81	358.10
40	150	0.02	3.47	53.06	56.55
43	150	0.02	3.21	40.05	43.28
44	150	0.02	1.15	62.50	63.66
46	125	0.02	1.89	52.86	54.77

Appendix B

Remineralisation in an OMZ

Table B.1: Sampling locations and dates.

Station ID	**Date**	**Latitude** °N	**Longitude** °W	**Area**
1	03-01-2014	13.35	91.20	Onshore
2	09-01-2014	13.26	91.22	Onshore
3	15-01-2014	13.25	91.22	Onshore
4	21-01-2014	13.21	91.22	Offshore
5	27-01-2014	13.13	91.17	Offshore
6	02-02-2014	13.04	91.11	Offshore

Table B.2: POC concentrations for the fast sinking, slow sinking and suspended particles and the total POC.

Station ID	**Depth** (m)	**Fast** (μg L^{-1})	**Slow** (μg L^{-1})	**Susp** (μg L^{-1})	**Total** (μg L^{-1})
1	40	2.24	10.46	205.87	217.71
	60	1.91	10.36	113.21	125.28
	80	1.98	4.60	59.89	65.58
	90	1.29	0.00	120.98	121.30
2	40	0.92	9.73	113.14	123.65
	60	0.55	4.81	102.75	107.36
	120	1.06	0.00	88.21	89.06
	150	0.90	1.24	64.86	66.14
3	50	0.53	0.86	105.47	106.40
	110	0.79	0.00	93.64	93.79
	170	0.87	7.95	14.53	22.82
	220	0.72	10.00	72.49	72.72
4	40	0.38	43.00	171.16	214.37
	120	0.36	0.00	131.25	131.36
	220	0.53	0.00	111.58	111.53
	350	0.56	0.00	112.01	112.56
5	70	0.52	10.81	111	123.05
	220	0.53	3.04	79.16	82.73
	350	0.32	11.12	49.17	60.62
6	40	0.79	0.00	205.94	206.72
	120	0.48	0.00	150.47	150.96
	220	0.37	0.00	73.82	74.19
	350	0.41	0.00	87.02	87.42

Table B.3: POC fluxes fast sinking, slow sinking and total particles.

Station ID	**Depth** (m)	**Fast** (mg C m^{-2} d^{-1})	**Slow** (mg C m^{-2} d^{-1})	**Total** (mg C m^{-2} d^{-1})
1	40	350	17	367
	60	309	168	477
	80	225	6	232
	90	140	0	140
2	40	143	28	171
	60	88	42	130
	120	121	0	121
	150	97	20	117
3	50	83	6	89
	110	128	0	128
	170	99	58	158
	220	78	0	78
4	40	58	345	403
	120	58	0	58
	220	60	0	60
	350	60	0	60
5	70	81	1140	221
	220	87	54	141
	350	37	57	95
6	40	122	0	122
	120	78	0	78
	220	42	2	44
	350	44	28	72

Table B.4: ANCOVA for the effect of depth and fraction on k.

Coefficients	**Estimate**	**s.e**	***t* value**	***p***
Intercept k (h^{-1}) Fast	-1.672	0.1592	-10.5	$<$ 2e-16
Depth k (h^{-1} m^{-1}) Fast	-0.0038	0.0014	-2.631	0.011
Δ Intercept Slow	1.01	0.25	4.03	0.00018
Δ k (h^{-1} m^{-1}) Slow v Fast	0.0066	0.002	3.088	0.003

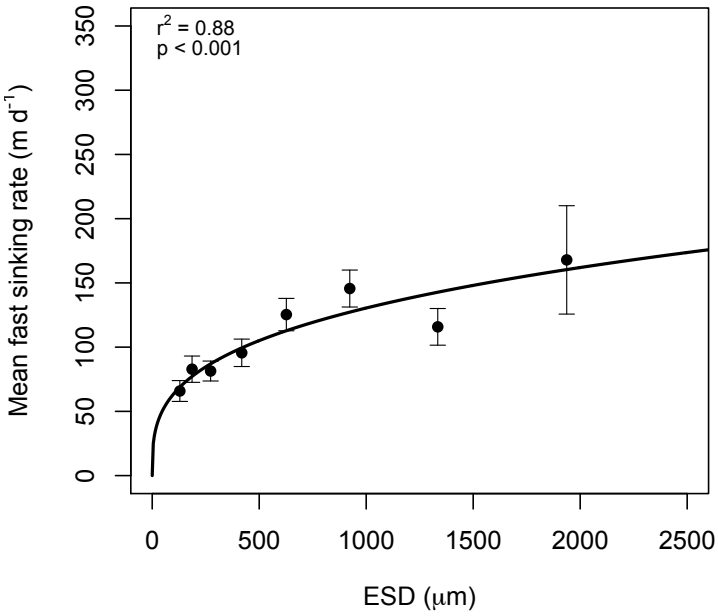

Figure B.1: ESD *vs.* sinking rate. Bins are by ESD and each 1.5 x larger than the previous bin.

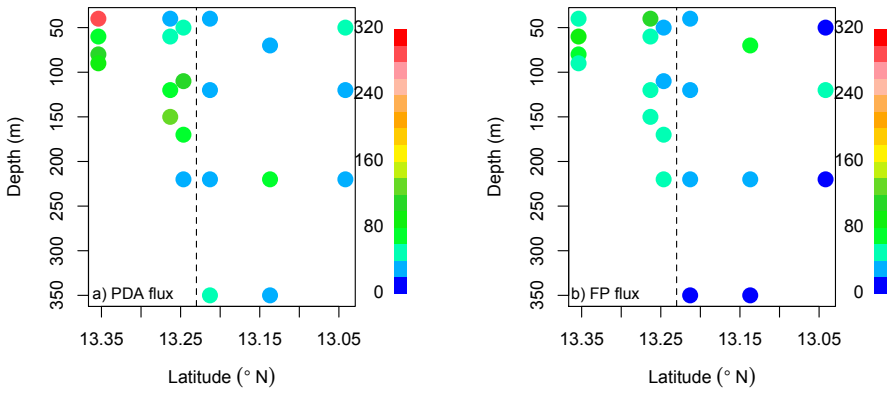

Figure B.2: Phytodetrital aggregate (a) and faecal pellet (b) POC fluxes (mg C m^{-2} d^{-1}) with depth.

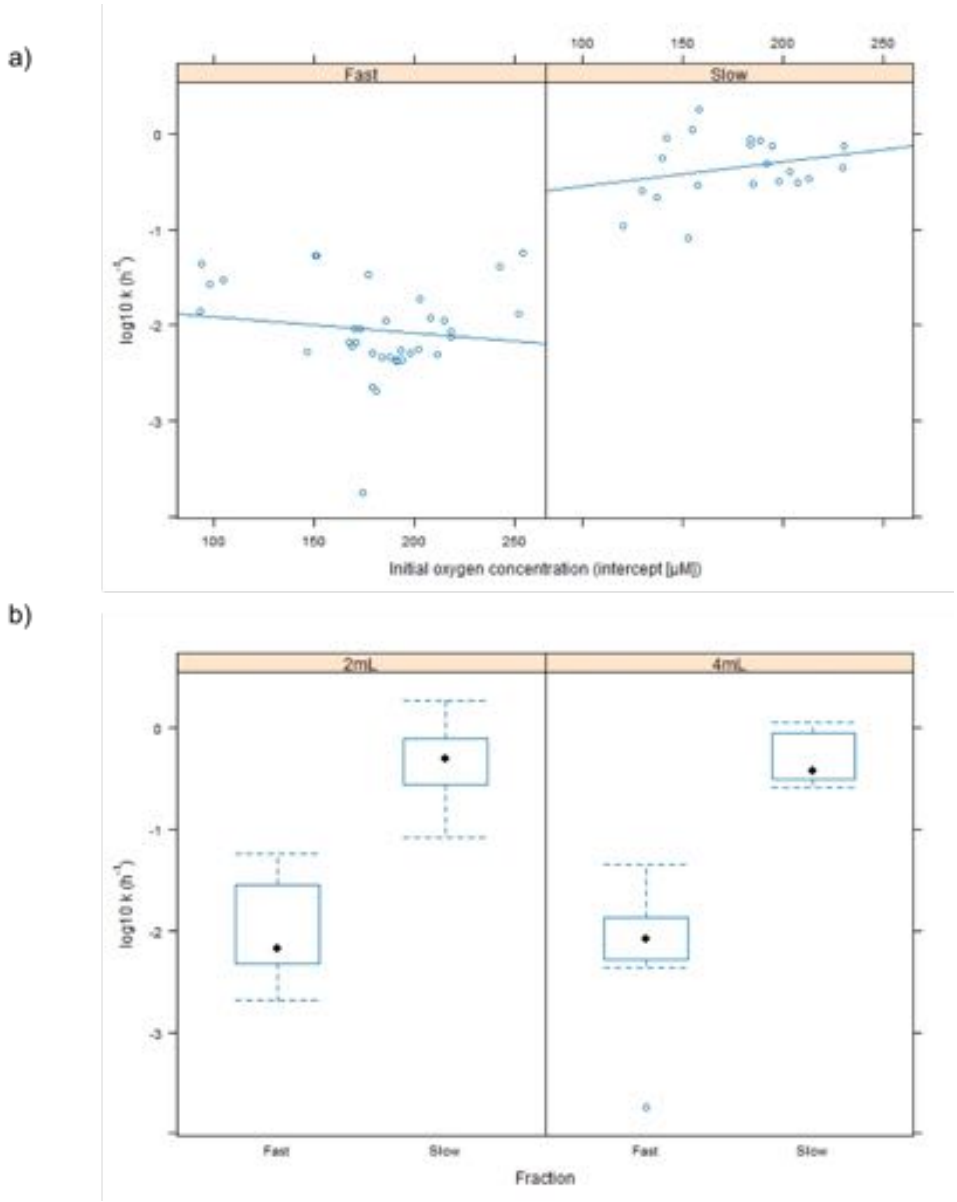

Figure B.3: Oxygen concentration (a) and chamber volume (b) on k for the fast and slow sinking particles. No significant effect on k was found ($p > 0.05$, t-tests). Data and figure by Mark Trimmer.

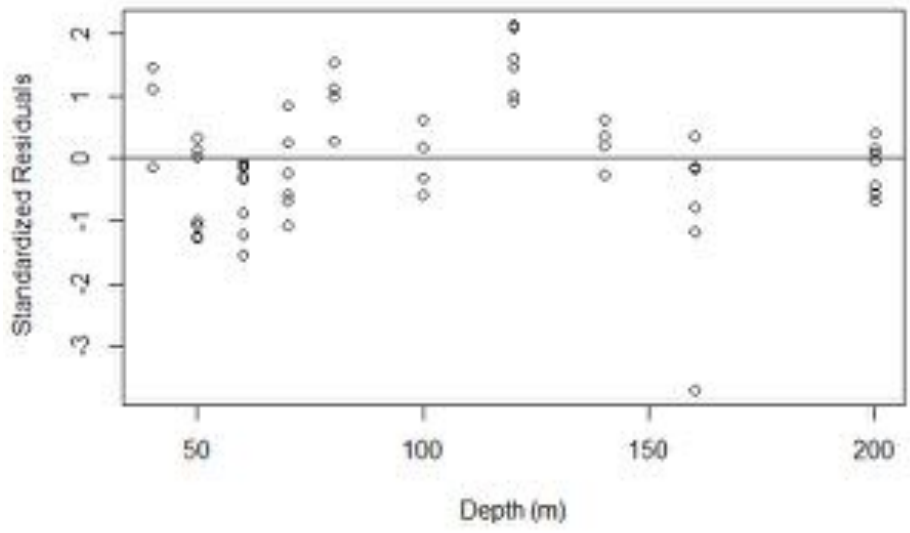

Figure B.4: Residuals from ANCOVA of depth on k. While the overall effect of depth might be interpreted as being significant, the basic assumptions underpinning a linear model are clearly violated as there should be no obvious pattern in the residuals from the linear ANCOVA model (Table B.4). Data and figure by Mark Trimmer.

Appendix C

Particle composition

Table C.1: Lipid compounds (Jeffreys *et al.*, 2009).

	Abbreviations	**Systematic name**
1	C14:0 acid	tetradecanoic acid
2	C14:0 alcohol	1-tetradecanol
3	*i*-C15:0 acid	13-methyltetradecanoic acid
4	*a*-C15:0 acid	12-methyltetradecanoic acid
5	C15:0 acid	pentadecanoic acid
6	C15:0 alcohol	1-pentadecanol
7	Δ^7-C16:1 acid	7-hexadecenoic acid
8	Δ^9-C16:1 acid	9-hexadecenoic acid
9	C16:0 acid	hexadecanoic acid
10	C16:0 alcohol	1-hexadecanol
11	*i*-C17:0 acid	15-methylhexadecanoic acid
12	*a*-C17:0 acid	14-methylhexadecanoic acid
13	C17:0 acid	heptadecanoic acid
14	C17:0 alcohol	1-heptadecanol
15	C18:3 acid	9,12,15-octadecatrienoic acid
16	C18:4 acid	3,6,9,12-octadecatetraenoic acid
17	C18:2 acid	6,9-octadecadienoic acid
18	C18:4 acid	6,9,12,15-octadecatetraenoic acid
19	C18:2 acid	9,11-octadecadienoic acid
20	C18:3 acid	6,9,12-octadecatrienoic acid
21	Δ^9-C18:1 acid	9-octadecenoic acid

Table C.1: Lipid compounds (Jeffreys *et al.*, 2009).

	Abbreviations	**Systematic name**
22	C18:2 acid	12,15-octadecadienoic acid
23	$\Delta^1$1-C18:1 acid	11-octadecenoic acid
24	C18:0 acid	octadecanoic acid
25	C18:0 alcohol	1-octadecanol
26	C19:0 acid	nonadecanoic acid
27	C19:0 alcohol	1-nonadecanol
28	C20:0 acid	eicosanoic acid
29	C20:0 alcohol	1-eicosanol
30	C21:0 acid	heneicosanoic acid
31	C21:0 alcohol	1-heneicosanol
32	C22:0 acid	docosanoic acid
33	C22:0 alcohol	1-docosanol
34	C23:0 acid	tricosanoic acid
35	C23:0 alcohol	1-tricosanol
36	C24:0 acid	tetracosanoic acid
37	C24:0 alcohol	1-tetracosanol
38	C25:0 acid	pentacosanoic acid
39	C26:0 acid	hexacosanoic acid
40	C26:0 alcohol	1-hexacosanol
41	C27$\Delta^{5,22}$ sterol	cholesta-5,22-dien-3β-ol
42	C27Δ^5 sterol	cholest-5-en-3β-ol
43	C27Δ^0 sterol	(5αH)-cholestan-3β-ol
44	C28$\Delta^{5,22}$ sterol	24-methylcholesta-5,22-dien-3β-ol
45	C29Δ^5 sterol	24-methylcholesta-5-en-3β-ol

Appendix D

Efficiency of the biological carbon pump

Table D.1: Sampling locations, depths dates in the Southern Ocean (SO), Porcupine Abyssal Plain (PAP) site and Equatorial Tropical Northern Pacific (ETNP).

Station ID	**Area**	**Latitude** °N	**Longitude** °E	**Date**	**Depth** (m)
1	SO	-59.9096	53.0300	15/01/2013	25, 125
2	SO	-58.51637	51.2597	16/01/2013	40, 140
3	SO	-59.91357	49.4159	17/01/2013	40, 140
4	SO	-60.97059	48.1354	18/01/2013	40, 140
5	SO	-57.97091	42.9343	20/01/2013	40, 140
6	SO	-55.20345	41.3218	21/01/2013	40, 140
7	SO	-52.90708	40.1359	22/01/2013	40, 140
8	SO	-50.28753	39.0203	23/01/2013	40, 140
9	SO	-50.95719	37.6151	24/01/2013	70, 170
10	SO	-52.68932	36.6230	25/01/2013	70, 170
11	SO	-51.68808	34.9765	28/01/2013	70, 170
12	SO	-51.36901	31.0913	29/01/2013	70, 170
13	SO	-53.6265	29.3274	30/01/2013	70, 170
14	SO	-55.92838	27.2584	31/01/2013	70, 170
15	SO	-58.08564	25.9257	01/02/2013	70, 170
16	SO	-63.25913	25.3539	03/02/2013	20, 120
17	SO	-62.26828	26.8482	04/02/2013	70, 170
18	SO	-60.14215	29.4865	05/02/2013	70, 170
19	PAP	48.3869	16.0842	04/06/2013	60, 160
20	PAP	48.3892	16.0858	05/06/2013	40, 140
21	PAP	48.3891	16.0857	07/06/2013	45, 145
22	PAP	48.3892	16.0875	07/06/2013	45, 145
23	PAP	48.3894	16.0858	09/06/2013	45, 145
24	ETNP	13.2464	91.2275	15/01/2014	40, 120
25	ETNP	13.2129	91.2278	21/01/2014	70, 220
26	ETNP	13.137	91.1791	27/01/2014	40, 120
27	ETNP	13.0418	91.1152	02/02/2014	50, 110

Bibliography

Abelmann, A., R. Gersonde, G. Cortese, G. Kuhn, & V. Smetacek (2006). Extensive phytoplankton blooms in the Atlantic sector of the glacial Southern Ocean. *Paleoceanography*, 21(1), 1–9.

Abramson, L., C. Lee, Z. Liu, S. Wakeham, & J. Szlosek (2010). Exchange between suspended and sinking particles in the northwest Mediterranean as inferred from the organic composition of in situ pump and sediment trap samples. *Limnology and Oceanography*, 55(2), 725–739.

Aksnes, D. & P. Wassmann (1993). Modeling the significance of zooplankton grazing for export production. *Limnology and Oceanography*, 38(5), 978–985.

Alldredge, A. (1976). Discarded appendicularian houses as sources of food, surface habitats, and particulate organic matter in planktonic environments. *Limnology and Oceanography*, 21(1), 14–23.

Alldredge, A. (1998). The carbon, nitrogen and mass content of marine snow as a function of aggregate size. *Deep-Sea Research I*, 45(4-5), 529–541.

Alldredge, A. & C. Gotschalk (1988). In situ settling behaviour of marine snow. *Limnology and Oceanography*, 33(3), 339–351.

Alldredge, A. & C. Gotschalk (1989). Direct observations of the mass flocculation of diatom blooms: characteristics, settling velocities and formation of diatom aggregates. *Deep Sea Research Part A. Oceanographic Research Papers*, 36(2), 159–171.

Alldredge, A., T. C. Granata, C. C. Gotschalk, & T. D. Dickey (1990). The physical strength of marine snow and its implications for particle disaggregation in the ocean. *Limnology and Oceanography*, 35(November), 1415–1428. ISSN 0024-3590.

Alldredge, A. & M. Youngbluth (1985). The significance of macroscopic aggregates (marine snow) as sites for heterotrophic bacterial production in the mesopelagic zone of the subtropical Atlantic. *Deep-Sea Research*, 12(12), 1445–1456.

Aller, R. C. (1994). Bioturbation and remineralization of sedimentary organic matter: effects of redox oscillation. *Chemical Geology*, 114(3-4), 331–345. ISSN 00092541.

Alonso-Gonzalez, J., J. Aristegui, C. Lee, A. Sanchez-Vidal, A. Calafat, J. Fabres, P. Sangra, P. Masque, A. Hernandez-Guerra, & V. Benitez-Barrios (2010). Role of slowly settling particles in the ocean carbon cycle. *Geophysical Research Letters*, 37.

Armstrong, R., C. Lee, J. Hedges, S. Honjo, & S. Wakeham (2002). A new, mechanistic model for organic carbon fluxes in the ocean based on the quantitative association of POC with ballast minerals. *Deep-Sea Research II*, 49(1-3), 219–236.

Arrigo, K. R., D. H. Robinson, D. L. Worthen, R. B. Dunbar, G. R. DiTullio, M. VanWoert, & M. P. Lizotte (1999). Phytoplankton community structure and the drawdown of nutrients and CO2 in the Southern Ocean. *Science*, 283(5400), 365–367.

Asper, V. (1987). Measuring the flux and sinking speed of marine snow aggregates. *Deep Sea Research*, 34(1), 1–17.

Atkinson, A., K. Schmidt, S. Fielding, S. Kawaguchi, & P. A. Geissler (2012). Variable food absorption by Antarctic krill: Relationships between diet, egestion rate and the composition and sinking rates of their fecal pellets. *Deep-Sea Research Part II: Topical Studies in Oceanography*, 59-60, 147–158.

Atkinson, A., V. Siegel, E. A. Pakhomov, & P. Rothery (2004). Long-term decline in krill stock and increase in salps within the Southern Ocean. *Nature*, 432(November), 100–103. ISSN 1476-4687.

Atkinson, A., P. Ward, R. Williams, & S. A. Poulet (1992). Feeding rates and diel vertical migration of copepods near South Georgia: comparison of shelf and oceanic sites. *Marine Biology*, 114(1), 49–56.

Aumont, O., C. Ethe, A. Tagliabue, L. Bopp, & M. Gehlen (2015). PISCES-v2: An ocean biogeochemical model for carbon and ecosystem studies. *Geoscientific Model Development*, 8(8), 2465–2513.

Azam, F., T. Fenchel, J. G. Field, J. S. Gray, L. A. Meyerreil, & F. Thingstad (1983). The Ecological Role of Water-Column Microbes in the Sea. *Marine Ecology Progress Series*, 10(3), 257–263.

Bach, L. T., U. Riebesell, S. Sett, S. Febiri, P. Rzepka, & K. G. Schulz (2012). An approach for particle sinking velocity measurements in the 3-400 μm size range and considerations on the effect of temperature on sinking rates. *Marine biology*, 159(8), 1853–1864.

Barker, S., J. a. Higgins, & H. Elderfield (2003). The future of the carbon cycle: review, calcification response, ballast and feedback on atmospheric CO2. *Philosophical transactions. Series A, Mathematical, physical, and engineering sciences*, 361(1810), 1977–98.

Bathmann, U. V., T. T. Noji, & B. von Bodungen (1991). Sedimentation of pteropods in the Norwegian Sea in autumn. *Deep Sea Research Part A. Oceanographic Research Papers*, 38(10), 1341–1360.

Becquevort, S. & W. Smith (2001). Aggregation, sedimentation and biodegradability of phytoplankton-derived material during spring in the Ross Sea, Antarctica. *Deep Sea Research Part II: Topical Studies in Oceanography*, 48(19-20), 4155–4178.

Behrenfeld, M. J. & P. G. Falkowski (1997). Photosynthetic rates derived from satellite-based chlorophyll concentration. *Limnology and Oceanography*, 42(1), 1–20.

Belcher, A., M. H. Iversen, C. Manno, S. A. Henson, G. A. Tarling, & R. Sanders (2016). The role of particle associated microbes in remineralisation of faecal pellets in the upper mesopelagic of the Scotia Sea, Antarctica. *Limnology and Oceanography*, 61(3), 1049–1064.

Benitez-Nelson, C., K. O. Buesseler, D. M. Karl, & J. Andrews (2001). A time-series study of particulate matter export in the North Pacific Subtropical Gyre based on 234Th:238U disequilibrium. *Deep Sea Research Part I: Oceanographic Research Papers*, 48(12), 2595–2611. ISSN 09670637.

Bianchi, D., E. D. Galbraith, D. A. Carozza, K. A. S. Mislan, & C. A. Stock (2013). Intensification of open-ocean oxygen depletion by vertically migrating animals. *Nature Geoscience*, 6(7), 545–548. ISSN 1752-0894.

Bienfang, P. (1981). SETCOL - A technologically simple and reliable method for measuring phtoplankton sinking rates. *Canadian Journal of Fisheries and Aquatic Sciences*, 38(10), 1289–1294.

Billett, D., R. Lampitt, & A. Rice (1983). Seasonal sedimentation of phytoplankton to the deep-sea benthos. *Nature*, 302(7), 520–522.

Bopp, L. & C. Le Quéré, Ocean Carbon Cycle. In *Surface Ocean–Lower Atmosphere Processes*. American Geophysical Union, 2009, pp. 181–195.

Boyd, P. & P. Newton (1999). Does planktonic community structure determine downward particulate organic carbon flux in different oceanic provinces? *Deep-Sea Research I*, 46(1), 63–91.

Boyd, P. & T. Trull (2007). Understanding the export of biogenic particles in oceanic waters: Is there consensus? *Progress in Oceanography*, 72(4), 276–312.

Brown, L., R. Sanders, G. Savidge, & C. H. Lucas (2003). The uptake of silica during the spring bloom in the Northeast Atlantic Ocean. *Limnology and Oceanography*, 48(5), 1831–1845.

Buesseler, K., A. N. Antia, M. Chen, S. W. Fowler, W. D. Gardner, O. Gustafsson, K. Harada, A. F. Michaels, M. R. van der Loeff'o, M. Sarin, D. K. Steinberg, & T. Trull (2007*a*). An assessment of the use of sediment traps for estimating upper ocean particle fluxes. *Journal of Marine Research*, 65(3), 345–416.

Buesseler, K., M. Bacon, J. Cochran, & H. Livingston (1992). Carbon and nitrogen export during the JGOFS North Atlantic Bloom Experiment estimated from 234Th:238U disequilibria. *Deep-Sea Research I*, 39(7-8), 1115–1137.

Buesseler, K. & P. Boyd (2009). Shedding light on processes that control particle export and flux attenuation in the twilight zone of the open ocean. *Limnology and Oceanography*, 54(4), 1210–1232.

Buesseler, K., C. Lamborg, P. Boyd, P. Lam, T. Trull, R. Bidigare, J. Bishop, K. Casciotti, F. Dehairs, M. Elskens, M. Honda, D. Karl, D. Siegel, M. Silver,

D. Steinberg, J. Valdes, B. Van Mooy, & S. Wilson (2007*b*). Revisiting carbon flux through the ocean's twilight zone. *Science (New York, N.Y.)*, 316(5824), 567–70.

Buesseler, K., A. M. P. McDonnell, O. M. E. Schofield, D. K. Steinberg, & H. W. Ducklow (2010). High particle export over the continental shelf of the west Antarctic Peninsula. *Geophysical Research Letters*, 37(22).

Buesseler, K., T. Trull, D. Steinber, M. Silver, D. Siegel, S. Saitoh, C. Lamborg, P. Lam, D. Karl, N. Jiao, M. Honda, M. Elskens, F. Dehairs, S. Brown, P. Boyd, J. Bishop, & R. Bidigare (2008). VERTIGO (VERtical Transport in the Global Ocean): A study of particle sources and flux attenuation in the North Pacific. *Deep-Sea Research II*, 55(14-15), 1522–1539.

Cabré, A., I. Marinov, R. Bernardello, & D. Bianchi (2015). Oxygen minimum zones in the tropical Pacific across CMIP5 models: mean state differences and climate change trends. *Biogeosciences Discussions*, 12(8), 6525–6587.

Cai, P., D. Zhao, L. Wang, B. Huang, & M. Dai (2015). Role of particle stock and phytoplankton community structure in regulating particulate organic carbon export in a large marginal sea. *Journal of Geophysical Research-Oceans*, 120.

Carson, R., *The Sea Around Us*. Oxford University Press, US, 1951.

Cavagna, A. J., F. Dehairs, S. Bouillon, V. Woule-Ebongué, F. Planchon, B. Delille, & I. Bouloubassi (2013). Water column distribution and carbon isotopic signal of cholesterol, brassicasterol and particulate organic carbon in the Atlantic sector of the Southern Ocean. *Biogeosciences*, 10, 2787–2801.

Cavan, E. L., F. A. Le Moigne, A. J. Poulton, G. A. Tarling, P. Ward, C. J. Daniels, G. M. Fragoso, & R. J. Sanders (2015). Attenuation of particulate organic carbon flux in the Scotia Sea, Southern Ocean, is controlled by zooplankton fecal pellets. *Geophysical Research Letters*, 42(3), 821–830.

Chen, B., M. R. Landry, B. Huang, & H. Liu (2012). Does warming enhance the effect of microzooplankton grazing on marine phytoplankton in the ocean? *Limnology and Oceanography*, 57(2), 519–526. ISSN 00243590.

Christie, W. (1982). Oil and fats group symposium influence of the diet on fat

deposition in animals. *Journal of the Science of Food and Agriculture*, 33(8), 809–812.

Clarke, A. & L. Peck (1990). The physiology of polar marine zooplankton. *Polar Research*, 10(2), 355–369.

Cochran, K. J., K. O. Buesseler, M. P. Bacon, & H. D. Livingston (1993). Thorium isotopes as indicators of particle dynamics in the upper ocean: results from the JGOFS North Atlantic Bloom experiment. *Deep-Sea Research Part I*, 40(8), 1569–1595.

Codispoti, L. (1995). Is the ocean loosing nitrate? *Nature*, 376, 724.

Collins, J. R., B. R. Edwards, K. Thamatrakoln, J. E. Ossolinski, G. R. Ditullio, K. D. Bidle, S. C. Doney, & B. A. S. V. Mooy (2015). The multiple fates of sinking particles in the North Atlantic Ocean. *Global Biogeochemical cycles*, 29, 1471–1494.

Davis, M. (1968). Pollen grains in lake sediments: Redeposition caused by seasonal water circulation. *Science*, 162, 796–799.

De La Rocha, C. & U. Passow (2007). Factors influencing the sinking of POC and the efficiency of the biological carbon pump. *Deep Sea Research Part II: Topical Studies in Oceanography*, 54(5-7), 639–658.

Devol, A. H. & H. E. Hartnett (2001). Role of the oxygen-deficient zone in transfer of organic carbon to the deep ocean. *Limnology and Oceanography*, 46(7), 1684–1690.

DiTullio, G. R., J. M. Grebmeier, K. R. Arrigo, M. P. Lizotte, D. H. Robinson, A. Leventer, J. B. Barry, M. L. VanWoert, & R. B. Dunbar (2000). Rapid and early export of Phaeocystis antarctica blooms in the Ross Sea, Antarctica. *Nature*, 404(6778), 595–598.

Doney, S., K. Lindsay, K. Caldeira, J. Campin, H. Drange, J.-C. Dutay, M. Follows, Y. Gao, A. Gnanadesikan, N. Gruber, A. Ishida, F. Joos, G. Madec, E. Maier-Reimer, J. C. Marshall, R. J. Matear, P. Monfray, A. Mouchet, R. Najjar, J. C. Orr, G. K. Plattner, J. Sarmiento, R. Schlitzer, R. Slater, I. J. Totterdell, M. F. Weirig, Y. Yamanaka, & A. Yool (2004). Evaluating

global ocean carbon models: The importance of realistic physics. *Global Biogeochemical Cycles*, 18(3).

Doney, S. C. (1999). Major challenges confronting marine biogeochemical modeling. *Global Biogeochemical Cycles*, 13(3), 705–714. ISSN 08866236.

Ducklow, H. W., M. Erickson, J. Kelly, M. Montes-Hugo, C. a. Ribic, R. C. Smith, S. E. Stammerjohn, & D. M. Karl (2008). Particle export from the upper ocean over the continental shelf of the west Antarctic Peninsula: A long-term record, 1992–2007. *Deep Sea Research Part II: Topical Studies in Oceanography*, 55(18-19), 2118–2131.

Ducklow, H. W., D. K. Steinberg, & K. O. Buesseler (2001). Upper ocean carbon export and the biological pump. *Oceanography*, 14(4), 50–58.

Dulaiova, H., M. V. Ardelan, P. B. Henderson, & M. A. Charette (2009). Shelf-derived iron inputs drive biological productivity in the southern Drake Passage. *Global Biogeochemical Cycles*, 23(4), 1–14.

Dunne, J. P., R. a. Armstrong, A. Gnanadesikan, & J. L. Sarmiento (2005). Empirical and mechanistic models for the particle export ratio. *Global Biogeochemical Cycles*, 19(4), GB4026.

Durkin, C. A., M. L. Estapa, & K. O. Buesseler (2015). Observations of carbon export by small sinking particles in the upper mesopelagic. *Marine Chemistry*, 175, 72–81.

Ebersbach, F., T. W. Trull, & S. G. Bray (2011). Controls on mesopelagic particle fluxes in the Sub-Antarctic and Polar Frontal Zones in the Southern Ocean south of Australia in summer—Perspectives from free-drifting sediment traps. *Deep Sea Research Part II: Topical Studies in Oceanography*, 58(21), 2260–2276. ISSN 09670645.

Engel, A., C. Borchard, A. Loginova, J. Meyer, H. Hauss, & R. Kiko (2015). Effects of varied nitrate and phosphate supply on polysaccharidic and proteinaceous gel particles production during tropical phytoplankton bloom experiments. *Biogeosciences Discussions*, 12(8), 6589–6635.

Falkowski, P. (1998). Biogeochemical Controls and Feedbacks on Ocean Primary Production. *Science*, 281(5374), 200–206.

Falkowski, P., R. Scholes, E. Boyle, J. Canadell, D. Canfield, J. Elser, N. Gruber, K. Hibbard, P. Hogberg, S. Linder, F. T. Mackenzie, B. Moore, T. Pedersen, Y. Rosenthal, S. Seitzinger, V. Smetacek, & W. Steffen (2000). The global carbon cycle: A test of our knowledge of earth as a system. *Science*, 290(5490), 291–296.

Fasham, M., H. W. Ducklow, & S. M. McKelvie (1990). A nitrogen-based model of plankton in the oceanic mixed layer. *Journal of Marine Research*, 48(3), 591–639.

Fasham, M. & G. Evans (1995). The use of optimization techniques to model marine ecosystem dynamics at the JGOFS station at 47N 20W. *Proceedings of the Royal Society of London, Series B*, 348, 203–209.

Fenchel, T., G. King, & H. Blackburn, *Bacterial Biogeochemistry*. Academic Press, California, 1998, 307 pp.

Fernández-Álamo, M. A. & J. Färber-Lorda (2006). Zooplankton and the oceanography of the eastern tropical Pacific: A review. *Progress in Oceanography*, 69(2-4), 318–359. ISSN 00796611.

Fiedler, P. C., V. Philbrick, & F. P. Chavez (1991). Oceanic upwelling and productivity in the eastern tropical Pacific. *Limnology and Oceanography*, 36(8), 1834–1850.

Fileman, T., D. Pond, R. Barlow, & R. Mantoura (1998). Vertical profiles of pigments, fatty acids and amino acids: Evidence for undegraded diatomaceous material sedimenting to the deep ocean in the Bellingshausen Sea, Antarctica. *Deep Sea Research Part I: Oceanographic Research Papers*, 45(2-3), 333–346.

Fowler, S. & G. Knauer (1986). Role of large particles in the transport of elements and organic compounds through the oceanic water column. *Progress in Oceanography*, 16(3), 147–194.

Fowler, S. W. (1977). Trace elements in zooplankton particulate products. *Nature*, 269(5623), 51–53.

François, R., S. Honjo, R. Krishfield, & S. Manganini (2002). Factors controlling the flux of organic carbon to the bathypelagic zone of the ocean. *Global Biogeochemical cycles*, 16(4), 1087.

Frankenberg, D. & K. L. Smith (1967). Coprophagy in marine animals. *Limnology and Oceanography*, 443–450.

Franks, P. J. S. (2002). NPZ Models of Plankton Dynamics: Their Construction, Coupling to Physics, and Application. *Journal of Oceanography*, 58(2), 379–387. ISSN 1573-868X.

Froneman, P. W., E. A. Pakhomov, R. Perissinotto, & V. Meaton (1998). Feeding and predation impact of two chaetognath species, Eukrohnia hamata and Sagitta gazellae, in the vicinity of Marion Island (southern ocean). *Marine Biology*, 131(1), 95–101.

Fulton, E. A., A. D. Smith, & C. R. Johnson (2003). Mortality and predation in ecosystem models: is it important how these are expressed? *Ecological Modelling*, 169(1), 157–178. ISSN 03043800.

Giani, M., A. Rinaldi, & D. Degobbis (2005). Mucilages in the Adriatic and Tyrrhenian Sea: an introduction. *The Science of the total environment*, 353(1-3), 3–9.

Giani, M., P. Sist, D. Berto, G. P. Serrazanetti, V. Ventrella, & R. Urbani (2012). The organic matrix of pelagic mucilaginous aggregates in the Tyrrhenian Sea (Mediterranean Sea). *Marine Chemistry*, 132-133, 83–94.

Giering, S., R. Sanders, R. Lampitt, T. Anderson, C. Tamburini, M. Boutrif, M. Zubkov, C. Marsay, S. Henson, K. Saw, K. Cook, & D. Mayor (2014). Reconciliation of the carbon budget in the ocean's twilight zone. *Nature*, 507(7493), 480–3.

Gilmartin, M., N. Revelante, & N. Revelenate (1974). The Island Mass Effect on the phytoplankton and primary production of the Hawaiian Islands. *Journal of Experimental Marine Biology and Ecology*, 16(2), 181–204.

Gleiber, M. R., D. K. Steinberg, & O. M. Schofield (2015). Copepod summer grazing and fecal pellet production along the Western Antarctic Peninsula. *Journal of Plankton Research*, 0(0), 1–19.

Gliwicz, M. Z. (1986). Predation and the evolution of vertical migration in zooplankton. *Nature*, 320(6064), 746–748.

Goericke, R., R. Olson, & A. Shalapyonok (2000). A novel niche for Prochlorococcus sp. in low-light suboxic environments in the Arabian Sea and the Eastern Tropical North Pacific. *Deep Sea Research Part I: Oceanographic Research Papers*, 47(7), 1183–1205.

Gonzalez, H. E. & V. Smetacek (1994). The possible role of the cyclopoid copepod Oithona in retarding vertical flux of zooplankton faecal material. *Marine Ecology Progress Series*, 113(3), 233–246.

Goutx, M., S. Wakeham, C. Lee, M. Duflos, C. Guigue, Z. F. Liu, B. Moriceau, R. Sempere, M. Tedetti, & J. H. Xue (2007). Composition and degradation of marine particles with different settling velocities in the northwestern Mediterranean Sea. *Limnology and Oceanography*, 52(4), 1645–1664.

Gram, L., H.-P. Grossart, A. Schlingloff, & T. Kiørboe (2002). Possible Quorum Sensing in Marine Snow Bacteria : Production of Acylated Homoserine Lactones by Roseobacter Strains Isolated from Marine Snow. *Applied and Environmental Microbiology*, 68(8), 4111–4116.

Grenfell, T. C. & G. A. Maykut (1977). The optical properties of ice and snow in the Arctic basin. *J. Glaciology*, 18(80), 445–463.

Gruber, N., The dynamics of the marine nitrogen cycle and its influence on atmospheric CO2 variations. In *The ocean carbon cycle and climate*. 2004, pp. 97–148.

Guidi, L., G. a. Jackson, L. Stemmann, J. C. Miquel, M. Picheral, & G. Gorsky (2008). Relationship between particle size distribution and flux in the mesopelagic zone. *Deep-Sea Research Part I: Oceanographic Research Papers*, 55, 1364–1374.

Hansen, A. N. & A. W. Visser (2016). Carbon export by vertically migrating zooplankton: an adaptive behaviour model. *Preprint submitted to Marine Ecology Progress Series*.

Hartnett, H. E., A. H. Devol, R. G. Keil, J. Hedges, & A. H. Devol (1998). Influence of oxygen exposure time on organic carbon preservation in continetal margin sediments. *Nature*, 391(February), 2–4.

Henson, S., R. Sanders, & E. Madsen (2012). Global patterns in efficiency of particulate organic carbon export and transfer to the deep ocean. *Global Biogeochemical cycles*, 26(1028), 14.

Henson, S., R. Sanders, E. Madsen, P. J. Morris, F. Le Moigne, & G. D. Quartly (2011). A reduced estimate of the strength of the ocean's biological carbon pump. *Geophysical Research Letters*, 38(4), L04606.

Henson, S., A. Yool, & R. Sanders (2015). Variability in efficiency of particulate organic carbon export: A model study. *Global Biogeochemical cycles*, 33–45.

Hernandez-Sanchez, M. T., J. Holtvoeth, R. A. Mills, E. H. Fisher, G. A. Wolff, & R. D. Pancost (2012). Signature of organic matter exported from naturally Fe-fertilised oceanic waters. *Deep Sea Research Part I: Oceanographic Research Papers*, 65, 59–72.

Herndl, G. & T. Reinthaler (2013). Microbial control of the dark end of the biological pump. *Nature geoscience*, 6(9), 718–724.

Heywood, K. J. & B. A. King (2002). Water masses and baroclinic transports in the South Atlantic and Southern oceans. *Journal of Marine Research*, 60(5), 639–676.

Hill, S. L., E. J. Murphy, K. Reid, P. N. Trathan, & A. J. Constable (2006). Modelling Southern Ocean ecosystems: krill, the food-web, and the impacts of harvesting. *Biological Reviews*, 81(September), 581–608.

Hilting, A. K., L. R. Kump, & T. J. Bralower (2008). Variations in the oceanic vertical carbon isotope gradient and their implications for the Paleocene-Eocene biological pump. *Paleoceanography*, 23(3), PA3222.

Holtvoeth, J., H. Vogel, B. Wagner, & G. A. Wolff (2010). Lipid biomarkers in Holocene and glacial sediments from ancient Lake Ohrid (Macedonia, Albania). *Biogeosciences*, 7, 3473–3489.

Honjo, S. (1982). Seasonality and Interaction of Biogenic and Lithogenic Particulate Flux at the Panama Basin. *Science*, 218(4575), 883–884.

Hopkins, T. L. & J. J. Torres (1989). Midwater food web in the vicinity of a marginal ice zone in the western Weddell Sea. *Deep Sea Research Part A. Oceanographic Research Papers*, 36(4), 543–560.

Huskin, I., L. Viesca, & R. Anadon (2004). Particle flux in the Subtropical Atlantic near the Azores: Influence of mesozooplankton. *Journal of Plankton Research*, 26(4), 403–415.

Iseki, K. (1981). Particulate Organic Matter Transport to the Deep Sea by Salp Fecal Pellets. *Marine Ecology Progress Series*, 5, 55–60.

Iversen, M. & H. Ploug (2013). Temperature effects on carbon-specific respiration rate and sinking velocity of diatom aggregates – potential implications for deep ocean export processes. *Biogeosciences Discussions*, 10(1), 371–399.

Iversen, M. & L. Poulsen (2007). Coprorhexy, coprophagy, and coprochaly in the copepods Calanus helgolandicus, Pseudocalanus elongatus, and Oithona similis. *Marine Ecology Progress Series*, 350(1990), 79–89.

Iversen, M. H. & H. Ploug (2010). Ballast minerals and the sinking carbon flux in the ocean: carbon-specific respiration rates and sinking velocity of marine snow aggregates. *Biogeosciences*, 7, 2613–2624.

Jeffreys, R. M., G. A. Wolff, & G. L. Cowie (2009). Influence of oxygen on heterotrophic reworking of sedimentary lipids at the Pakistan margin. *Deep Sea Research Part II: Topical Studies in Oceanography*, 56(6-7), 358–375.

Jónasdóttir, S. H., A. W. Visser, K. Richardson, & M. R. Heath (2015). Seasonal copepod lipid pump promotes carbon sequestration in the deep North Atlantic. *Proceedings of the National Academy of Sciences*, 112(39), 12122–12126.

Jones, E. M., D. C. Bakker, H. J. Venables, & A. J. Watson (2012). Dynamic seasonal cycling of inorganic carbon downstream of South Georgia, Southern Ocean. *Deep Sea Research Part II: Topical Studies in Oceanography*, 59-60, 25–35.

Kahru, M., S. Mitchell, S. Gille, C. D. Hewes, & O. Holm-Hansen (2007). Eddies enhance biological production in the Weddell-Scotia Confluence of the Southern Ocean. *Geophys. Res. Lett.*, 34.

Kalvelage, T., G. Lavik, P. Lam, S. Contreras, L. Arteaga, C. R. Löscher, A. Oschlies, A. Paulmier, L. Stramma, & M. M. M. Kuypers (2013). Nitrogen cycling driven by organic matter export in the South Pacific oxygen minimum zone. *Nature Geoscience*, 6(February), 228–234.

Kamykowski, D. & S.-J. Zentara (1990). Hypoxia in the world as recorded in the Historical Data Set. *Deep-Sea Research*, 37(12), 1861–1874.

Kawaguchi, K., S. Ishikawa, & O. Matsuda (1986). The overwintering of Antarctic krill under the coastal fast ice off the Ongul Islands in Lutzow-Holm Bay, Antarctica. *Memoirs of the National Institute of Polar Research*, 44, 67–85.

Keil, R. G. & G. L. Cowie (1999). Organic matter preservation through the oxygen-deficient zone of the NE Arabian Sea as discerned by organic carbon:mineral surface area ratios. *Marine Geology*, 161(1), 13–22.

Keil, R. G., J. Neibauer, C. Biladeau, K. van der Elst, & A. H. Devol (2016). A multiproxy approach to understanding the "enhanced" flux of organic matter through the oxygen deficient waters of the Arabian Sea. *Biogeosciences*, 13, 2077–2092.

Kiko, R., H. Hauss, F. Buchholz, & F. Melzner (2016). Ammonium excretion and oxygen respiration of tropical copepods and euphausiids exposed to oxygen minimum zone conditions. *Biogeosciences*, 13, 2241–2255.

Kilops, S. & V. Kilops, *Introduction to Organic Chemistry*. Blackwell Science, 2005, 2nd edition, 393 pp.

Kindler, K., A. Khalili, & R. Stocker (2010). Diffusion-limited retention of porous particles at density interfaces. *Proceedings of the National Academy of Sciences of the United States of America*, 107(51), 22163–8.

Kiørboe, T. (2011). How zooplankton feed: mechanisms, traits and trade-offs. *Biological reviews of the Cambridge Philosophical Society*, 86(2), 311–39. ISSN 1469-185X.

Kiriakoulakis, K., B. J. Bett, M. White, & G. A. Wolff (2004). Organic biogeochemistry of the Darwin Mounds, a deep-water coral ecosystem, of the NE Atlantic. *Deep-Sea Research Part I: Oceanographic Research Papers*, 51(12), 1937–1954.

Klaas, C. & D. Archer (2002). Association of sinking organic matter with various types of mineral ballast in the deep sea: Implications for the rain ratio. *Global Biogeochemical cycles*, 16(4), 1116.

Kobari, T., D. K. Steinberg, A. Ueda, A. Tsuda, M. W. Silver, & M. Kitamura (2008). Impacts of ontogenetically migrating copepods on downward carbon flux in the western subarctic Pacific Ocean. *Deep Sea Research Part II: Topical Studies in Oceanography*, 55(14-15), 1648–1660.

Korb, R. E., M. J. Whitehouse, P. Ward, M. Gordon, H. J. Venables, & A. J. Poulton (2012). Regional and seasonal differences in microplankton biomass, productivity, and structure across the Scotia Sea: Implications for the export of biogenic carbon. *Deep Sea Research Part II: Topical Studies in Oceanography*, 59-60, 67–77.

Kwon, E., F. Primeau, & J. Sarmiento (2009). The impact of remineralization depth on the air-sea carbon balance. *nature Geoscience*, 2, 630–635.

Lam, P., S. C. Doney, & J. K. B. Bishop (2011). The dynamic ocean biological pump: Insights from a global compilation of particulate organic carbon, CaCO3, and opal concentration profiles from the mesopelagic. *Global Biogeochemical Cycles*, 25(3), 1–14.

Lam, P., G. Lavik, M. M. Jensen, J. van de Vossenberg, M. Schmid, D. Woebken, D. Gutiérrez, R. Amann, M. S. M. Jetten, & M. M. M. Kuypers (2009). Revising the nitrogen cycle in the Peruvian oxygen minimum zone. *Proceedings of the National Academy of Sciences of the United States of America*, 106(12), 4752–7.

Lam, P. J. & J. K. B. Bishop (2007). High biomass, low export regimes in the Southern Ocean. *Deep-Sea Research II*, 54(5-7), 601–638.

Lampitt, R. (1985). Evidence for the seasoanl deposition of detritus ot the deep-sea floor and its subsequent resuspension. *Deep-Sea Research*, 32, 1885–1897.

Lampitt, R., B. Bett, K. Kiriakoulakis, E. Popova, O. Ragueneau, A. Vangriesheim, & G. A. Wolff (2001). Material supply to the abyssal seafloor in the Northeast Atlantic. *Progress in Oceanography*, 50(1-4), 27–63.

Lampitt, R., W. Hillier, & P. Challenor (1993). Seasonal and diel variation in the open ocean concentration of marine snow aggregates. *Nature*, 363, 737–739.

Lampitt, R., T. Noji, & B. Bodungen (1990). What happens to zooplankton faecal pellets? Implications for vertical flux. *Marine Biology*, 23, 15–23.

Lampitt, R. S., B. Boorman, L. Brown, M. Lucas, I. Salter, R. Sanders, K. Saw, S. Seeyave, S. J. Thomalla, & R. Turnewitsch (2008). Particle export from the euphotic zone: Estimates using a novel drifting sediment trap, Th-234 and new production. *Deep-Sea Research Part I-Oceanographic Research Papers*, 55(11), 1484–1502.

Lancraft, T. M., T. L. Hopkins, J. J. Torres, & J. Donnelly (1991). Oceanic micronektonic/macrozooplanktonic community structure and feeding in ice covered Antarctic waters during the winter (AMERIEZ 1988). *Polar Biology*, 11(3), 157–167.

Landry, M. R. & R. P. Hassett (1982). Estimating the grazing impact of marine micro-zooplankton. *Marine Biology*, 67(3), 283–288. ISSN 1432-1793.

Laufkötter, C., M. Vogt, & N. Gruber (2013). Long-term trends in ocean plankton production and particle export between 1960–2006. *Biogeosciences Discussions*, 10(3), 5923–5975.

Laufkötter, C., M. Vogt, N. Gruber, L. Bopp, J. Dunne, J. Hauck, J. John, I. Lima, R. Seferian, & C. Volker (2015). Projected decreases in future marine export production : the role of the carbon flux through the upper ocean ecosystem. *Biogeosciences Discussions*, 12(4), 3731–3824.

Laws, A., G. Falkowski, O. Smith, J. Hugh, & J. Mccarthy (2000). Temperature effects on export production in the open ocean. *Global Biogeochemical cycles*, 14(4), 1231–1246.

Le Moigne, F., M. Gallinari, E. Laurenceau, & C. De La Rocha (2013*a*). Enhanced rates of particulate organic matter remineralization by microzooplankton are diminished by added ballast minerals. *Biogeosciences Discussions*, 10(2), 3597–3625.

Le Moigne, F., S. Henson, R. Sanders, & E. Madsen (2013*b*). Global database of surface ocean particulate organic carbon export fluxes diagnosed from the 234 Th technique. *Earth system science data*, 5, 295–304.

Le Moigne, F., K. Pabortsava, C. Marcinko, & P. Martin (2014). Where is mineral ballast important for surface export of particulate organic carbon in the ocean? *Geophysical Research Letters*, 41, 8460–8468.

Le Moigne, F., R. Sanders, M. Villa-Alfageme, A. P. Martin, K. Pabortsava, H. Planquette, P. Morris, & S. Thomalla (2012). On the proportion of ballast versus non-ballast associated carbon export in the surface ocean. *Geophysical Research Letters*, 39(15).

Le Moigne, F., M. Villa, R. Sanders, C. Marsay, R. Garcia-Tenorio, & S. Henson (2013*c*). Insights from a POC and biominerals Th and Po derived export fluxes study at the Porcupine Abyssal Plain: Implications for the ballast hypothesis. *Deep Sea Research I*, 72, 88–101.

Le Moigne, F. A., S. A. Henson, E. Cavan, C. Georges, K. Pabortsava, E. P. Achterberg, E. Ceballos-Romero, M. Zubkov, & R. J. Sanders (2016). What causes the inverse relationship between primary production and export efficiency in the Southern Ocean? *Geophysical Research Letters*.

Le Quéré, C., E. T. Buitenhuis, R. Moriarty, S. Alvain, O. Aumont, L. Bopp, S. Chollet, C. Enright, D. J. Franklin, R. J. Geider, S. P. Harrison, A. Hirst, S. Larsen, L. Legendre, T. Platt, I. C. Prentice, R. B. Rivkin, S. Sathyendranath, N. Stephens, M. Vogt, S. Sailley, & S. M. Vallina (2015). Role of zooplankton dynamics for Southern Ocean phytoplankton biomass and global biogeochemical cycles. *Biogeosciences Discussions*, 12(14), 11935–11985.

Lee, C., D. Murray, R. Barber, K. Buesseler, J. Dymond, J. Hedges, S. Honjo, S. Manganini, J. Marra, C. Moser, M. Peterson, W. Prell, & S. Wakeham (1998). Particulate organic carbon fluxes: compilation of results from the 1995 US JGOFS Arabian Sea Process Study. *Deep-Sea Research II*, 45(10-11), 2489–2501.

Li, W. K. W. (1998). Annual average abundance of heterotrophic bacteria and Synechococcus in surface ocean waters. *Limnology and Oceanography*, 43(7), 1746–1753.

Lima, I. D., P. J. Lam, & S. C. Doney (2013). Dynamics of particulate organic carbon flux in a global ocean model. *Biogeosciences Discussions*, 10(9), 14715–14767.

Lombard, F., M. Koski, & T. Kiørboe (2013). Copepods use chemical trails to find sinking marine snow aggregates. *Limnology and Oceanography*, 58(1), 185–192.

Löscher, C. R., A. Bourbonnais, J. Dekaezemacker, C. N. Charoenpong, M. A. Altabet, H. W. Bange, R. Czeschel, C. Hoffmann, & R. Schmitz (2016). N2 fixation in eddies of the eastern tropical South Pacific Ocean. *Biogeosciences*, 13(10), 2889–2899.

Maiti, K., M. a. Charette, K. O. Buesseler, & M. Kahru (2013). An inverse relationship between production and export efficiency in the Southern Ocean. *Geophysical Research Letters*, 40(November 2012).

Manno, C., G. Stowasser, P. Enderlein, S. Fielding, & G. A. Tarling (2015). The contribution of zooplankton faecal pellets to deep-carbon transport in the Scotia Sea (Southern Ocean). *Biogeosciences*, 12(6), 1955–1965.

Marsay, C., R. Sanders, S. Henson, K. Pabortsava, E. Achterberg, & R. Lampitt (2015). Attenuation of sinking particulate organic carbon flux through the mesopelagic ocean. *Proceedings of the National Academy of Sciences*, 12(4), 1089–1094.

Martin, J., G. Knauler, D. Karl, & W. Broenkow (1987). VERTEX: carbon cycling in the north east Pacific. *Deep-Sea Research*, 34(2), 267–285.

Martin, J. H. (1990). Glacial-Interglacial CO2 Change: The Iron Hypothesis. *Paleoceanography*, 5(1), 1–13.

Mayor, D. J., R. Sanders, S. L. C. Giering, & T. R. Anderson (2014). Microbial gardening in the ocean's twilight zone. *BioEssays : news and reviews in molecular, cellular and developmental biology*, 36(12), 1132–7.

Mayzaud, P., M. Boutoute, S. Gasparini, & L. Mousseau (2014). Lipids and fatty acid composition of particulate matter in the North Atlantic: importance of spatial heterogeneity, season and community structure. *Marine Biology*, 161(9), 1951–1971.

McCave, I. N. (1975). Vertical flux of particles in the ocean. *Deep-Sea Research and Oceanographic Abstracts*, 22(December 1974), 491–502.

Mcdonnell, A. M. P., P. W. Boyd, & K. O. Buesseler (2015). Effects of sinking velocities and microbial respiration rates on the attenuation of particulate carbon fluxes through the mesopelagic zone. *Global Biogeochemical cycles*, 29, 175–193.

McDonnell, A. M. P. & K. O. Buesseler (2010). Variability in the average sinking velocity of marine particles. *Limnology and Oceanography*, 55(5), 2085–2096.

Menzies, R. J., R. Y. George, & R. G. T, *Abyssal environment and ecology of the world oceans*. Wiley-Interscience, New York, 1973, 488 pp.

Miller, M. B. & B. L. Bassler (2001). Quorum sensing in bacteria. *Annual Review of Microbiology*, 55, 165–199.

Mislan, K., C. Stock, J. Dunne, & J. Sarmiento (2014). Group behaviour among model bacteria influences particulate carbon reminerlisation depths. *Journal of Marine Research*, 72, 183–218.

Mulder, A., A. van de Graaf, L. Robertson, & J. Kuenen (1995). Anaerobic ammonium oxidation discovered in a denitrifying fluidized bed reactor. *Fems Microbiology Ecology*, 16(3), 177–183.

Murphy, E., E. Hofmann, J. Watkins, N. Johnston, A. Piñones, T. Ballerini, S. Hill, P. Trathan, G. Tarling, R. Cavanagh, E. Young, S. Thorpe, & P. Fretwell (2013). Comparison of the structure and function of Southern Ocean regional ecosystems: The Antarctic Peninsula and South Georgia. *Journal of Marine Systems*, 109-110, 22–42.

Okuyama, H., Y. Orikasa, & T. Nishida (2008). Significance of antioxidative functions of eicosapentaenoic and docosahexaenoic acids in marine microorganisms. *Applied and environmental microbiology*, 74(3), 570–4.

Olson, M. & K. L. Daly (2013). Micro-grazer biomass, composition and distribution across prey resource and dissolved oxygen gradients in the far eastern tropical north Pacific Ocean. *Deep-Sea Research Part I: Oceanographic Research Papers*, 75, 28–38.

Orsi, A. H., T. Whitworth, & W. D. Nowlin (1995). On the meridional extent and fronts of the Antarctic Circumpolar Current. *Deep-Sea Research Part I*, 42(5), 641–673.

Pakhomov, A. E. & D. C. McQuaid (1996). Distribution of surface zooplankton and seabirds across the Southern Ocean. *Polar Biology*, 16(4), 271–286. ISSN 1432-2056.

Parekh, P., S. Dutkiewicz, M. J. Follows, & T. Ito (2006). Atmospheric carbon dioxide in a less dusty world. *Geophysical Research Letters*, 33.

Park, J., I.-S. Oh, H.-C. Kim, & S. Yoo (2010). Variability of SeaWiFs chlorophyll-a in the southwest Atlantic sector of the Southern Ocean: Strong topographic effects and weak seasonality. *Deep Sea Research Part I: Oceanographic Research Papers*, 57(4), 604–620.

Paulmier, A. & D. Ruiz-Pino (2009). Oxygen minimum zones (OMZs) in the modern ocean. *Progress in Oceanography*, 80(3-4), 113–128.

Peterson, M. L., S. G. Wakeham, C. Lee, M. Askea, & J. C. Miquel (2005). Novel techniques for collection of sinking particles in the ocean and determining their settling rates. *Limnology and Oceanography*, 3, 520–532.

Piontek, J., M. Massmig, S. Endres, F. A. C. Le Moigne, H. W. Bange, & A. Engel, Bacterial Activity and Organic Matter Turnover in Oxygen Deficient Waters of the Baltic Sea. In *Ocean Sciences Meeting*. 2016.

Planchon, F., A.-J. Cavagna, D. Cardinal, L. André, & F. Dehairs (2013). Late summer particulate organic carbon export and twilight zone remineralisation in the Atlantic sector of the Southern Ocean. *Biogeosciences*, 10(2), 803–820.

Ploug, H. & H. P. Grossart (2000). Bacterial growth and grazing on diatom aggregates: Respiratory carbon turnover as a function of aggregate size and sinking velocity. *Limnology and Oceanography*, 47(7), 1467–1475.

Ploug, H., M. Iversen, & G. Fischer (2008). Ballast, sinking velocity, and apparent diffusivity within marine snow and zooplankton fecal pellets: Implications for substrate turnover by attached bacteria. *Limnology and Oceanography*, 53(5), 1878–1886.

Pollard, R. T., I. Salter, R. J. Sanders, M. I. Lucas, C. M. Moore, R. A. Mills, P. J. Statham, J. T. Allen, A. R. Baker, D. C. E. Bakker, M. A. Charette, S. Fielding, G. R. Fones, M. French, A. E. Hickman, R. J. Holland, J. A. Hughes, T. D. Jickells, R. S. Lampitt, P. J. Morris, F. H. Nedelec, M. Nielsdottir, H. Planquette, E. E. Popova, A. J. Poulton, J. F. Read, S. Seeyave, T. Smith, M. Stinchcombe, S. Taylor, S. Thomalla, H. J. Venables, R. Williamson, & M. V. Zubkov (2009). Southern Ocean deep-water carbon export enhanced by natural iron fertilization. *Nature*, 457(7229), 577–U81.

Poulton, A., R. Sanders, P. Holligan, M. Stinchcombe, T. Adey, L. Brown, & K. Chamberlain (2006). Phytoplankton mineralization in the tropical and subtropical Atlantic Ocean. *Global Biogeochemical cycles*, 20(4).

Poulton, A. J., M. C. Stinchcombe, E. P. Achterberg, D. C. E. Bakker, C. Dumousseaud, H. E. Lawson, G. A. Lee, S. Richier, D. J. Suggett, & J. R. Young (2014). Coccolithophores on the north-west European shelf: calcification rates and environmental controls. *Biogeosciences Discussions*, 11(2), 2685–2733.

Precali, R., M. Giani, M. Marini, F. Grilli, C. Ferrari, O. Pecar, & E. Paschini (2005). Mucilaginous aggregates in the northern Adriatic in the period 1999-2002: typology and distribution. *The Science of the total environment*, 353(1-3), 10–23.

Redfield, A., *On the proportions of organic derivatives in sea water and their relation to the composition of plankton.* University Press of Liverpool, 1934, 177–192 pp.

Reimers, C. E., Y. Alleau, J. E. Bauer, J. Delaney, P. R. Girguis, P. S. Schrader, & H. A. Stecher (2013). Redox effects on the microbial degradation of refractory organic matter in marine sediments. *Geochimica et Cosmochimica Acta*, 121, 582–598. ISSN 00167037.

Rembauville, M., S. Blain, L. Armand, B. Quéguiner, & I. Salter (2015). Export fluxes in a naturally iron-fertilized area of the Southern Ocean – Part 2: Importance of diatom resting spores and faecal pellets for export. *Biogeosciences*, 12(11), 3171–3195.

Richardson, A. J. (2008). In hot water: zooplankton and climate change. *ICES Journal of Marine Science*, 65(3), 279–295.

Richardson, T. L. & G. A. Jackson (2007). Small phytoplankton and carbon export from the surface ocean. *Science*, 315(5813), 838–840.

Richier, S., E. P. Achterberg, C. Dumousseaud, a. J. Poulton, D. J. Suggett, T. Tyrrell, M. V. Zubkov, & C. M. Moore (2014). Phytoplankton responses and associated carbon cycling during shipboard carbonate chemistry manipulation experiments conducted around Northwest European shelf seas. *Biogeosciences*, 11(17), 4733–4752.

Riley, J., R. Sanders, C. Marsay, F. Le Moigne, E. Achterberg, & A. Poulton (2012). The relative contribution of fast and slow sinking particles to ocean carbon export. *Global Biogeochemical cycles*, 26.

Rokop, F. J. (1974). Reproductive patterns in the deep-sea benthos. *Science*, 186, 743–745.

Roullier, F., L. Berline, L. Guidi, X. Durrieu De Madron, M. Picheral, A. Sciandra, S. Pesant, & L. Stemmann (2014). Particle size distribution and estimated carbon flux across the Arabian Sea oxygen minimum zone. *Biogeosciences*, 11(16), 4541–4557.

Sabine, C., R. Feely, N. Gruber, R. Key, K. Lee, J. Bullister, R. Wanninkhof, C. S. Wong, D. Wallace, B. Tilbrook, F. J. Millero, T. H. Peng, A. Kozyr, T. Ono, & A. F. Rios (2004). The oceanic sink for anthropogenic CO2. *Science*, 305(5682), 367–371.

Sailley, S., H. Ducklow, H. Moeller, W. Fraser, O. Schofield, D. K. Steinberg, L. Garzio, & S. Doney (2013). Carbon fluxes and pelagic ecosystem dynamics near two western Antarctic Peninsula Adélie penguin colonies: an inverse model approach. *Marine Ecology Progress Series*, 492, 253–272.

Salter, I., A. E. S. Kemp, C. M. Moore, R. S. Lampitt, G. a. Wolff, & J. Holtvoeth (2012). Diatom resting spore ecology drives enhanced carbon export from a naturally iron-fertilized bloom in the Southern Ocean. *Global Biogeochemical Cycles*, 26(1), GB1014.

Salter, I., R. S. Lampitt, R. Sanders, A. Poulton, A. E. S. Kemp, B. Boorman, K. Saw, & R. Pearce (2007). Estimating carbon, silica and diatom export from a naturally fertilised phytoplankton bloom in the Southern Ocean using PELAGRA: A novel drifting sediment trap. *Deep-Sea Research Part Ii-Topical Studies in Oceanography*, 54(18-20), 2233–2259.

Sanders, R., S. A. Henson, M. Koski, C. L. De La Rocha, S. C. Painter, A. J. Poulton, J. Riley, B. Salihoglu, A. Visser, A. Yool, R. Bellerby, & A. P. Martin (2014). The Biological Carbon Pump in the North Atlantic. *Progress in Oceanography*, 129, 200–218.

Sanders, R., P. J. Morris, A. J. Poulton, M. C. Stinchcombe, A. Charalampopoulou, M. I. Lucas, & S. J. Thomalla (2010). Does a ballast effect occur in the surface ocean? *Geophysical Research Letters*, 37(8).

Schartau, M. & A. Oschlies (2003). Simultaneous data-based optimization of a 1D-ecosystem model at three locations in the North Atlanric: Part 1 - Method and parameter estimates. *Journal of Marine Research*, 61(6), 765 – 793.

Schlitzer, R. (2002). Carbon export fluxes in the Southern Ocean: results from inverse modeling and comparison with satellite-based estimates. *Deep Sea Research Part II: Topical Studies in Oceanography*, 49(9-10), 1623–1644.

Schunck, H., G. Lavik, D. K. Desai, T. Großkopf, T. Kalvelage, C. R. Löscher, A. Paulmier, S. Contreras, H. Siegel, M. Holtappels, P. Rosenstiel, M. B. Schilhabel, M. Graco, R. A. Schmitz, M. M. M. Kuypers, & J. LaRoche (2013). Giant Hydrogen Sulfide Plume in the Oxygen Minimum Zone off Peru Supports Chemolithoautotrophy. *PLoS ONE*, 8(8), e68661. ISSN 1932-6203.

Sedwick, P. N. & G. R. DiTullio (1997). Regulation of algal blooms in Antarctic Shelf Waters by the release of iron from melting sea ice. *Geophysical Research Letters*, 24(20), 2515–2518.

Siegel, V., A. Skibowski, & U. Harm (1992). Community structure of the epipelagic zooplankton community under the sea-ice of the northern Weddell Sea. *Polar Biology*, 12(1), 15–24.

Sieracki, C. K., M. E. Sieracki, & C. M. Yentsch (1998). An imaging analysis system for automated analysis for marine microplankton. *Mar Ecol Prog Ser*, 168, 285–296.

Slagstad, D., K. Downing, F. Carlotti, & H. Hirche (1999). Modelling the carbon export and air-sea flux of CO2 in the Greenland Sea. *Deep-Sea Research Part II: Topical Studies in Oceanography*, 46, 1511–1530.

Smith, K. L., A. D. Sherman, T. J. Shaw, A. E. Murray, M. Vernet, & A. O. Cefarelli (2011). Carbon export associated with free-drifting icebergs in the Southern Ocean. *Deep-Sea Research Part II: Topical Studies in Oceanography*, 58(11-12), 1485–1496.

Steinberg, D. K. (1995). Diet of copepods (Scopalatum vorax) associated with mesopelagic detritus (giant larvacean houses) in Monterey Bay, California. *Marine Biology*, 122(4), 571–584.

Steinberg, D. K., C. a. Carlson, N. R. Bates, S. a. Goldthwait, L. P. Madin, & A. F. Michaels (2000). Zooplankton vertical migration and the active transport of dissolved organic and inorganic carbon in the Sargasso Sea. *Deep Sea Research Part I: Oceanographic Research Papers*, 47(1), 137–158.

Steinberg, D. K., B. A. S. Van Mooy, K. O. Buesseler, P. W. Boyd, T. Kobari, & D. M. Karl (2008). Bacterial vs. zooplankton control of sinking particle flux in the ocean's twilight zone. *Limnology and Oceanography*, 53(4), 1327–1338.

Stevens, H. & O. Ulloa (2008). Bacterial diversity in the oxygen minimum zone of the eastern tropical South Pacific. *Environmental microbiology*, 10(5), 1244–59.

Stramma, L., G. C. Johnson, J. Sprintall, & V. Mohrholz (2008). Expanding oxygen-minimum zones in the tropical oceans. *Science*, 320(5876), 655–658.

Stramma, L., S. Schmidtko, L. a. Levin, & G. C. Johnson (2010). Ocean oxygen minima expansions and their biological impacts. *Deep-Sea Research Part I: Oceanographic Research Papers*, 57(4), 587–595.

Suess, E. (1980). Particulate organic carbon in the oceans-surface productivity and oxygen utilisation. *Nature*, 288(20).

Sun, M.-Y., S. G. Wakeham, & C. Lee (1997). Rates and mechanisms of fatty acid degradation in oxic and anoxic coastal marine sediments of Long Island Sound, New York, USA. *Geochimica et Cosmochimica Acta*, 61(2), 341–355.

Takahashi, T., S. Sutherland, C. Sweeney, A. Poisson, N. Metzl, B. Tilbrook, N. Bates, R. Wanninkhof, R. Feely, C. Sabine, J. Olafsson, & Y. Nojiri (2002). Global sea–air CO2 flux based on climatological surface ocean pCO2, and seasonal biological and temperature effects. *Deep Sea Research Part II: Topical Studies in Oceanography*, 49(9-10), 1601–1622.

Tarling, G., P. Ward, A. Atkinson, M. Collins, & E. Murphy (2012). DISCOVERY 2010: Spatial and temporal variability in a dynamic polar ecosystem. *Deep Sea Research Part II: Topical Studies in Oceanography*, 59-60, 1–13.

Tarling, G. A. (2013). JR274 Sea Surface Ocean Acidification Consortium Cruise to the Southern Ocean. Technical report, British Antarctic Survey, Cambridge, UK.

Tarling, G. A., R. Shreeve, P. Ward, & A. Hirst (2004). Life-cycle phenotypic composition and mortality of Calanoides actus in the Scotia Sea; a modeling approach. *Marine Ecology Progress Series*, 272, 165–181.

Taylor, M. H., M. Losch, & A. Bracher (2013). On the drivers of phytoplankton blooms in the Antarctic marginal ice zone: A modeling approach. *Journal of Geophysical Research: Oceans*, 118(1), 63–75.

Thomalla, S., A. Poulton, R. Sanders, R. Turnewitsch, P. Holligan, & M. Lucas (2008). Variable export fluxes and efficiencies for calcite, opal, and organic carbon in the Atlantic Ocean: A ballast effect in action? *Global Biogeochemical cycles*, 22(1), GB1010.

Thomalla, S., R. Turnewitsch, M. Lucas, & A. Poulton (2006). Particulate organic carbon export from the North and South Atlantic gyres: The Th-234/U-238 disequilibrium approach. *Deep-Sea Research Part Ii-Topical Studies in Oceanography*, 53(14-16), 1629–1648.

Thorpe, S. (2014). JR274 physical oceanographic analyses. Technical report, Bristish Antartic Survey.

Tiano, L., E. Garcia-Robledo, & N. P. Revsbech (2014). A new highly sensitive method to assess respiration rates and kinetics of natural planktonic communities by use of the switchable trace oxygen sensor and reduced oxygen concentrations. *PLoS ONE*, 9(8), e105399.

Tolosa, I., S. Fiorini, B. Gasser, J. Martín, & J. C. Miquel (2013). Carbon sources in suspended particles and surface sediments from the Beaufort Sea revealed by molecular lipid biomarkers and compound-specific isotope analysis. *Biogeosciences*, 10(3), 2061–2087.

Turner, J. T. (2004). The Importance of Small Pelagic Planktonic Copepods and Their Role in Pelagic Marine Food Webs. *Zoological Studies*, 43(2), 255–266.

Ulloa, O. & S. Pantoja (2009). The oxygen minimum zone of the eastern South

Pacific. *Deep Sea Research Part II: Topical Studies in Oceanography*, 56, 987–991.

Van Mooy, B. A. S., R. G. Keil, & A. H. Devol (2002). Impact of suboxia on sinking particulate organic carbon : Enhanced carbon flux and preferential degradation of amino acids via denitrification. *Geochimica et Cosmochimica Acta*, 66(3), 457–465.

Veit, R., E. Silverman, & I. Everson (1993). Aggregation Patterns of Pelagic Predators and their Principal Prey , Antarctic Krill, near South Georgia. *Journal of Animal Ecology*, 62(3), 551–564.

Venables, H., M. P. Meredith, A. Atkinson, & P. Ward (2012). Fronts and habitat zones in the Scotia Sea. *Deep Sea Research Part II: Topical Studies in Oceanography*, 59-60, 14–24.

Villareal, T. a. (1988). Positive buoyancy in the oceanic diatom Rhizosolenia debyana H. Peragallo. *Deep Sea Research Part A. Oceanographic Research Papers*, 35(6), 1037–1045.

Volk, T. & M. Hoffert, Ocean Carbon Pumps: Analysis of Relative Strengths and Efficiencies in Ocean-Driven Atmospheric CO2 Changes. In *The Carbon Cycle and Atmospheric CO2: Natural Variations Archean to Present*. American Geophysical Union, 1991, pp. 99–110.

Wakeham, S. G. (1995). Lipid biomarkers for heterotrophic alteration of suspended particulate organic matter in oxygenated and anoxic water columns of the ocean. *Deep Sea Research Part I: Oceanographic Research Papers*, 42(10), 1749–1771.

Wakeham, S. G. & E. a. Canuel (1988). Organic geochemistry of particulate matter in the eastern tropical North Pacific Ocean: Implications for particle dynamics. *Journal of Marine Research*, 46, 183–213.

Wakeham, S. G., J. W. Farrington, R. M. Gagosian, C. Lee, H. DeBaar, G. E. Nigrelli, B. W. Tripp, S. O. Smith, & N. M. Frew (1980). Organic matter fluxes from sediment traps in the equatorial Atlantic Ocean.

Wakeham, S. G. & C. Lee (1989). Organic geochemistry of particulate matter

in the ocean: The role of particles in oceanic sedimentary cycles. *Organic Geochemistry*, 14(I), 83–96.

Wakeham, S. G., C. Lee, M. L. Peterson, Z. F. Liu, J. Szlosek, I. F. Putnam, & J. H. Xue (2009). Organic biomarkers in the twilight zone-Time series and settling velocity sediment traps during MedFlux. *Deep-Sea Research Part Ii-Topical Studies in Oceanography*, 56(18), 1437–1453.

Ward, P., A. Atkinson, & G. Tarling (2012*a*). Mesozooplankton community structure and variability in the Scotia Sea: A seasonal comparison. *Deep Sea Research Part II: Topical Studies in Oceanography*, 59-60, 78–92.

Ward, P., A. Atkinson, H. J. Venables, G. a. Tarling, M. J. Whitehouse, S. Fielding, M. a. Collins, R. Korb, A. Black, G. Stowasser, K. Schmidt, S. E. Thorpe, & P. Enderlein (2012*b*). Food web structure and bioregions in the Scotia Sea: A seasonal synthesis. *Deep Sea Research Part II: Topical Studies in Oceanography*, 59-60, 253–266.

Whitehouse, M. J., A. Atkinson, R. E. Korb, H. J. Venables, D. W. Pond, & M. Gordon (2012). Substantial primary production in the land-remote region of the central and northern Scotia Sea. *Deep-Sea Research Part II: Topical Studies in Oceanography*, 59-60, 47–56.

Wiebe, P. H., L. P. Madin, L. R. Haury, G. R. Harbison, & L. M. Philbin (1979). Diel vertical migration bySalpa aspera and its potential for large-scale particulate organic matter transport to the deep-sea. *Marine Biology*, 53(3), 249–255.

Williams, R. L., S. Wakeham, R. McKinney, & K. F. Wishner (2014). Trophic ecology and vertical patterns of carbon and nitrogen stable isotopes in zooplankton from oxygen minimum zone regions. *Deep-Sea Research Part I: Oceanographic Research Papers*, 90(1), 36–47.

Wilson, S., H. Ruhl, & K. Smith (2013). Zooplankton fecal pellet flux in the abyssal northeast Pacific : A 15 year time-series study. *Limnology and Oceanography*, 58(3), 881–892.

Wilson, S., D. Steinberg, & K. Buesseler (2008). Changes in fecal pellet characteristics with depth as indicators of zooplankton repackaging of particles in the

mesopelagic zone of the subtropical and subarctic North Pacific Ocean. *Deep-Sea Research Part Ii-Topical Studies in Oceanography*, 55(14-15), 1636–1647.

Wishner, K. F., C. Gelfman, M. M. Gowing, D. M. Outram, M. Rapien, & R. L. Williams (2008). Vertical zonation and distributions of calanoid copepods through the lower oxycline of the Arabian Sea oxygen minimum zone. *Progress in Oceanography*, 78(2), 163–191.

Wishner, K. F., D. M. Outram, B. A. Seibel, K. L. Daly, & R. L. Williams (2013). Zooplankton in the eastern tropical north Pacific: Boundary effects of oxygen minimum zone expansion. *Deep Sea Research Part I: Oceanographic Research Papers*, 79, 122–140.

Wolff, G. a., D. S. M. Billett, B. J. Bett, J. Holtvoeth, T. FitzGeorge-Balfour, E. H. Fisher, I. Cross, R. Shannon, I. Salter, B. Boorman, N. J. King, A. Jamieson, & F. Chaillan (2011). The effects of natural iron fertilisation on deep-sea ecology: The Crozet Plateau, southern Indian ocean. *PLoS ONE*, 6(6).

Worthington, E. B. (1931). Vertical movements of freshwater Macroplankton. *International review of Hydrobiologie and Hydrographie*, 25(5-6), 394–436.

Wright, J. J., K. M. Konwar, & S. J. Hallam (2012). Microbial ecology of expanding oxygen minimum zones. *Nature Reviews Microbiology*, 10(6), 381–394.

Wyrtki, K. (1964). Upwelling in the Costa Rica Dome. *Fishery Bulletin*, 63(2), 355–372.

Yool, A., E. Popova, & T. R. Anderson (2011). Medusa-1.0: a new intermediate complexity plankton ecosystem model for the global domain. *Geoscientific Model Development*, 4(2), 381–417.

Yool, A., E. E. Popova, & T. R. Anderson (2013). MEDUSA-2.0: an intermediate complexity biogeochemical model of the marine carbon cycle for climate change and ocean acidification studies. *Geoscientific Model Development*, 6(5), 1767–1811.

Yvon-Durocher, G., J. M. Caffrey, A. Cescatti, M. Dossena, P. del Giorgio, J. M. Gasol, J. M. Montoya, J. Pumpanen, P. A. Staehr, M. Trimmer, G. Woodward,

& A. P. Allen (2012). Reconciling the temperature dependence of respiration across timescales and ecosystem types. *Nature*, 487(7408), 472–476.

Zielinski, U. & R. Gersonde (1997). Diatom distribution in Southern Ocean surface sediments (Atlantic sector): Implications for paleoenvironmental reconstructions. *Palaeogeography, Palaeoclimatology, Palaeoecology*, 129(3-4), 213–250.

Zuur, A., E. Ieno, N. Walker, A. Saveliev, & G. Smith, *Mixed Effects Models and Extensions in Ecology with R.* Springer-Verlag, New York, 2009, 1st edition, 574 pp.